APPENDIX D

METEOROLOGICAL MODELING

2021 REGIONAL HAZE STATE IMPLEMENTATION PLAN
REVISION

PROJECT NUMBER 2019-112-SIP-NR
SFR-122/2019-112-SIP-NR

This page intentionally left blank

TABLE OF CONTENTS

LIST OF TABLES

LIST OF FIGURES

CHAPTER 1: WEATHER RESARCH AND FORECASTING (WRF) MODELING OVERVIEW

The Texas Commission on Environmental Quality (TCEQ) used version 3.8.1 of the WRF model to generate the meteorological inputs for the photochemical modeling supporting this 2021 Regional Haze State Implementation Plan (SIP) Revision. The WRF modeling system was developed by a broad user community including the Air Force Weather Agency, national laboratories, and academia (WRF, 2017).

1.1 MODELING DOMAIN

The WRF modeling was conducted for the entire Continental United States (CONUS) for the year of 2016. A summary is provided in Table 1-1: *CONUS 2016 Meteorological Modeling*.

Table 1-1: CONUS 2016 Meteorological Modeling

Episode	Begin Date/Time (UTC)	End Date/Time (UTC)
2016 Calendar Year	December 16, 2015 00:00	December 31, 2016 00:00

A Lambert Conformal Conic (LCC) map projection with geographical coordinates defined in Table 1-2: *Lambert Conformal Map Projections* was used for the WRF modeling.

Table 1-2: Lambert Conformal Map Projections

Projection Parameter	Value
First True Latitude (Alpha)	33˚N
Second True Latitude (Beta)	45˚N
Central Longitude (Gamma)	97˚W
Projection Origin	97˚W, 40˚N
Spheroid	Perfect Sphere, Radius = 6370 km

WRF was configured with a single 12 kilometer (km) grid covering almost all of North America. Figure 1-1: *WRF 2016 Regional Haze Modeling Domain* shows the single WRF domain in light red that includes all Canadian Provinces, Mexico, and portions of Central America and Venezuela and the smaller concentric CAMx domain in dark red. The easting and northing ranges in the LCC projection are defined in Table 1-3: *WRF Modeling Domain Definitions* in units of km. Table 1-4: *Vertical Layer Structure* provides details regarding the heights, in units of meters above ground level (m AGL), and thickness, in units meters (m), of the vertical layers in WRF.

Figure 1-1: WRF 2016 Regional Haze Modeling Domain

Table 1-3: WRF Modeling Domain Definitions

Domain	Easting Range (km)	Northing Range (km)	East/West Grid Points	North/South Grid Points
12 km	-3492,3492	-1324,3024	583	505

Table 1-4: Vertical Layer Structure

WRF Layer	Sigma Level	Top (m AGL)	Center (m AGL)	Thickness (m)
44	0.000	20581	20054	1054
43	0.010	19527	18888	1278
42	0.025	18249	17573	1353
41	0.045	16896	16344	1103
40	0.065	15793	15215	1156
39	0.090	14637	14144	987
38	0.115	13650	13136	1029
37	0.145	12621	12168	906
36	0.175	11716	11245	941
35	0.210	10774	10294	962
34	0.250	9813	9379	867
33	0.290	8946	8550	792
32	0.330	8154	7790	729
31	0.370	7425	7128	594
30	0.405	6830	6551	559
29	0.440	6271	6007	528
28	0.475	5743	5492	501
27	0.510	5242	5037	410
26	0.540	4832	4636	393
25	0.570	4439	4250	378
24	0.600	4061	3878	365
23	0.630	3696	3520	352
22	0.660	3344	3173	341
21	0.690	3003	2838	330
20	0.720	2673	2513	320
19	0.750	2353	2224	259
18	0.775	2094	1967	253
17	0.800	1841	1717	247
16	0.825	1593	1472	242
15	0.850	1352	1280	143
14	0.865	1209	1138	141
13	0.880	1068	999	139
12	0.895	929	860	137
11	0.910	792	746	91
10	0.920	701	656	90
9	0.930	611	566	89
8	0.940	522	477	89
7	0.950	433	389	88
6	0.960	345	301	87
5	0.970	258	214	87
4	0.980	171	128	86
3	0.990	85	60	51
2	0.996	34	26	17
1	0.998	17	8	17
0	1.000	0	0	0

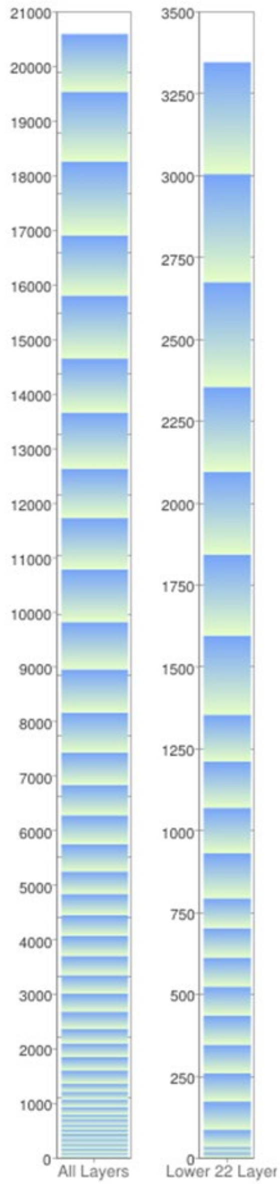

Figure 1-2: WRF Vertical Layer Structure

The WRF vertical layer structure is intended to provide higher resolution in the lowest part of the atmosphere where pollutant mixing is critical, as shown in Figure 1-2: *WRF Vertical Layer Structure*.

1.2 WRF MODEL CONFIGURATION

The selection of the final meteorological modeling configuration for the 2016 episode year resulted from numerous sensitivity tests and model performance evaluation. The final WRF parameterization schemes and options selected are shown in Table 1-5: *2016 WRF Configuration*. This WRF configuration is very similar to that used by the United States Environmental Protection Agency (EPA), which has done their own evaluations with a 12 km grid configuration. However, TCEQ modeling differs from EPA modeling in part by having a larger number of vertical levels. Another important difference is that TCEQ WRF modeling has its initialization and boundary conditions developed using the European Re-Analysis Interim (ERA-Interim) analyses. This is discussed in Section 2.1: *WRF Preprocessing System.*

Table 1-5: 2016 WRF Configuration

Model Version	Domain	Nudging Type	PBL	Cumulus	Radiation	Land-Surface	Micro-physics
WRF 3.8.1	12 km	3-D Analysis	ACM2	Kain-Fritsch	RRTM / Dudhia	Pleim-Xiu (PX)	Morrison

Note: ACM2 = Asymmetric Convective Model, version 2, RRTM = Rapid Radiative Transfer Model

The selected WRF configuration used the PX land surface model (LSM) with soil nudging. The PX soil nudging does not use new soil or soil moisture data. Instead, this is a force restore technique that adjusts soil moisture provided by the National Centers for Environmental Prediction (NCEP) archived data to more closely match the two-meter temperature and humidity in the WRF Surface Four-Dimensional Data Assimilation (WRFSFDDA) file.

WRF output was post-processed using the WRFCAMx utility to convert the WRF meteorological fields to the Comprehensive Air Quality Model with Extensions (CAMx) grid and input format (Ramboll, 2019). The WRFCAMx utility aggregates or interpolates, as necessary, between the 12 km WRF grid and the 36 km CAMx grid since they share the same map projection. The WRFCAMx utility also generates several alternative vertical diffusivity (K_v) files based upon multiple methodologies for estimating mixing given the same WRF meteorological fields. The WRF K_v option selected was the Community Multiscale Air Quality model (CMAQ) planetary boundary layer profile.

CHAPTER 2: WRF PREPARATION

2.1 WRF PREPROCESSING SYSTEM (WPS)

The preparation of WRF input files involves the execution of different models within the WPS as described below. The requirement to initialize and develop boundary conditions for WRF on a large domain precluded the use archived data sets from the NCEP Eta data archive used in other SIP projects. Among global models, the ERA-Interim archived by the European Centre for Medium-Range Weather Forecasts (ECMWF) has a sophisticated use of four-dimensional variational analysis, and variational bias correction of satellite data. The archive includes 60 model levels archived every six hours. A detailed description is provided at https://www.ecmwf.int/en/elibrary/8174-era-interim-archive-version-20.

2.1.1 GEOGRID

- GEOGRID defined the WRF grids on a Lambert-Conformal Projection (see Table 1-2) and allocated the Land Use/Land Cover (LULC) data. New LULC data was included in the WRF v3.8.1 release.

2.1.2 UNGRIB/METGRID

- UNGRIB unpacked the surface- and upper-level meteorological data from the Gridded Binary (GRIB) files of the ERA-Interim analyses to standard pressure levels native to the ERA-Interim analyses.
- METGRID re-gridded the unpacked data onto the WRF grids defined in GEOGRID into a Network Common Data Form (NetCDF) format.

2.1.3 OBSGRID

- This optional program was used to develop the WRFSFDDA for the 12 km grid. Running the WRF model with the PX land surface model with soil nudging requires the WRFSFDDA file.

2.1.4 REAL

- The REAL program defined the WRF sigma level vertical structure (Figure 1-2) and mapped the archived data retrieved on pressure levels to the sigma levels defined by the WRF user, consistent with surface land use data and definitions of the upper atmosphere. Base state variables were set to Texas summer values: 1013 hPa sea-level pressure, a reference temperature lapse rate of 45 (K/ln p), and a 304 degrees K sea-level temperature. The REAL program produced the WRF initial condition files, boundary condition files, and WRF Four-Dimensional Data Assimilation (WRFFDDA) nudging files, where the four dimensions are three spatial dimensions plus time.

CHAPTER 3: WRF MODEL PERFORMANCE EVALUATION (MPE)

3.1 OBSERVATIONS

To evaluate the performance of WRF, surface data for wind speed, wind direction, temperature and specific humidity were collected from the NOAA ds472.0 dataset and the Meteorological Assimilation Data Ingest System (MADIS). Across the 12 km domain there were over 2800 stations as shown in Figure 3-1: *All ds472.0 Data Used for Model Validation in the 12 km Domain*. These sites provided wind speed, temperature, and humidity data for the analysis discussed below.

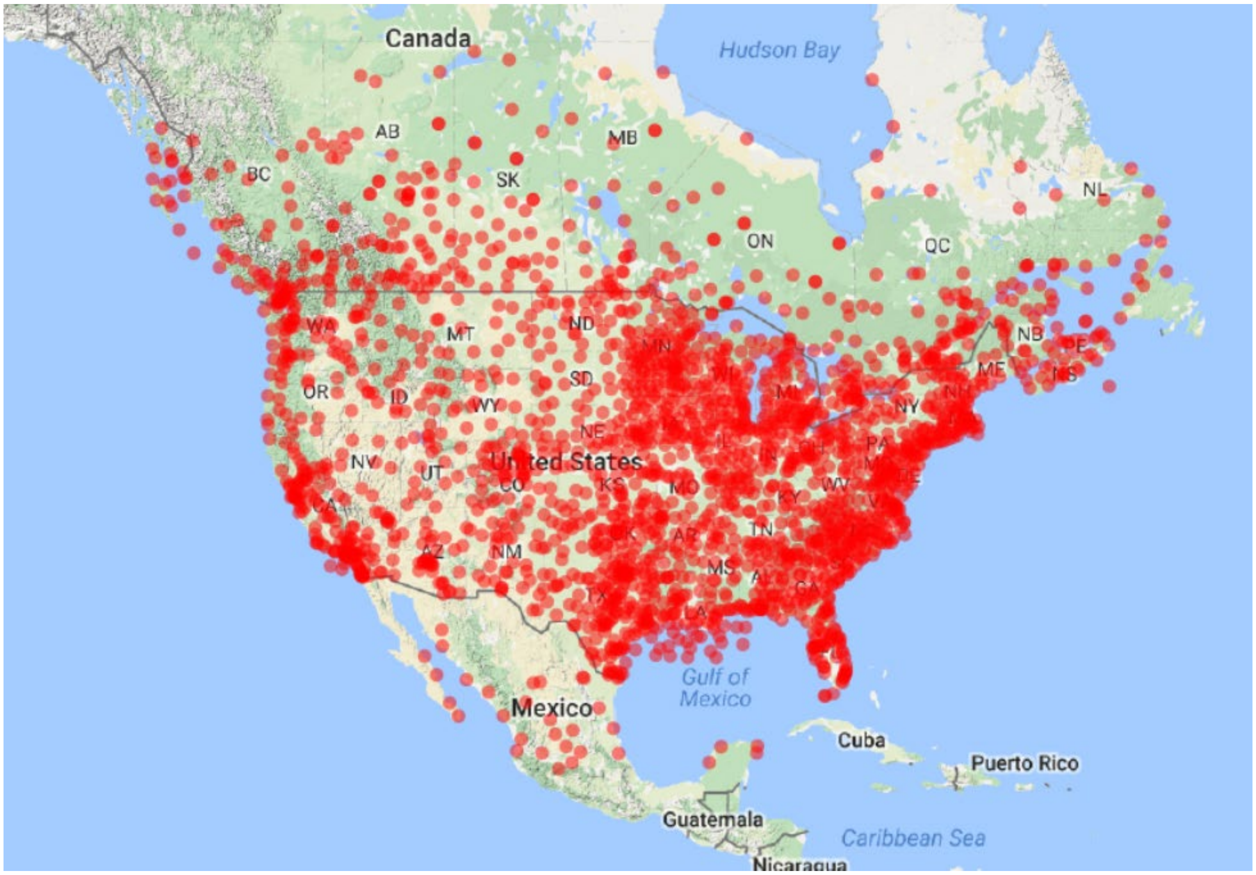

Figure 3-1: All ds472.0 Data Used for Model Validation in the 12 km Domain

For the model performance evaluation, WRF predicted values for wind speed, direction, temperature, and humidity were compared to ds472 observations in daily averaged monthly time series. The time series compare WRF modeled values to averages across the CONUS or within a south-central region domain that includes Texas and its surrounding states plus Missouri. Alternative ways of aggregating and averaging data provide other performance information. For that reason, in addition to evaluation of daily time series of model performance across the entire domain, WRF monthly mean biases for wind speed, temperature, and humidity at individual ds472 sites were calculated and plotted on United States (U.S.) maps. Table 3-1: *Simple and Complex Meteorological Modeling Performance Benchmarks for Meteorological Surface Variables* provides a summary of meteorological benchmarks for simple and complex terrains from three different sources. As air quality modeling is now used for longer study periods with more synoptic variability and in regions with mountains and land sea breezes, additional benchmarks for complex meteorology were proposed. The discussion of these benchmarks can be found in the Western Regional Air Partnership (WRAP) West-wide Jump-start Air Quality Modeling Study (WestJumpAQMS) Final Report (WRAP, 2013).

Table 3-1: Simple and Complex Meteorological Modeling Performance Benchmarks for Meteorological Surface Variables

Meteorological Variable	Simple Benchmark (Emery et al., 2001)	Complex Benchmark (McNally, 2009)	Complex Benchmark (WRAP, 2013)
Temperature Bias	≤ ±0.5 ˚K	≤ ±1.0 ˚K	≤ ±2.0 ˚K
Temperature Error	≤ 2.0 ˚K	≤ 3.0 ˚K	≤ 3.5 ˚K
Mixing Ratio Bias	≤ ±1.0 g/kg		
Mixing Ratio Error	≤ 2.0 g/kg		
Wind speed Bias	≤ ±0.5 m/s		≤ ±1.5 m/s
Wind Speed RMSE	≤ 2.0 m/s		≤ 2.5 m/s
Wind Direction Bias	≤ ±10 degrees		
Wind Direction Error	≤ 30 degrees		≤ 55 degrees

Note: ˚K is degree Kelvin; g/kg is grams/kilogram; m/s is meters/second

There are no “bright lines” for model performance. Rather, the benchmarks summarize a broad consensus of performance goals across different modeling exercises. Expectations are higher and corresponding meteorology benchmarks are more stringent when terrain and meteorology are simple. For example, if the modeling domain includes complex terrain, and if the meteorological regimes include frontal passages, then the benchmarks are relaxed to reflect the greater challenges capturing all the relevant phenomena.

Although the ds472 dataset are point measurements, as Figure 3-1 shows, there is adequate spatial coverage across the CONUS. Another means of quantifying WRF performance is to evaluate cloud development. Clouds impact gas phase chemistry by affecting photolytic reactions, either by enhanced diffuse scattering, enhanced reflection above low clouds, or by inhibiting photolytic chemistry below. Aqueous aerosol chemistry directly depends upon clouds. However, verifying cloud placement, transport, and removal happen on timescales as short as an hour or perhaps across a few days. For a year-long episode, precipitation totals serve as a surrogate for the average placement of clouds on the timescale of monthly analysis. The WRF predicted gridded precipitation can be compared to the PRISM (Parameter-elevation Relationships on Independent Slopes Model) dataset maintained by Oregon State University. Precipitation data is collected from approximately 13,000 locations, temperatures from about 10,000 locations, and dependence of model grid cells on site data is constructed from a weighted regression for multiple climatological and topographical data. This methodology is explained in detail at: http://prism.oregonstate.edu/documents/Daly2008_PhysiographicMapping_IntJnlClim.pdf. WRF accumulations are instantaneous values while PRISM data is accumulated hourly values. The WRF magnitudes may generally match the PRISM data but show more granularity of precipitation patterns.

3.2 WRF JANUARY PERFORMANCE

3.2.1 CONUS January Timeseries

Daily performance was evaluated using monthly time series panels comparing hourly modeled and observed data that were averaged across for all ds472 sites and the south-central region. Time series for wind speed, wind direction, temperature, and humidity were calculated for each month of 2016. An example of the January 2016 wind performance for the CONUS is shown in *Figure 3-2: WRF CONUS Wind Performance for January 2016* which shows hourly wind speed averaged over all ds472 sites. The x-axis of the time series panels is the date and time in Central Standard Time (CST) of the modeling episode. The y-axis represents the range of values of the plotted parameter (e.g., wind speed).

Compared to the benchmarks in Table 3-1, wind speed bias and wind direction are within the recommended bounds as shown in Figure 3-2. Nocturnal temperature sometimes exceeds 1.5 ºC as depicted in Figure 3-3: *WRF CONUS Temperature Performance for January 2016*; however, given that this is a winter month with great variability across latitude and includes complex terrain, this bias seems acceptable. Specific humidity, or mixing ratio, also look reasonable although the bias becomes more noticeably positive by the end of the month as shown in Figure 3-4: *WRF CONUS Humidity Performance for January 2016*.

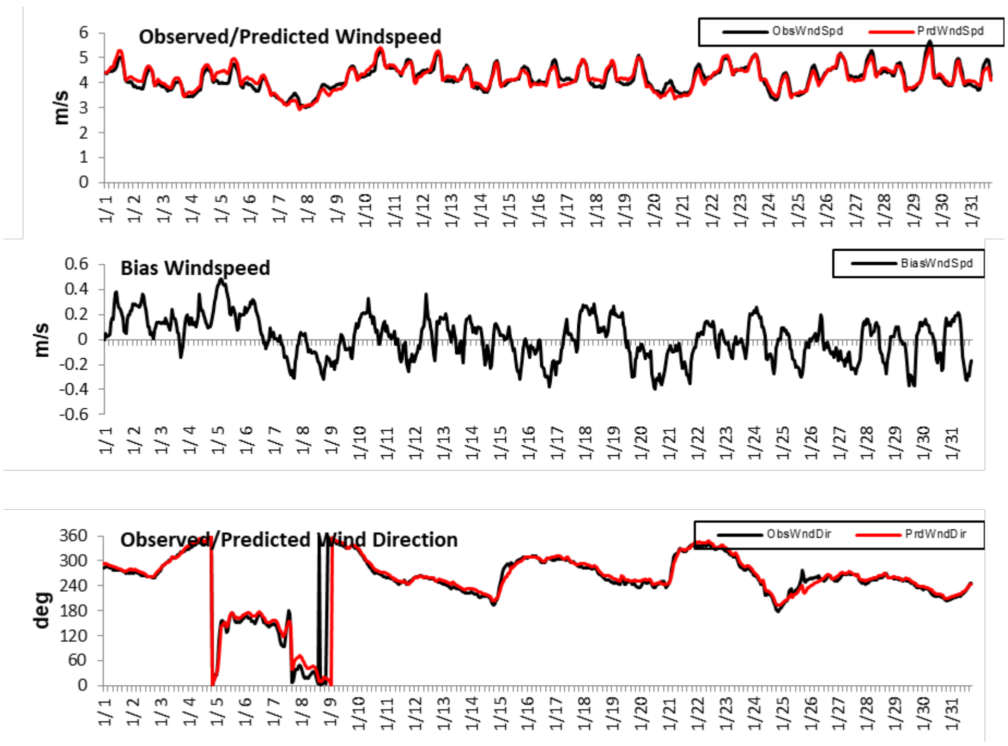

Figure 3-2: WRF CONUS Wind Performance for January 2016

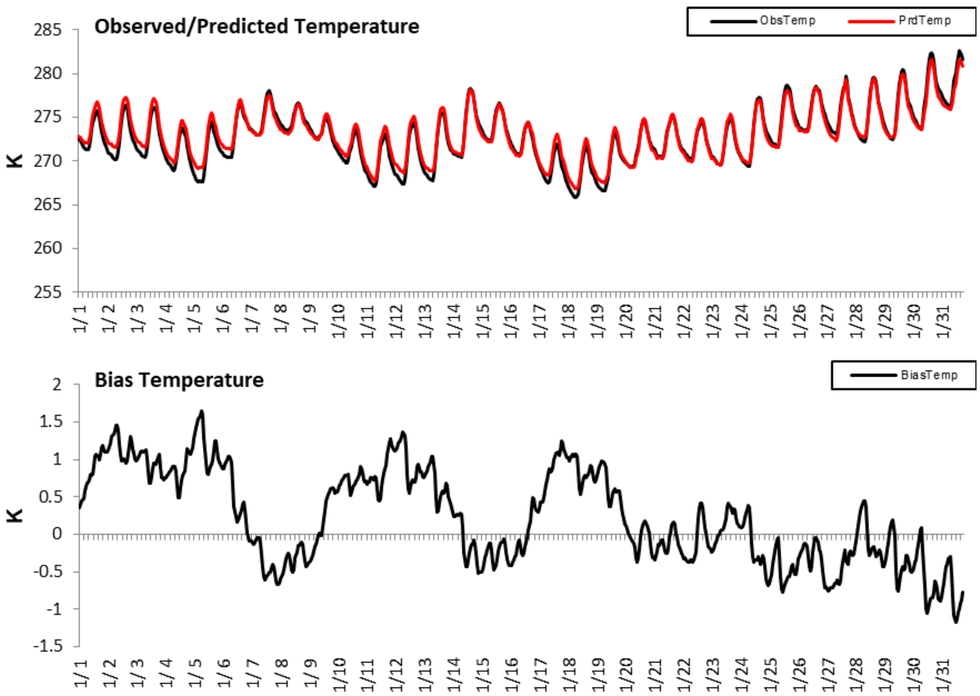

Figure 3-3: WRF CONUS Temperature Performance for January 2016

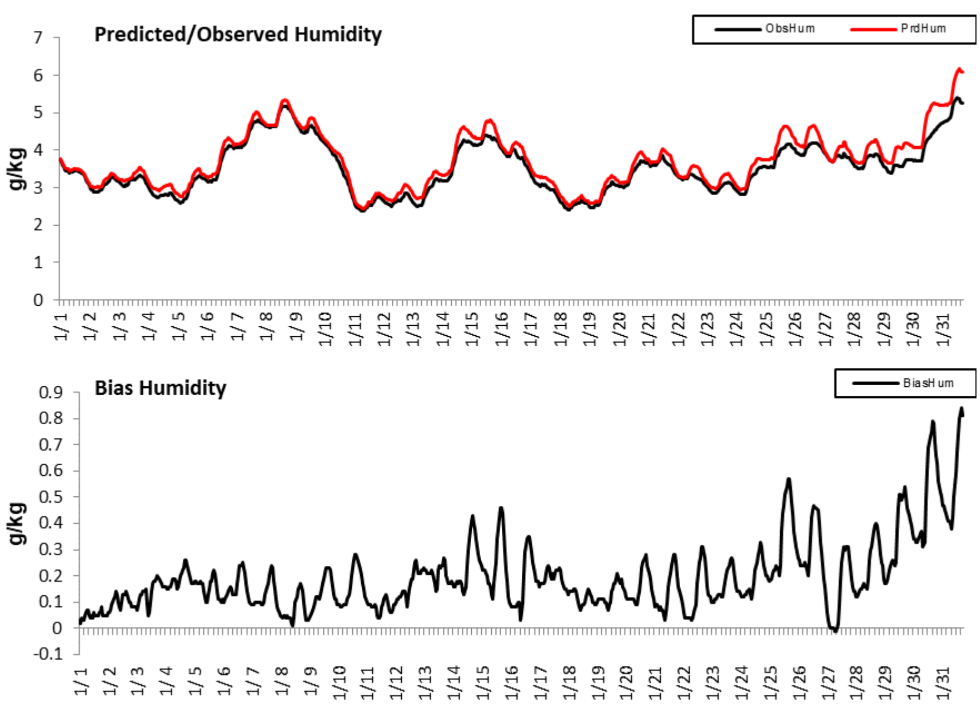

Figure 3-4: WRF CONUS Humidity Performance for January 2016

3.2.2 South-Central Region January Timeseries

Applying the same benchmarks to a smaller region often reflect more variability due to averaging over fewer predicted-observed data pairs. In this section, daily mean bias and error is calculated for the south-central region, an area that includes Texas and surrounding states (New Mexico, Oklahoma, Missouri, Arkansas, and Louisiana). Observation locations are shown in Figure 3-5: *ds472 Sites in the South-Central Region*. For this month, wind speed and direction as well as humidity (Figure 3-8: *WRF South-Central Region Humidity Performance for January 2016*) show good performance. Temperatures have larger biases associated with the overprediction of night-time temperatures (Figure 3-7: *WRF South-Central Region Temperature Performance for January 2016*).

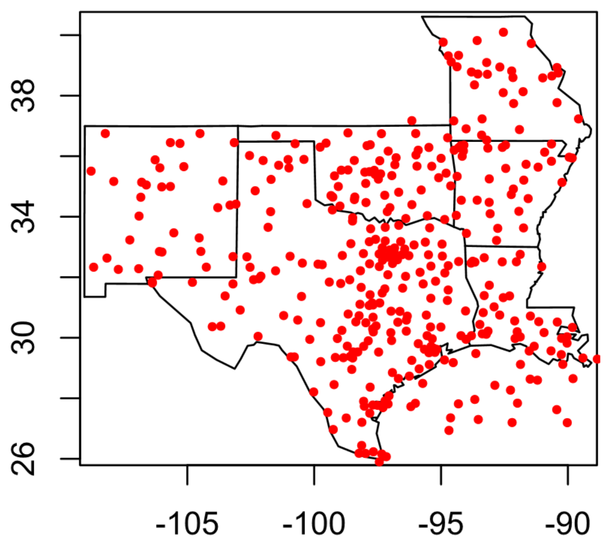

Figure 3-5: ds472 Sites in the South-Central Region

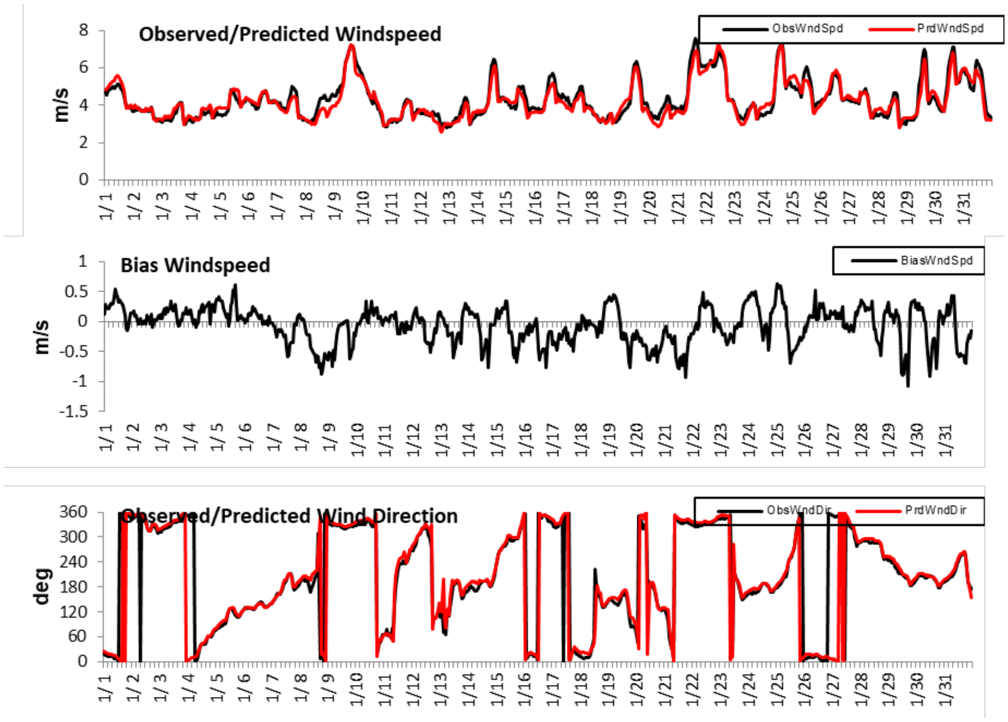

Figure 3-6: WRF South-Central Region Wind Performance for January 2016

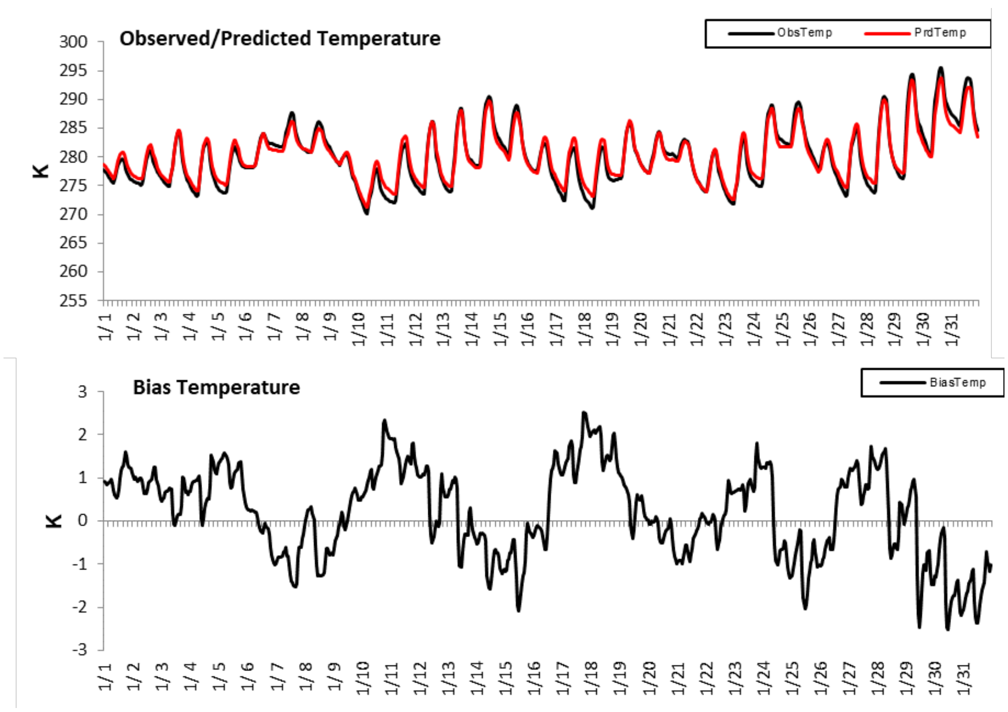

Figure 3-7: WRF South-Central Region Temperature Performance for January 2016

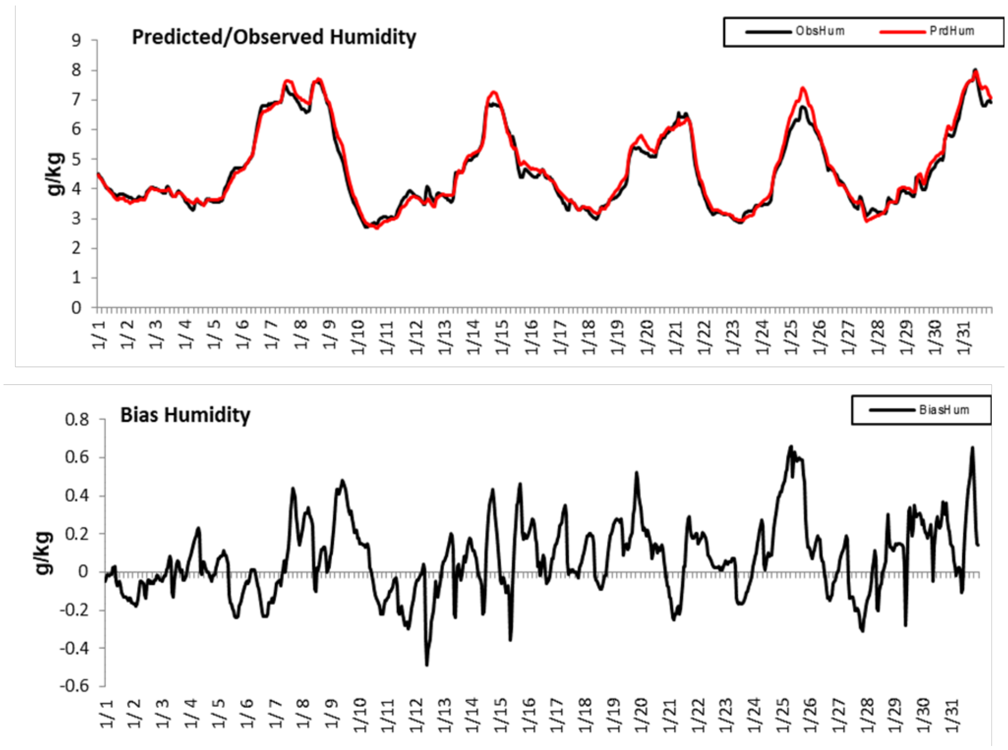

Figure 3-8: WRF South-Central Region Humidity Performance for January 2016

3.2.3 January Spatial Bias Plots

In this section, biases are calculated at each individual site in the ds472 dataset for the entire month. Wind speed biases, seen in Figure 3-9: *Mean Bias of Wind Speed for January 2016*, were low throughout east Texas, most of Oklahoma, Missouri, and Arkansas. However, New Mexico showed many sites with a negative bias of 1.5 m/s, and some sites had an even larger negative wind speed bias. Temperatures biases, shown in Figure 3-10: *Mean Temperature Bias for January 2016*, tended to be low across the south-central region, but were up to 2.0 degrees too warm near Big Bend and north-central New Mexico. The humidity comparison showed most of the CONUS had a bias near zero while western Texas was too dry by about 1.5 g/kg as shown in Figure 3-11: *Mean Mixing Ratio Bias for January 2016*.

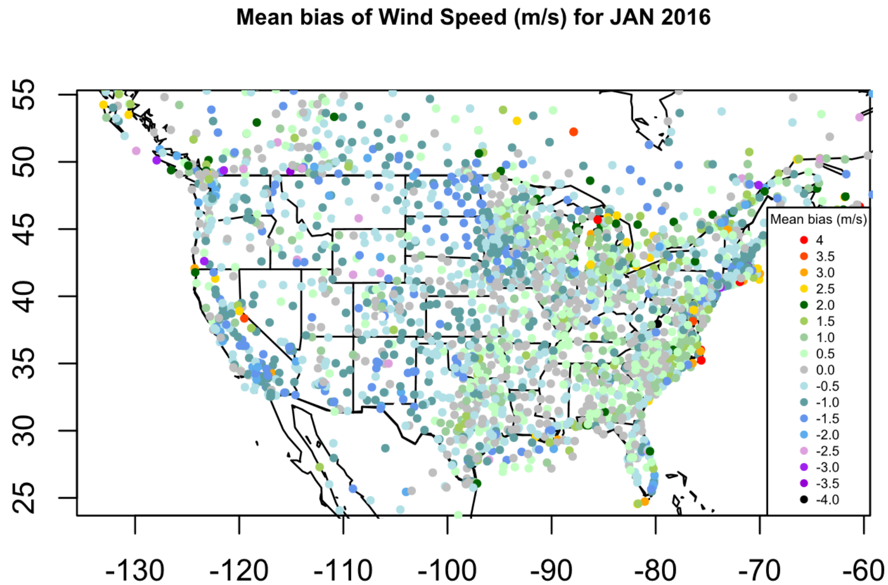

Figure 3-9: Mean Bias of Wind Speed for January 2016

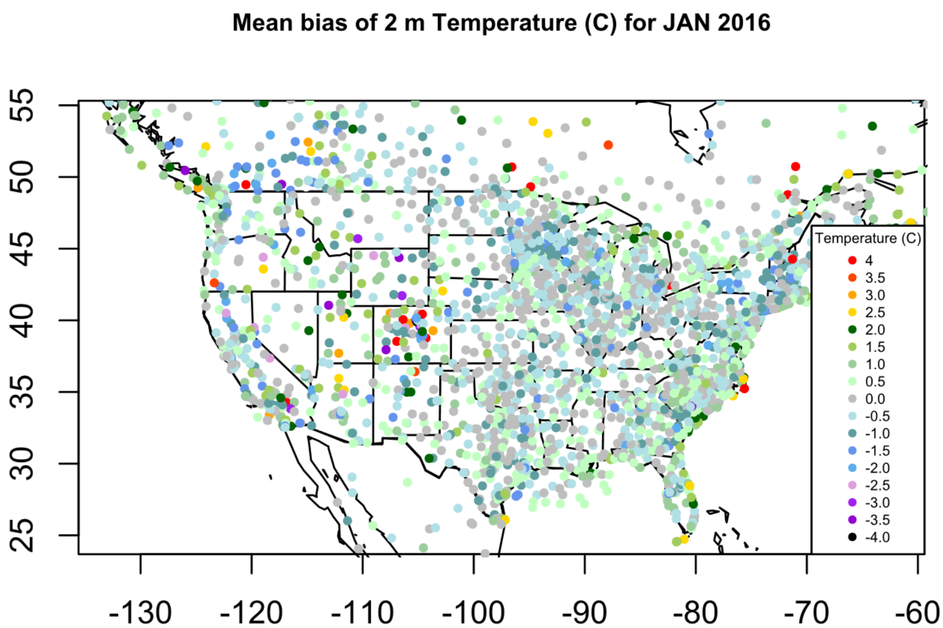

Figure 3-10: Mean Temperature Bias for January 2016

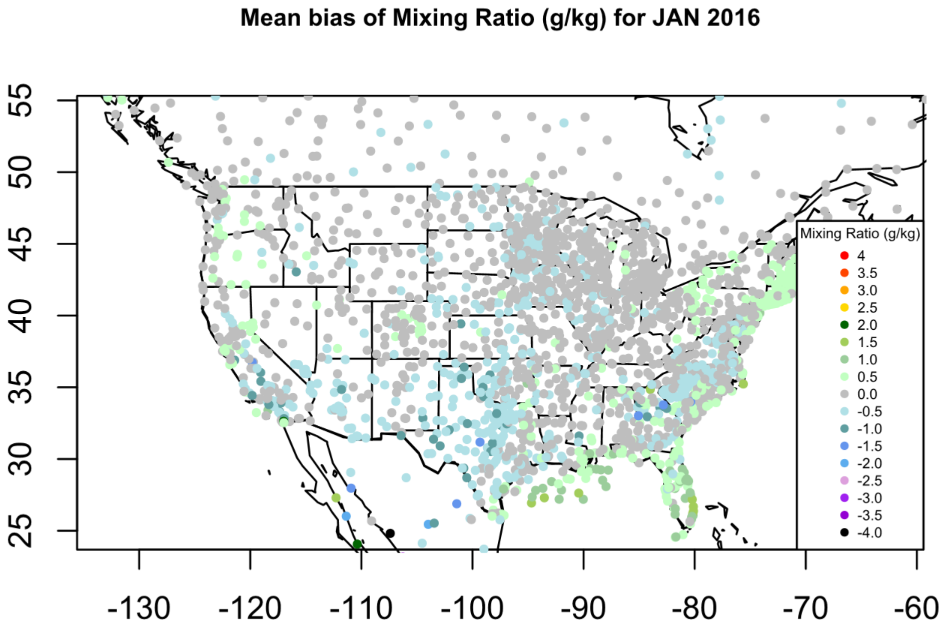

Figure 3-11: Mean Mixing Ratio Bias for January 2016

3.2.4 January Accumulated Precipitation

The patterns of accumulated precipitation shown in Figure 3-12: *WRF Accumulated Monthly Precipitation in Inches for January 2016* and Figure 3-13: *PRISM Accumulated Monthly Precipitation for January 2016* look very similar. The west coast and northwest U.S. had the most precipitation although the extent of heavy WRF precipitation there was less than the PRISM data. Both data sets showed very little precipitation across the Great Plains. The general magnitude of precipitation matched in east Texas although the areal extent of precipitation was a bit less.

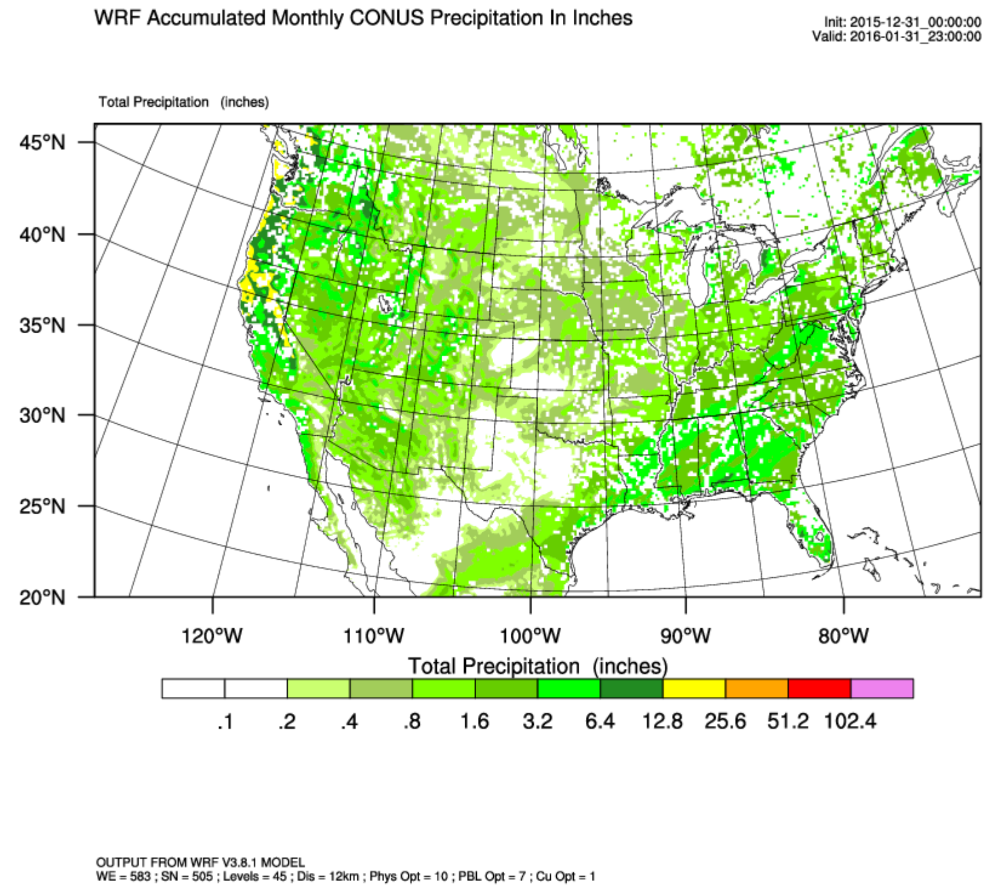

Figure 3-12: WRF Accumulated Monthly Precipitation in Inches for January 2016

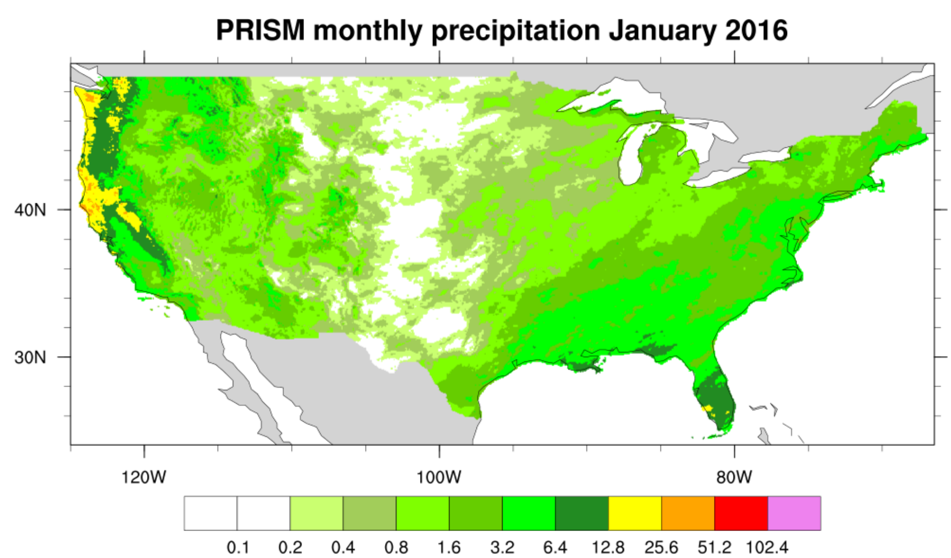

Figure 3-13: PRISM Accumulated Monthly Precipitation for January 2016

3.3 WRF FEBRUARY PERFORMANCE

Time series for wind speed and direction looked very good across the CONUS and the south-central region as shown in Figure 3-14: *WRF CONUS Wind Performance for February 2016* and Figure 3-17: *WRF South-Central Region Wind Performance for February 2016*. Nocturnal over-prediction of temperatures resulted in higher daily temperature biases as shown in Figure 3-15: *WRF CONUS Temperature Performance for February 2016* and Figure 3-18: *WRF South-Central Region Temperature Performance for February 2016*. In general, specific humidity performance was good as shown in Figure 3-16: *WRF CONUS Humidity Performance for February 2016* and Figure 3-19: *WRF South-Central Region Humidity Performance for February 2016*.

3.3.1 CONUS February Timeseries

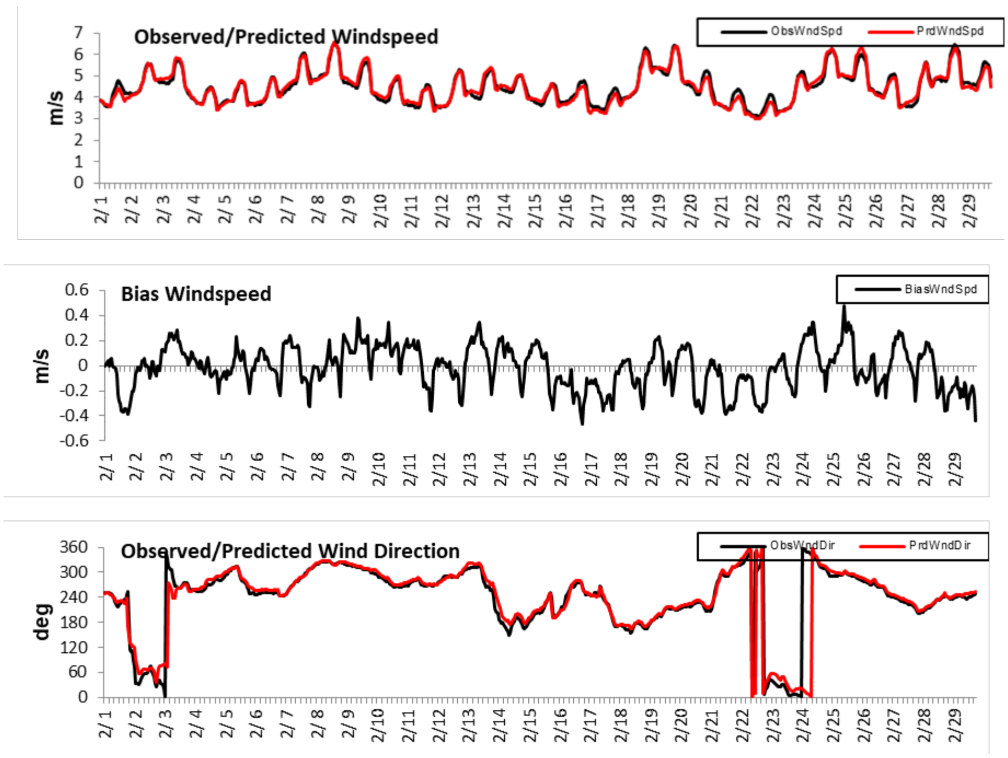

Figure 3-14: WRF CONUS Wind Performance for February 2016

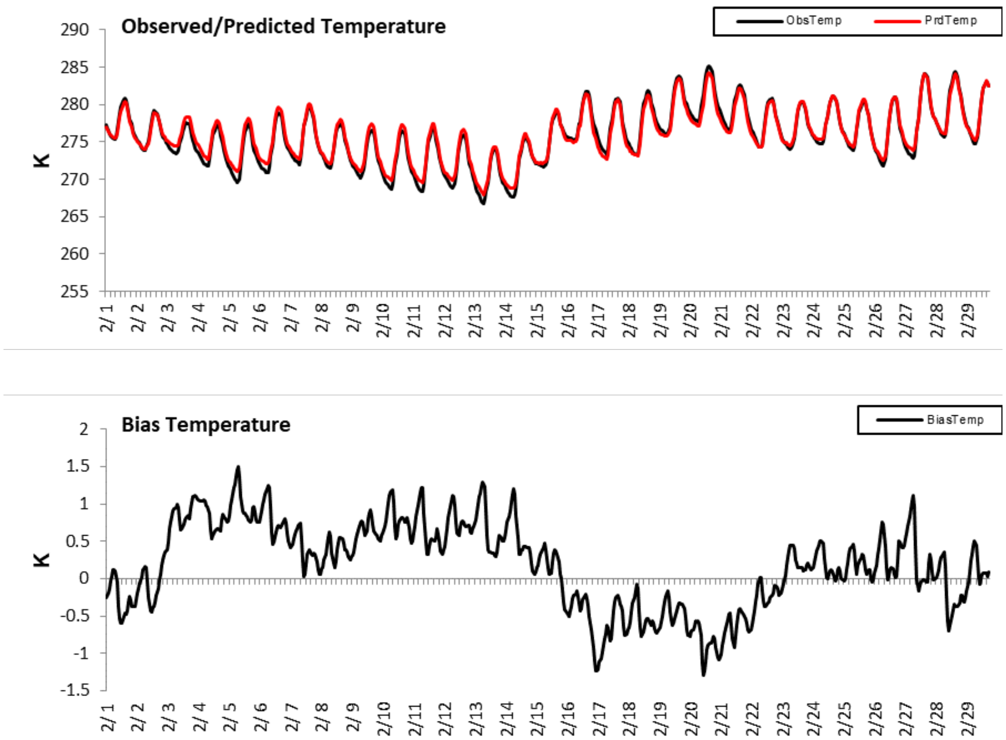

Figure 3-15: WRF CONUS Temperature Performance for February 2016

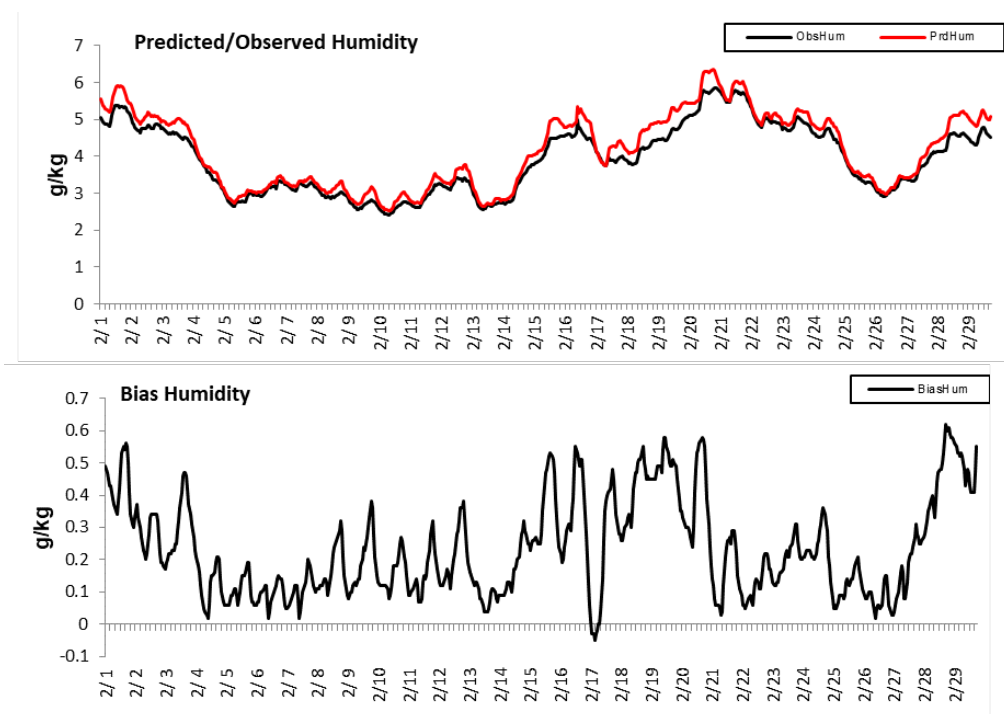

Figure 3-16: WRF CONUS Humidity Performance for February 2016

3.3.2 South-Central Region February Timeseries

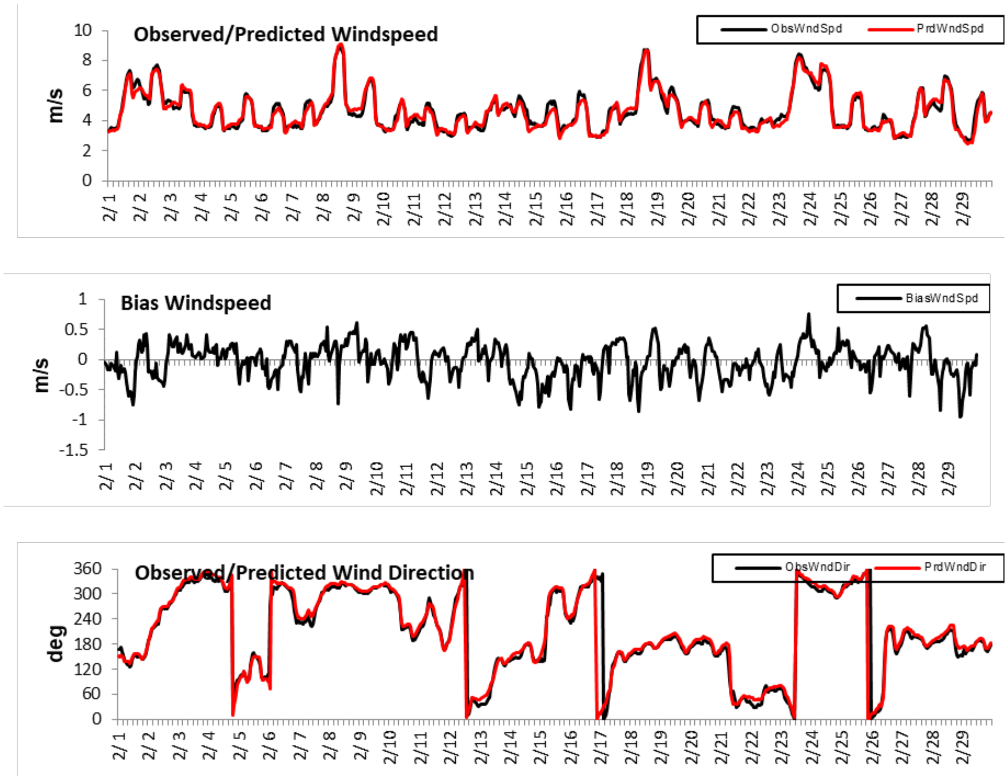

Figure 3-17: WRF South-Central Region Wind Performance for February 2016

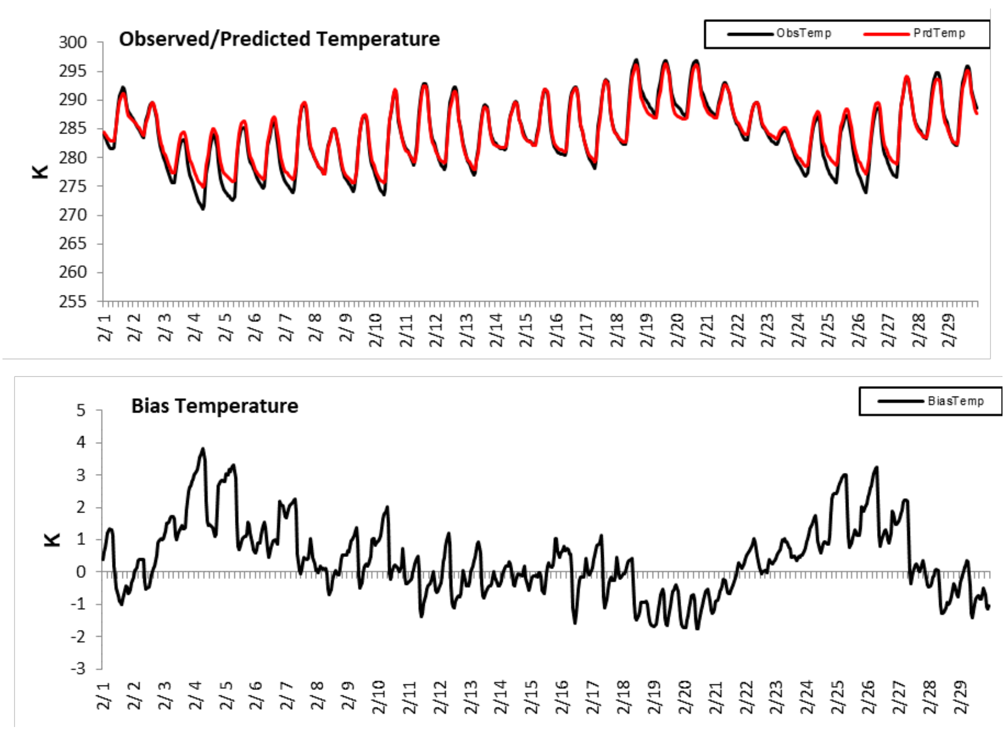

Figure 3-18: WRF South-Central Region Temperature Performance for February 2016

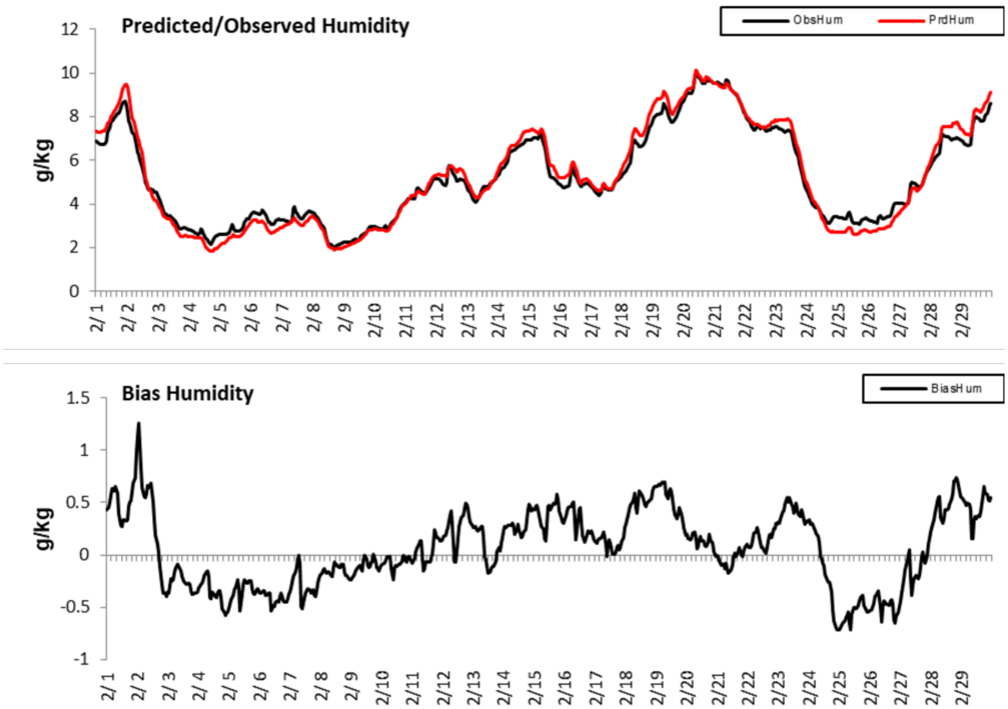

Figure 3-19: WRF South-Central Region Humidity Performance for February 2016

3.3.3 February Spatial Bias Plots

Wind speed biases were low across most of the south-central region with exception of a strong negative bias of -4 m/s at Guadalupe Mountains National Park and negative biases of 1 to 2 m/s over New Mexico as shown in Figure 3-20: *Mean Bias of Windspeed for February 2016*. Temperature biases tended to be a low to slightly negative across Texas and the region excepting a high temperature bias near Big Bend National Park as shown in Figure 3-21: *Mean Bias of Temperature for February 2016*. The periods of slight overprediction and underprediction shown in Figure 3-19 tend to balance and show the low monthly biases shown in Figure 3-22: *Mean Bias of Mixing Ratio for February 2016*.

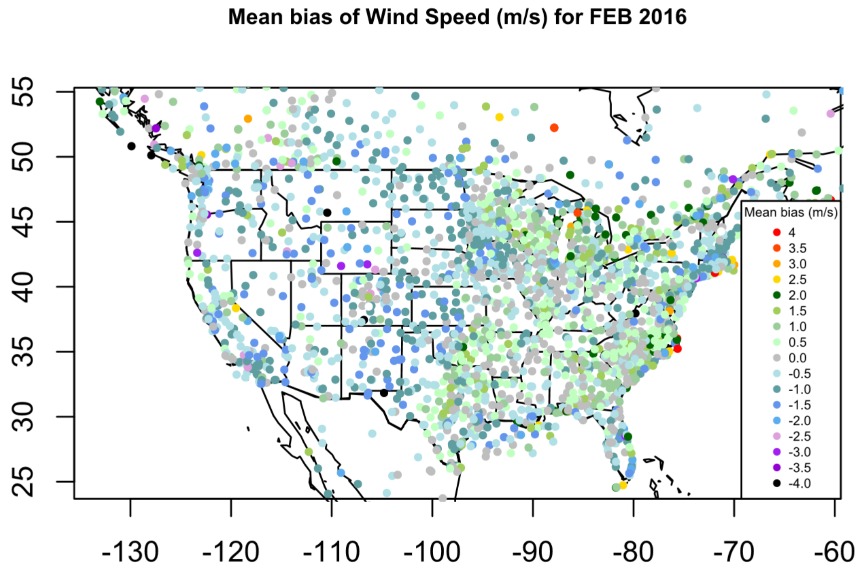

Figure 3-20: Mean Bias of Windspeed for February 2016

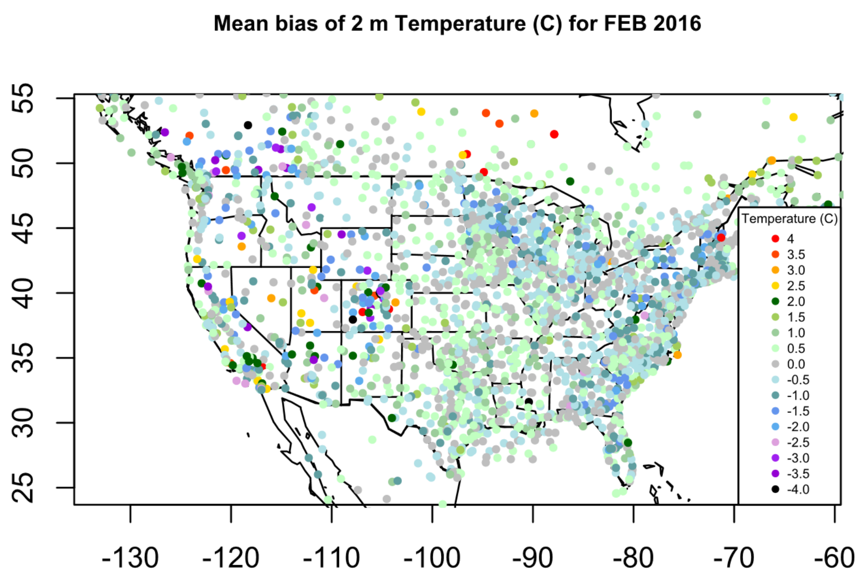

Figure 3-21: Mean Bias of Temperature for February 2016

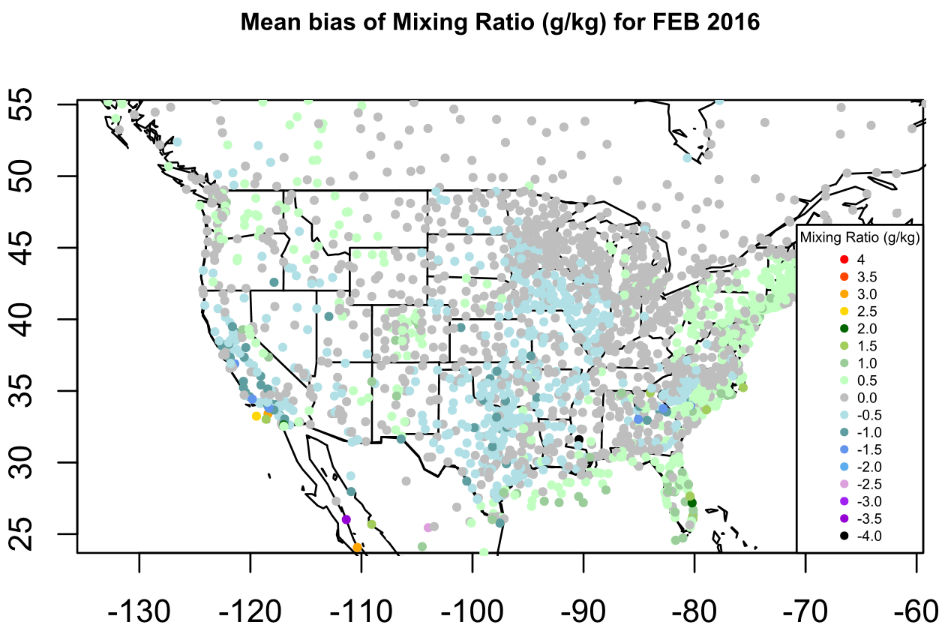

Figure 3-22: Mean Bias of Mixing Ratio for February 2016

3.3.4 February Accumulated Precipitation

Precipitation patterns are similar for both WRF (Figure 3-23: *WRF Accumulated Monthly Precipitation for February 2016*) and PRISM data (Figure 3-24: *PRISM Accumulated Monthly Precipitation for February 2016*) for February.

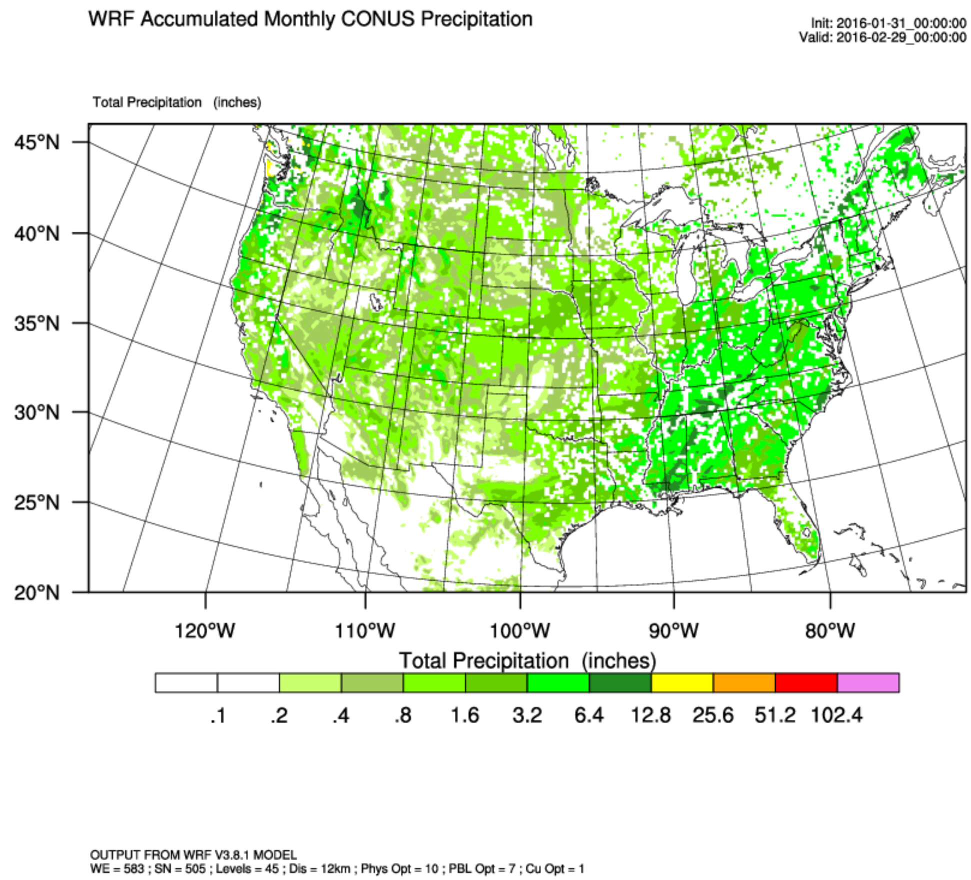

Figure 3-23: WRF Accumulated Monthly Precipitation for February 2016

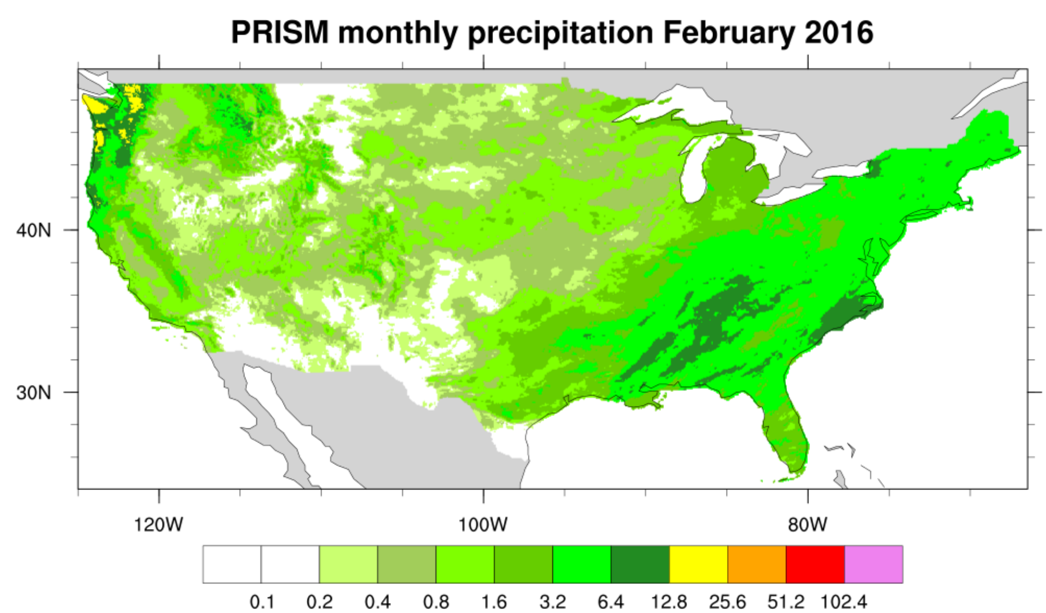

Figure 3-24: PRISM Accumulated Monthly Precipitation for February 2016

3.4 WRF MARCH PERFORMANCE

Time series for wind speed and direction looked very good across the CONUS and across the south-central region as shown in Figure 3-25: *WRF CONUS Wind Performance for March 2016* and Figure 3-28: *WRF South-Central Region Wind Performance for March 2016*. Higher daily temperature biases resulted from nocturnal overprediction during periods of the month with cooler temperatures as shown in Figure 3-26: *WRF CONUS Temperature Performance for March 2016* and Figure 3-29: *WRF South-Central Region Temperature Performance for March 2016*. Humidity performance was generally good although there were periods with modest overprediction as shown in Figure 3-27: *WRF CONUS Humidity Performance* and Figure 3-30: *WRF South-Central Region Humidity Performance for March 2016*.

3.4.1 CONUS March Timeseries

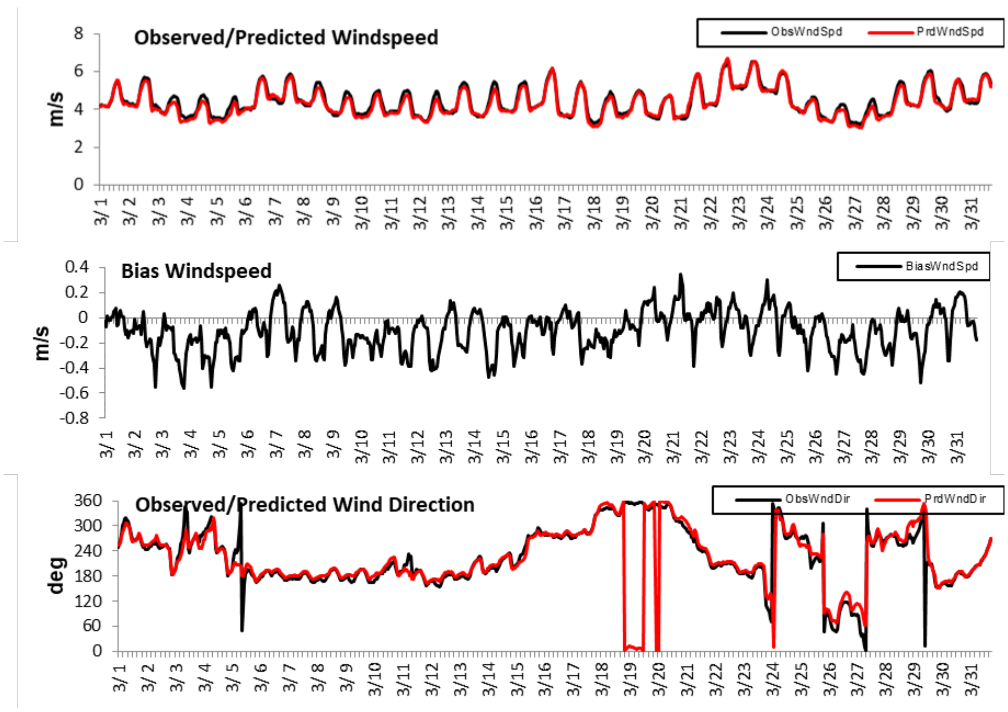

Figure 3-25: WRF CONUS Wind Performance for March 2016

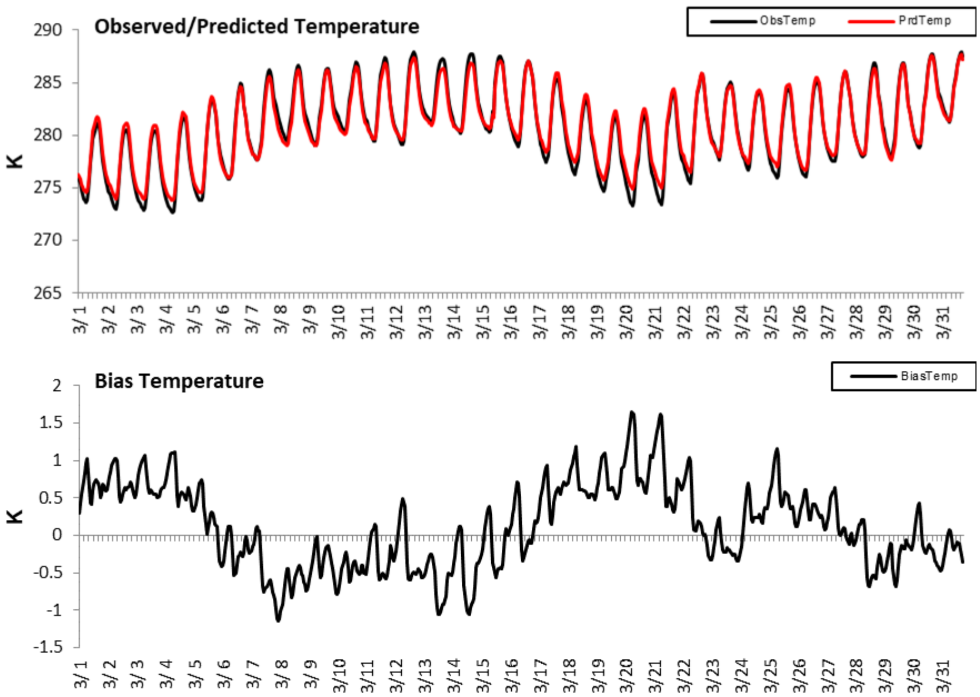

Figure 3-26: WRF CONUS Temperature Performance for March 2016

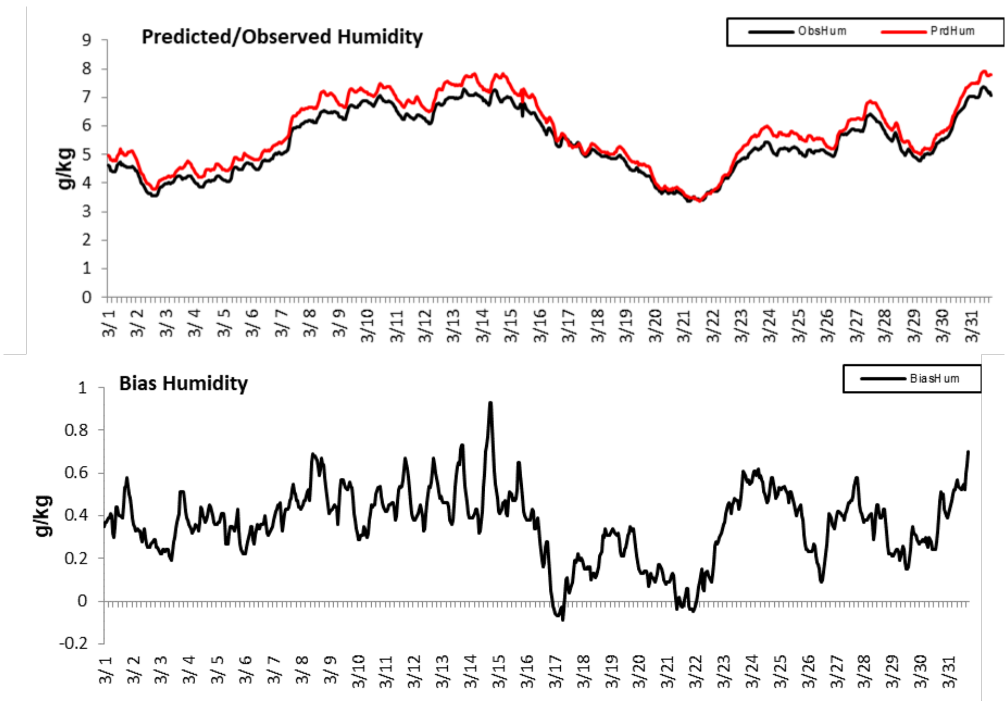

Figure 3-27: WRF CONUS Humidity Performance for March 2016

3.4.2 South-Central Region March Timeseries

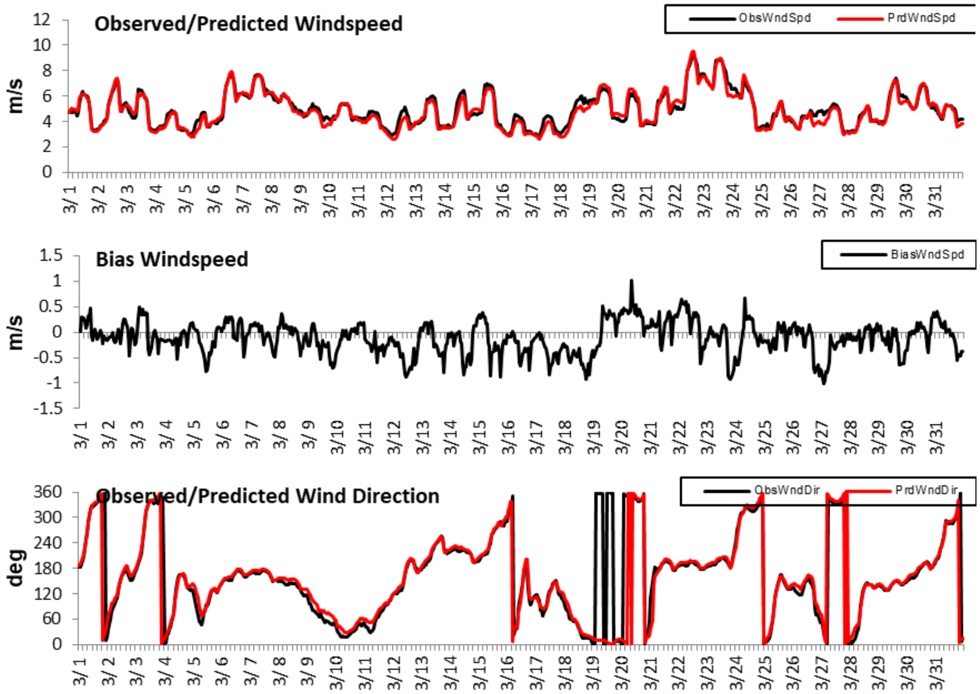

Figure 3-28: WRF South-Central Region Wind Performance for March 2016

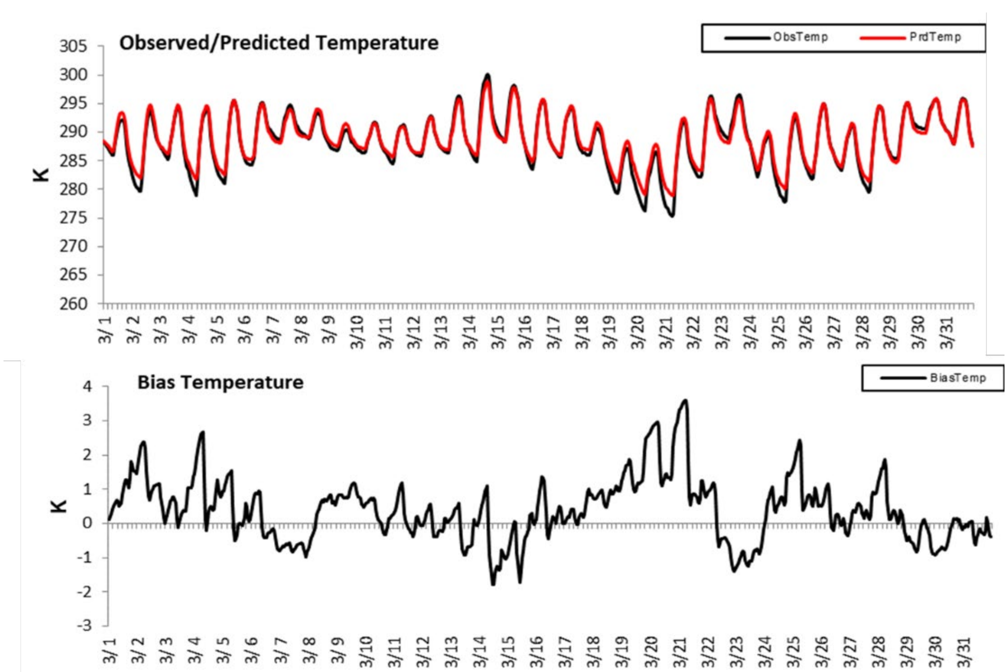

Figure 3-29: WRF South-Central Region Temperature Performance for March 2016

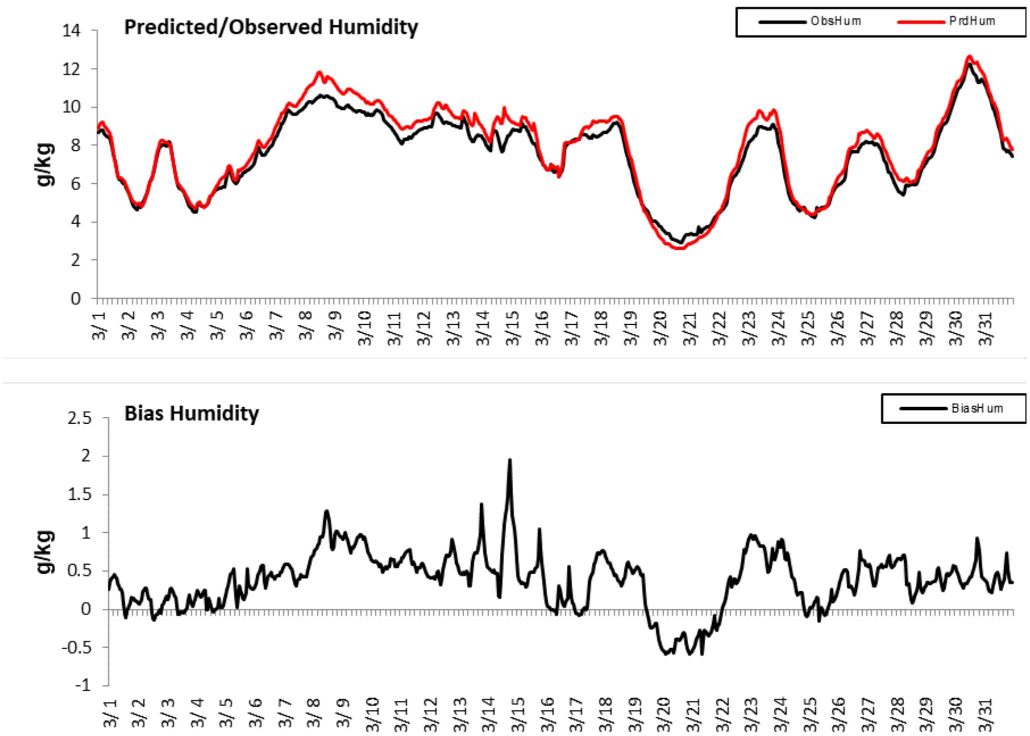

Figure 3-30: WRF South-Central Region Humidity Performance for March 2016

3.4.3 March Spatial Bias Plots

The modest negative bias in wind speed shown in Figure 3-28 for most of the month is captured in the monthly averages of ds472 sites in the south-central region in Figure 3-31: *Mean Bias of Wind Speed for March 2016*. New Mexico had larger negative wind speed biases than elsewhere in this region. Temperature (Figure 3-32: *Mean Bias of Temperature for March 2016*) and humidity (Figure 3-33: *Mean Bias of Mixing Ratio for March 2016*) looked generally good, although as in February, Big Bend had a high temperature bias.

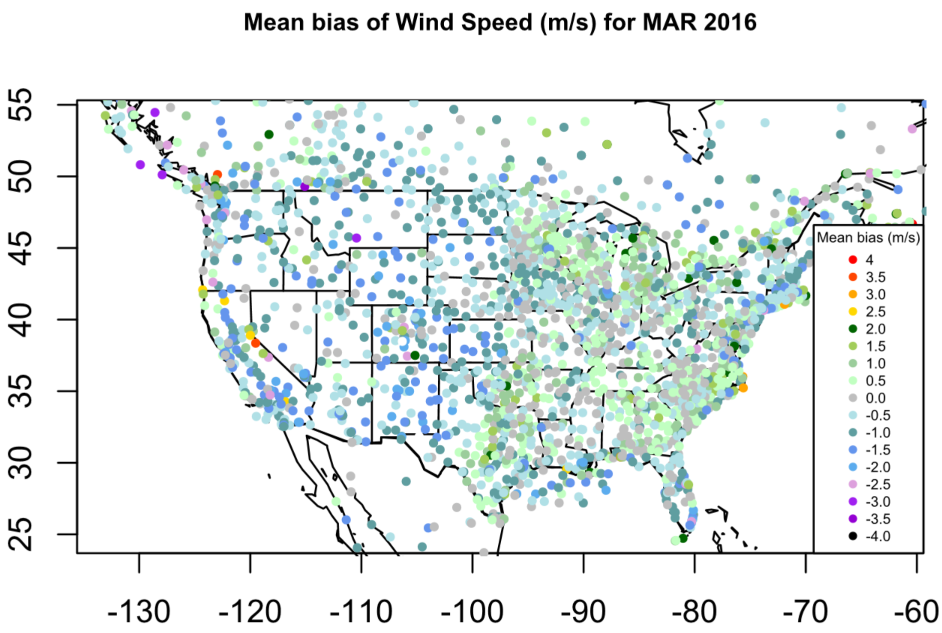

Figure 3-31: Mean Bias of Wind Speed for March 2016

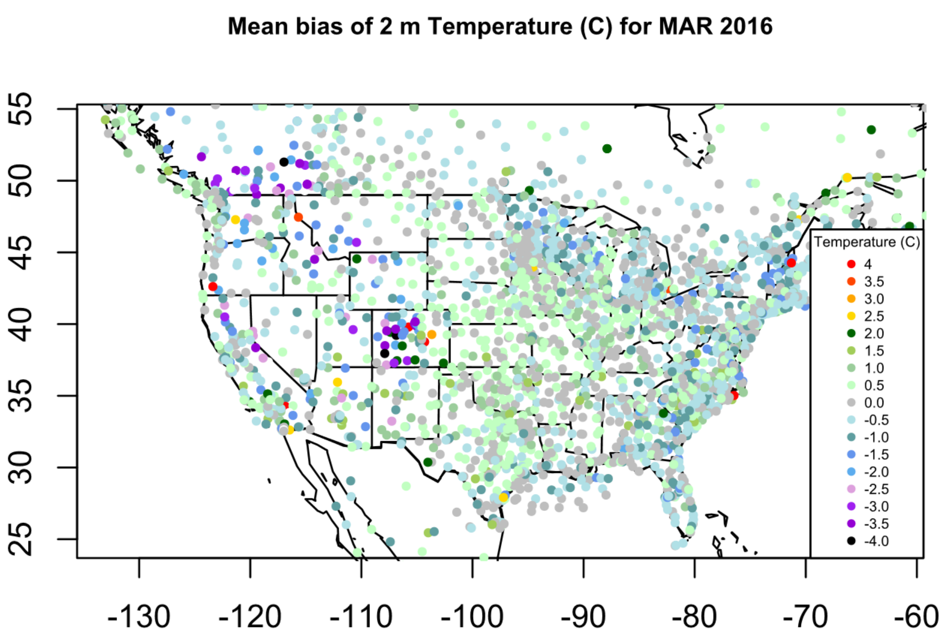

Figure 3-32: Mean Bias of Temperature for March 2016

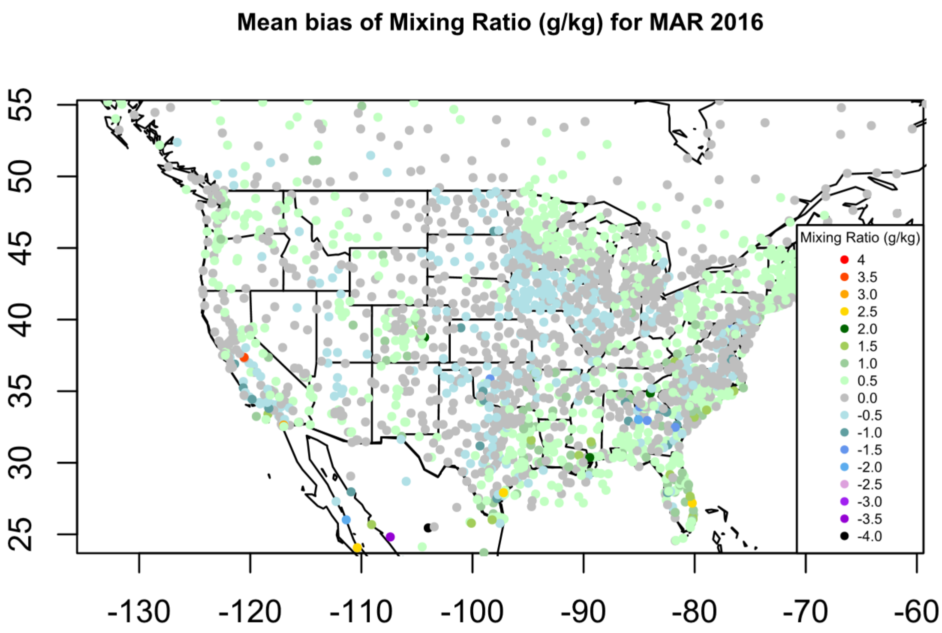

Figure 3-33: Mean Bias of Mixing Ratio for March 2016

3.4.4 March Accumulated Precipitation

Patterns of precipitation for March generally matched observations. WRF predicted heavy accumulations between Houston and Beaumont and in central Arkansas as shown in Figure 3-34: *WRF Accumulate Precipitation for March 2016*. The PRISM data showed eastern Texas, Arkansas, and northern Louisiana to have comparable magnitudes over a larger area as shown in Figure 3-35: *PRISM Accumulated Monthly Precipitation for March 2016*.

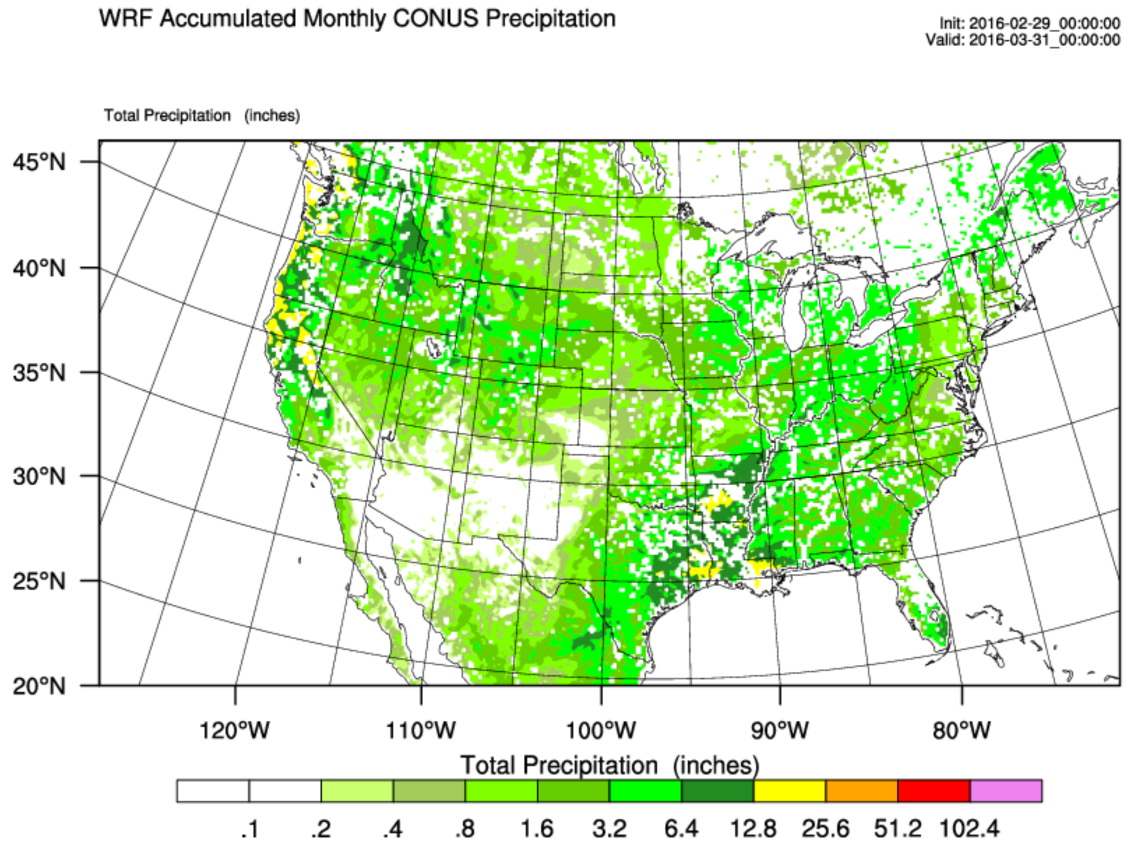

Figure 3-34: WRF Accumulate Precipitation for March 2016

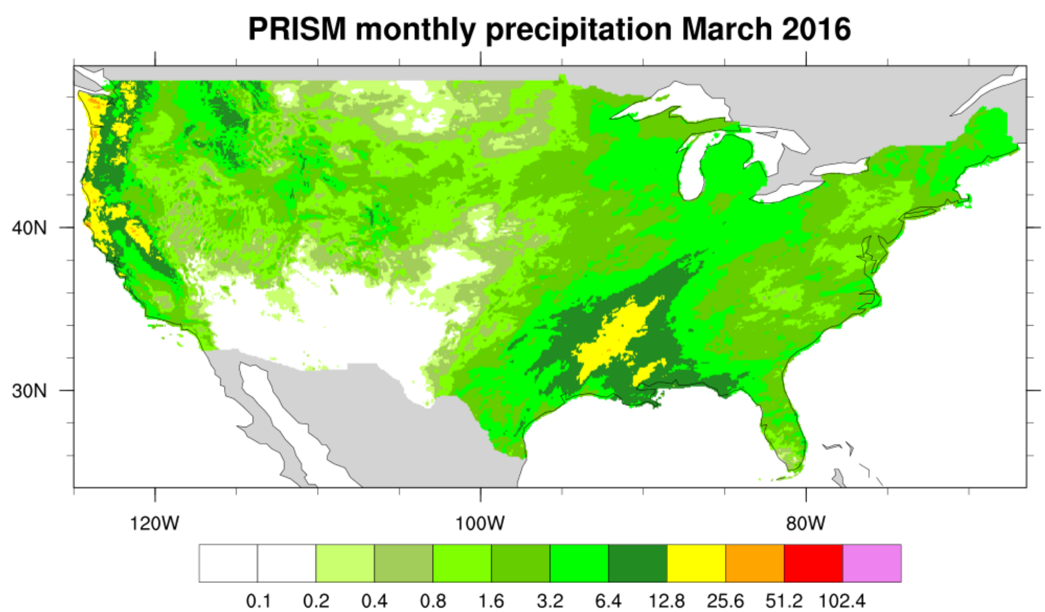

Figure 3-35: PRISM Accumulated Monthly Precipitation for March 2016

3.5 WRF APRIL PERFORMANCE

Time series for wind speed and direction are good for both CONUS and the south-central region as shown in Figure 3-36: *WRF CONUS Wind Performance for April 2016*, Figure 3-39: *WRF South-Central Region Wind Performance for April 2016*, and Figure 3-42: *Mean Bias of Wind Speed for April 2016*. Nocturnal biases in temperature are generally lower than observed in March as shown in Figure 3-37: *WRF CONUS Temperature Performance for April 2016*, Figure 3-40: *WRF South-Central Region Temperature Performance for April 2016*, and Figure 3-43: *Mean Bias of Temperature for April*. Humidity performance is good as shown in Figure 3-38: *WRF CONUS Humidity Performance for April 2016*, Figure 3-41: *WRF South-Central Region Humidity Performance for April 2016*, and Figure 3-44: *Mean Bias of Mixing Ratio for April 2016*.

3.5.1 CONUS April Timeseries

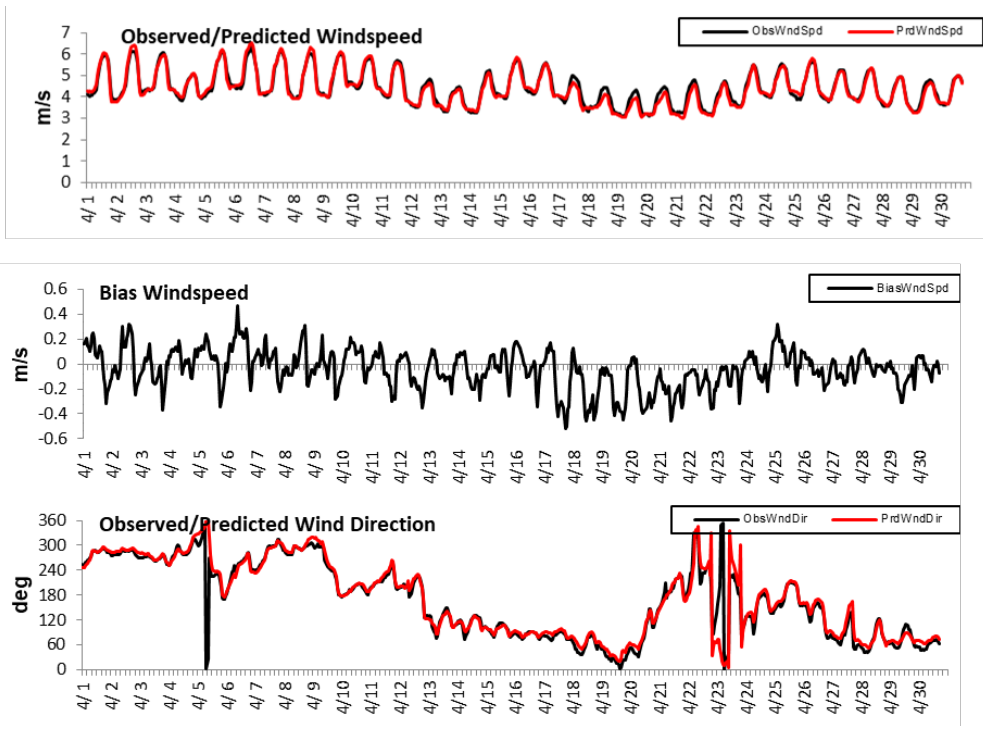

Figure 3-36: WRF CONUS Wind Performance for April 2016

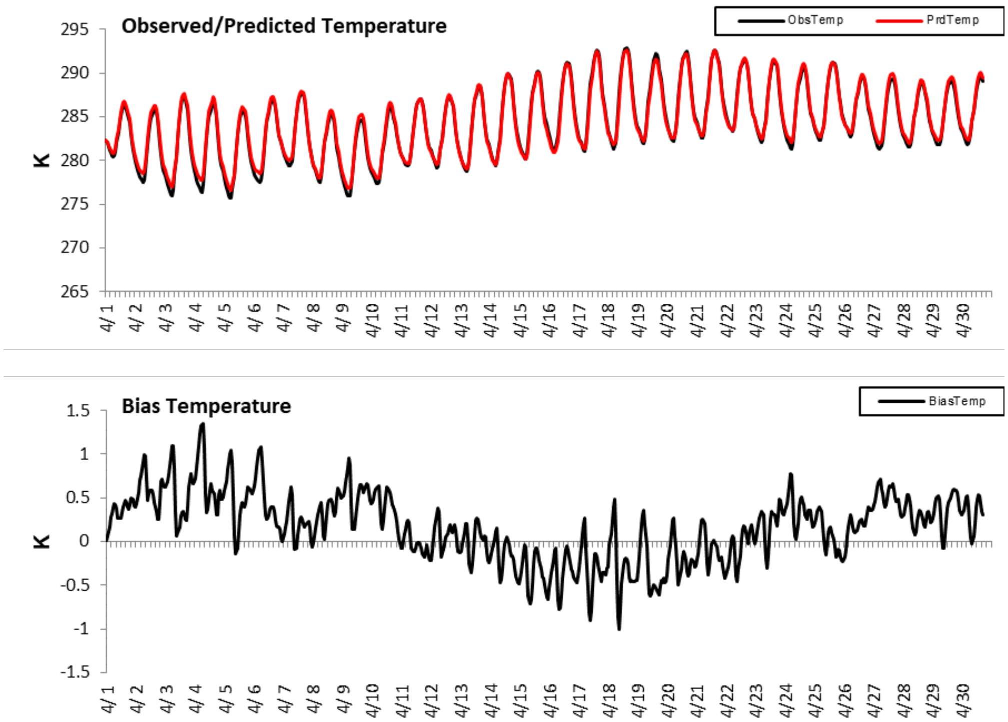

Figure 3-37: WRF CONUS Temperature Performance for April 2016

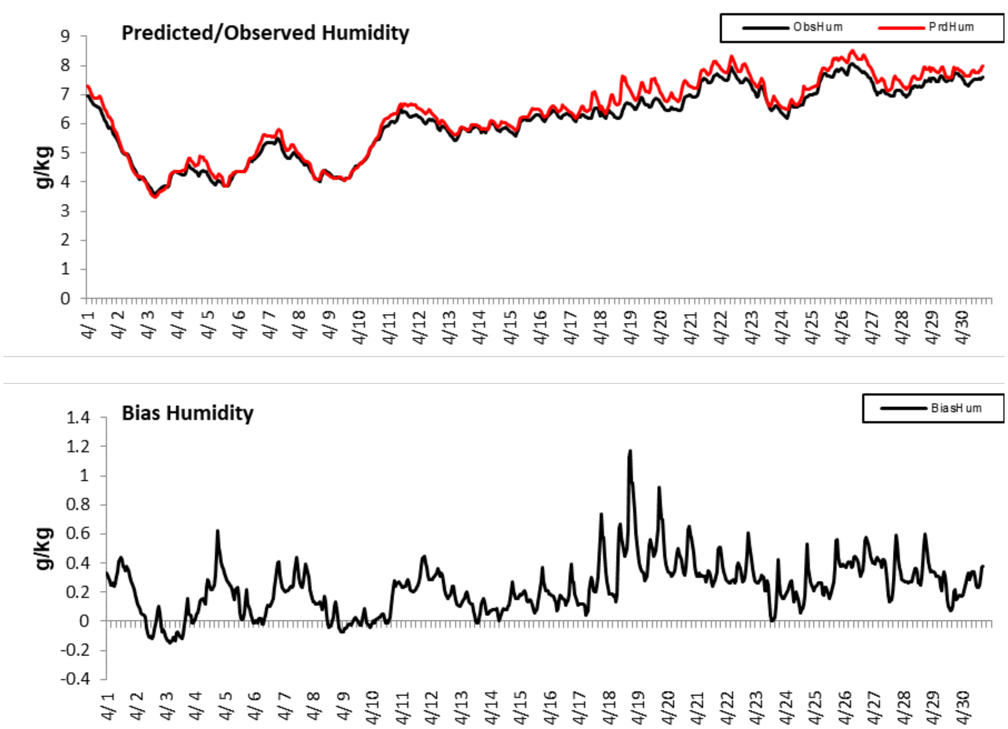

Figure 3-38: WRF CONUS Humidity Performance for April 2016

3.5.2 South-Central Region April Timeseries

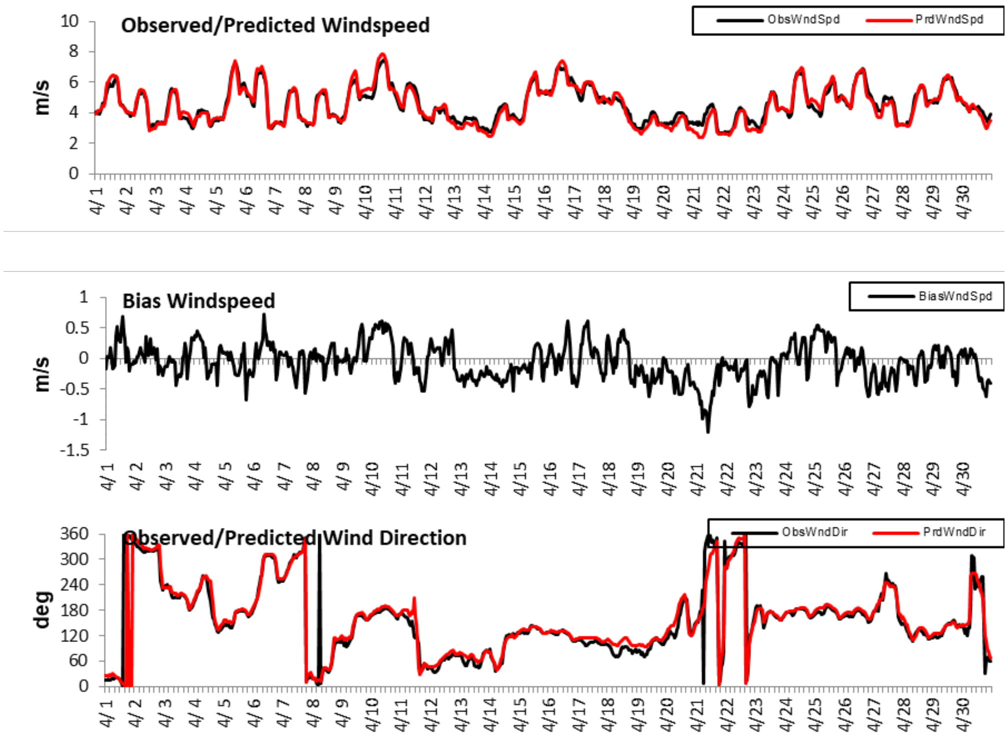

Figure 3-39: WRF South-Central Region Wind Performance for April 2016

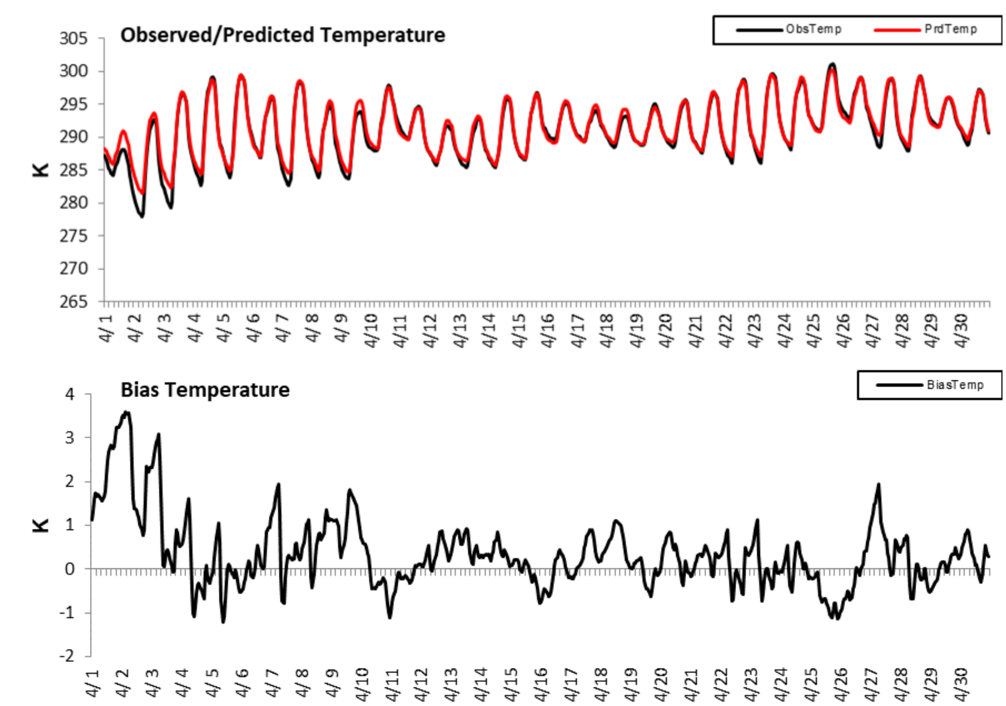

Figure 3-40: WRF South-Central Region Temperature Performance for April 2016

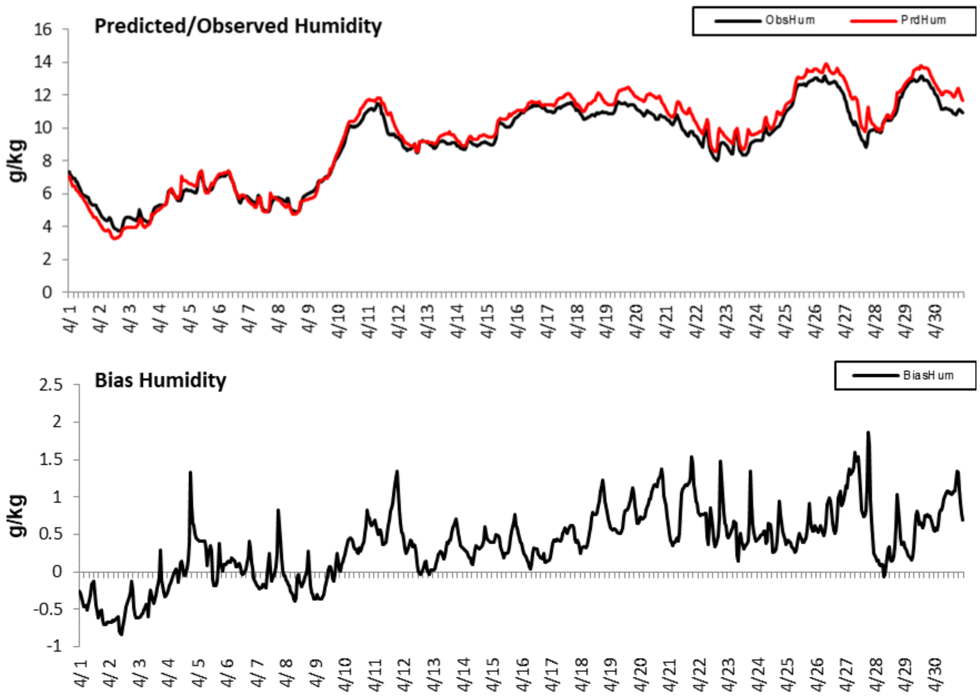

Figure 3-41: WRF South-Central Region Humidity Performance for April 2016

3.5.3 April Spatial Bias Plots

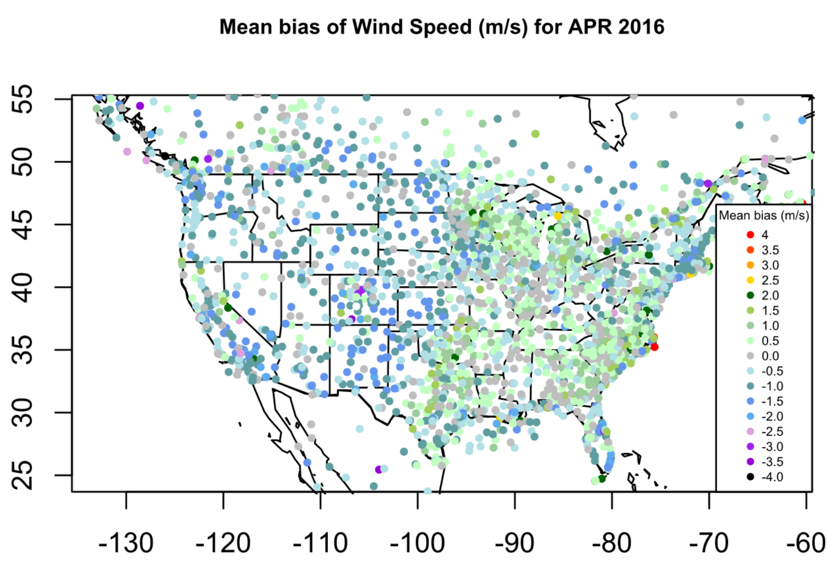

Figure 3-42: Mean Bias of Wind Speed for April 2016

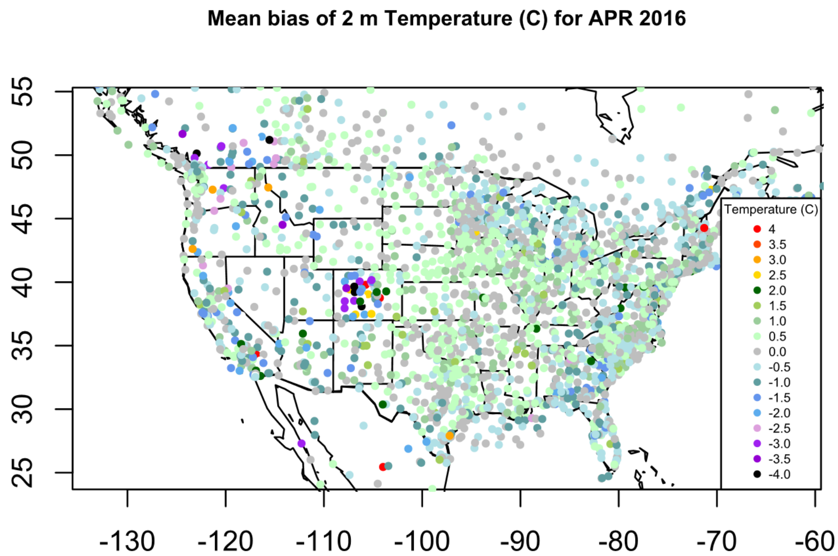

Figure 3-43: Mean Bias of Temperature for April

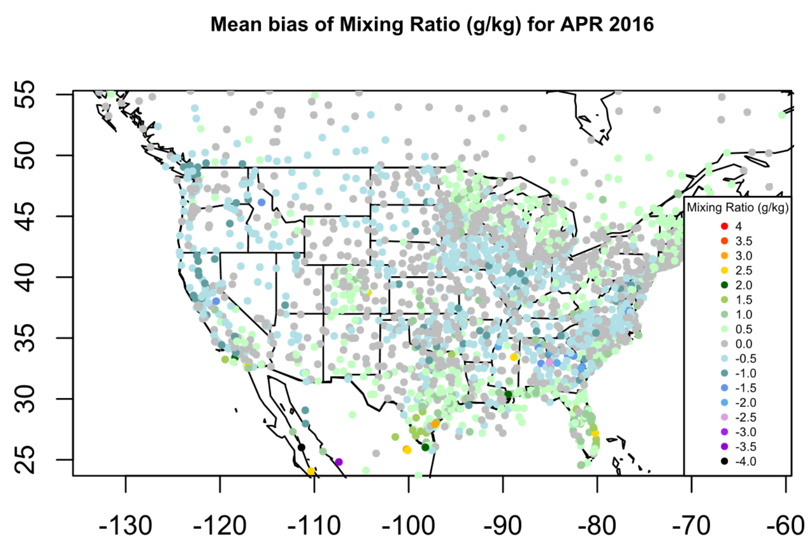

Figure 3-44: Mean Bias of Mixing Ratio for April 2016

3.5.4 April Accumulated Precipitation

April has some discrepancies in accumulated precipitation. Although patterns are reasonable, WRF (Figure 3-45: *WRF Accumulated Precipitation for April 2016*) under predicts measured rainfall amounts (Figure 3-46: *PRISM Accumulated Precipitation for April 2016*) in eastern Oklahoma, Arkansas, and portions of Louisiana.

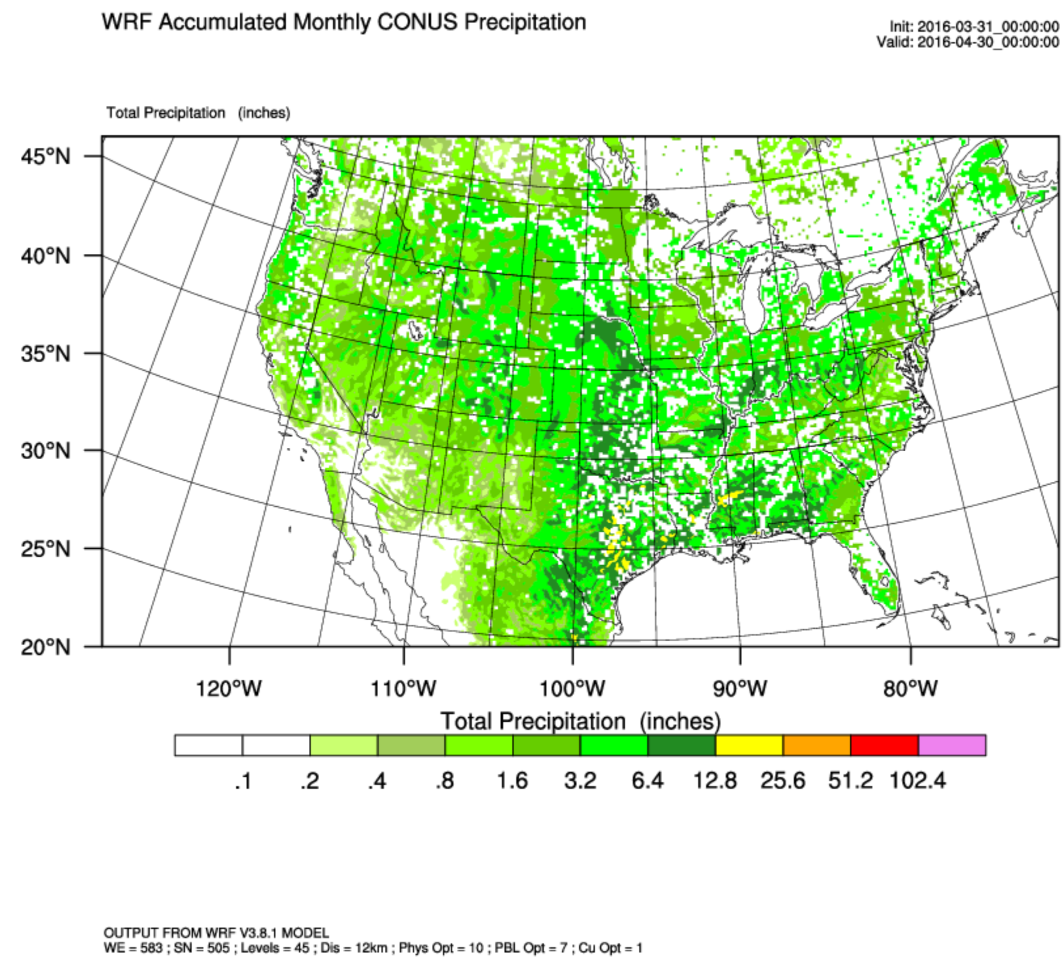

Figure 3-45: WRF Accumulated Precipitation for April 2016

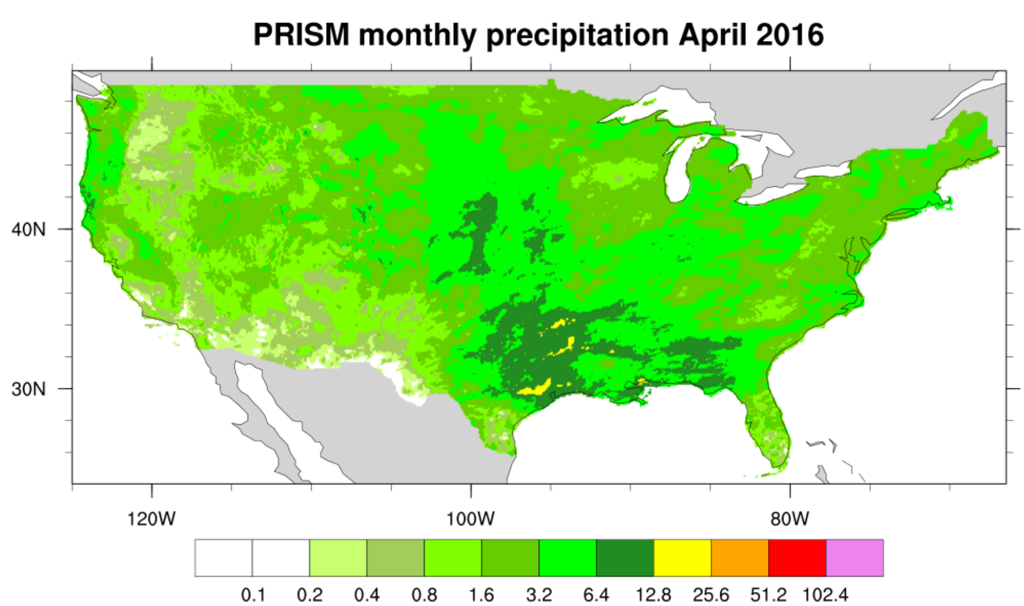

Figure 3-46: PRISM Accumulated Precipitation for April 2016

3.6 WRF MAY PERFORMANCE

Wind speed performance is good across the CONUS and the south-central region as shown in Figure 3-47: *WRF CONUS Wind Performance for May 2016* and Figure 3-50: *WRF South-Central Region Wind Performance for May 2016*. Although temperature biases are lower across the CONUS than during the winter months (Figure 3-48: *WRF CONUS Temperature Performance for May 2016*), across the smaller south-central region, Figure 3-51: *WRF South-Central Region Temperature Performance for May 2016* shows periods of nocturnal bias during cooler periods of the month. Nocturnal humidity has a high bias during the May on the CONUS and the south-central region, as can be seen in Figure 3-49: *WRF CONUS Humidity Performance for May 2016* and Figure 3-52: *WRF South-Central Region Humidity Performance for May 2016.*

3.6.1 CONUS May Timeseries

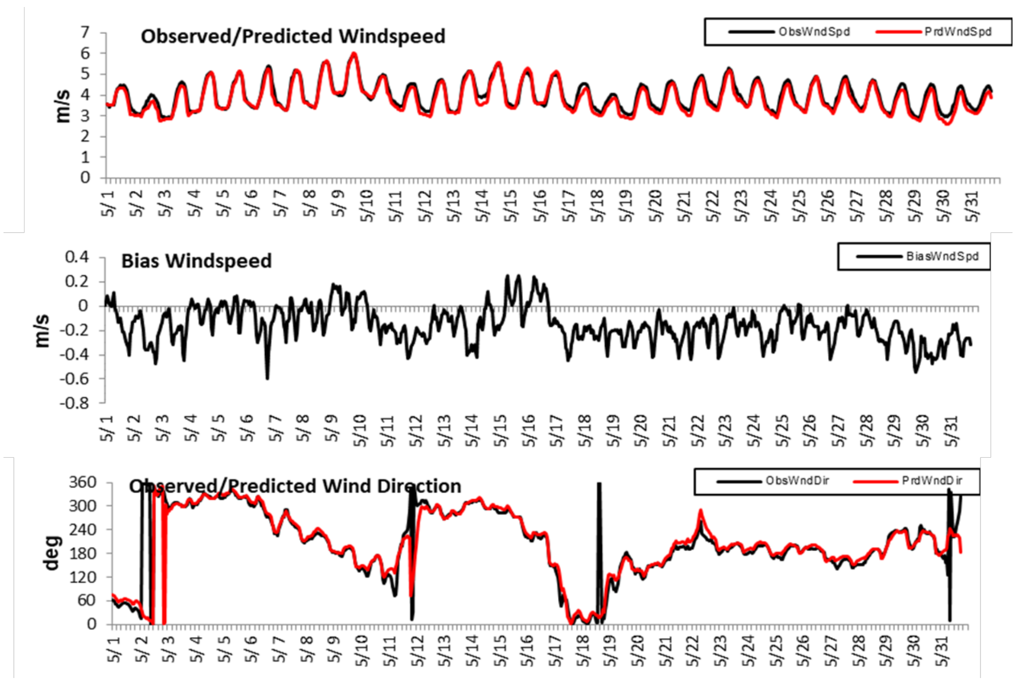

Figure 3-47: WRF CONUS Wind Performance for May 2016

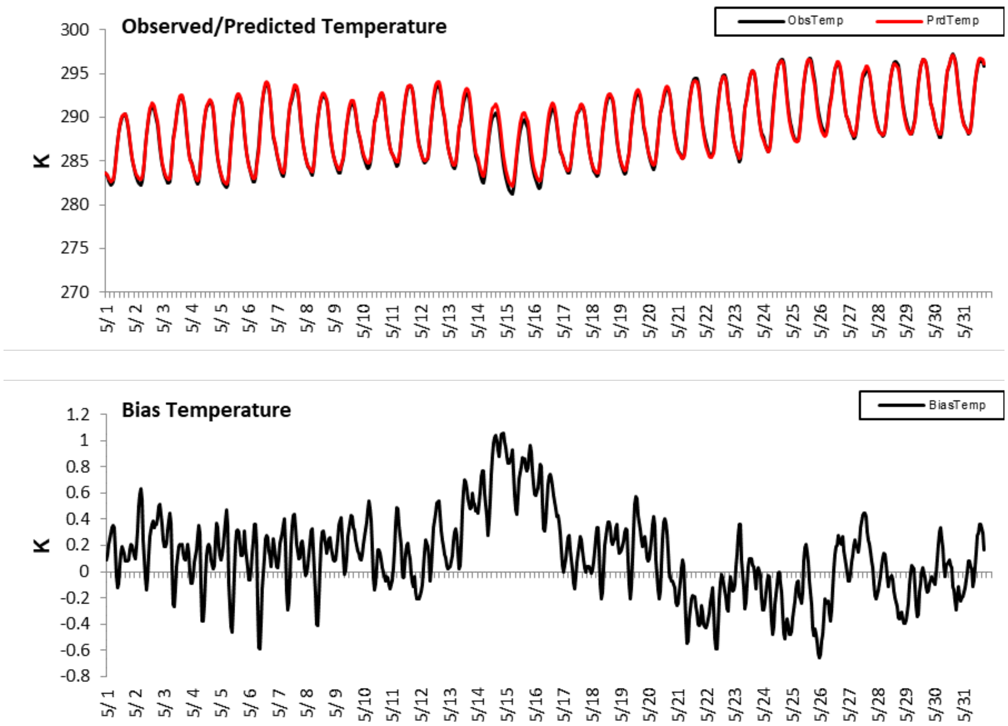

Figure 3-48: WRF CONUS Temperature Performance for May 2016

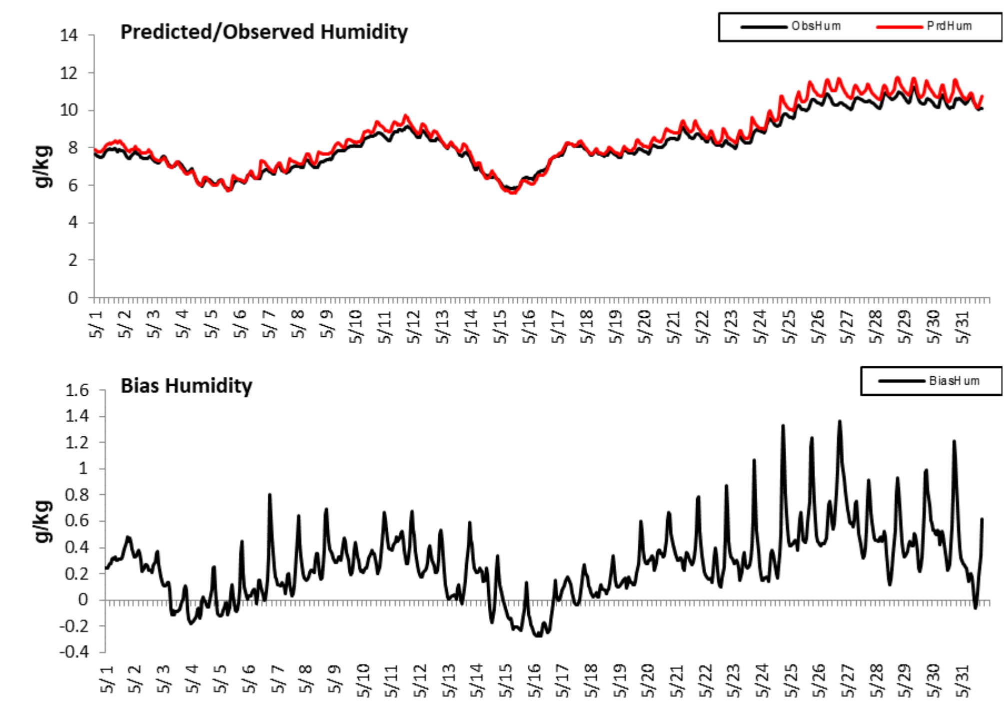

Figure 3-49: WRF CONUS Humidity Performance for May 2016

3.6.2 South-Central Region May Timeseries

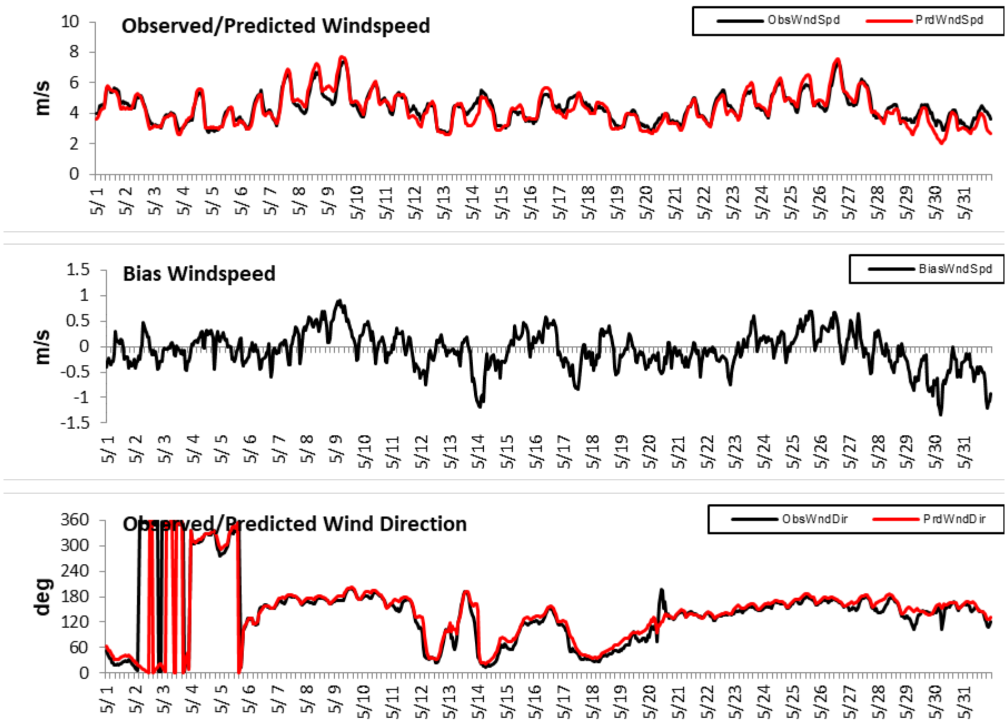

Figure 3-50: WRF South-Central Region Wind Performance for May 2016

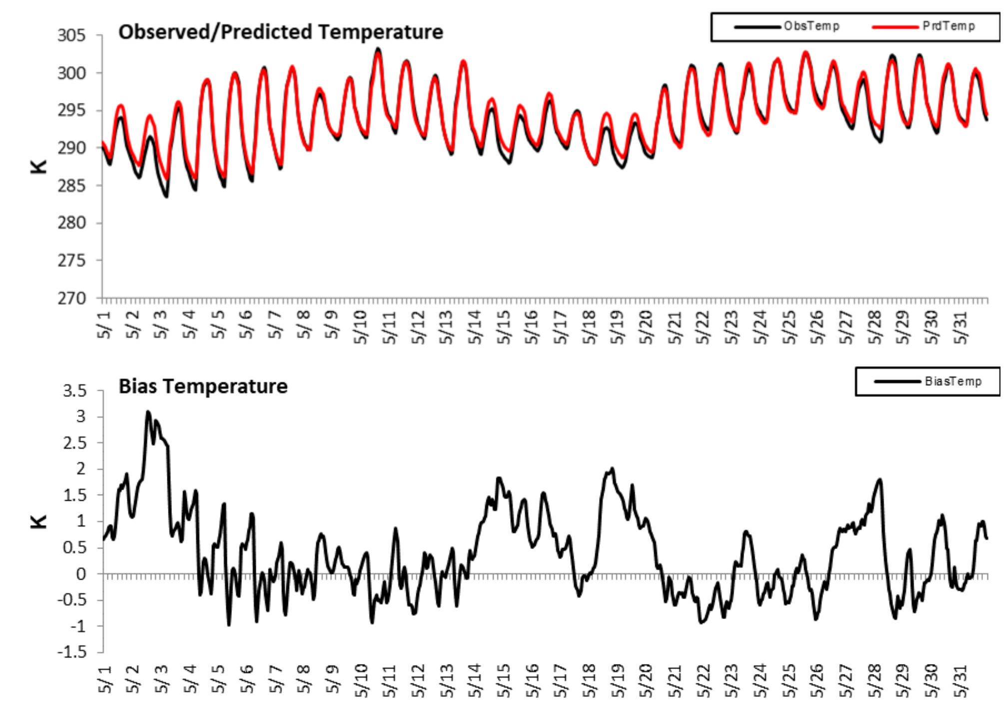

Figure 3-51: WRF South-Central Region Temperature Performance for May 2016

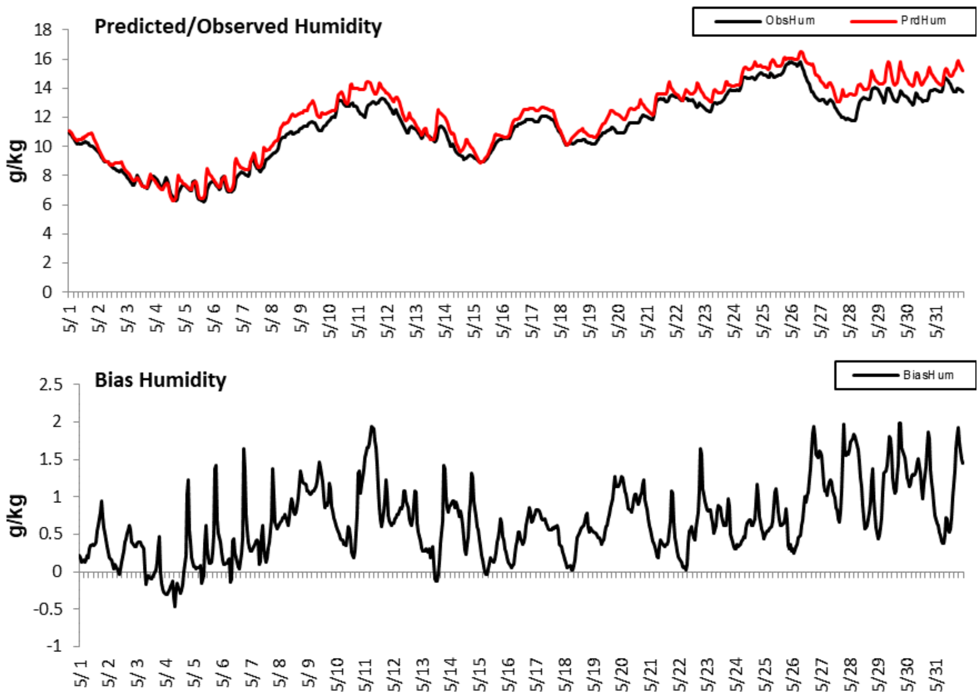

Figure 3-52: WRF South-Central Region Humidity Performance for May 2016

3.6.3 May Spatial Bias Plots

Portions of central Texas and southern Oklahoma have a positive wind speed bias of approximately 1.5 m/s as shown in Figure 3-53: *Mean Bias of Wind Speed for May 2016*. New Mexico again shows several sites with a negative wind speed bias. Otherwise, much of Texas and surrounding states have many sites with very little bias. Figure 3-54: *Mean Bias of Temperature for May 2016* shows most sites with good temperature performance, but some sites in central Texas, the south Texas coast, and along the Texas-Oklahoma border show noticeable high temperature biases. Figure 3-55: *Mean Bias of Mixing Ratio for May 2016* shows sites along the Red River and Rio Grande also having a high humidity bias.

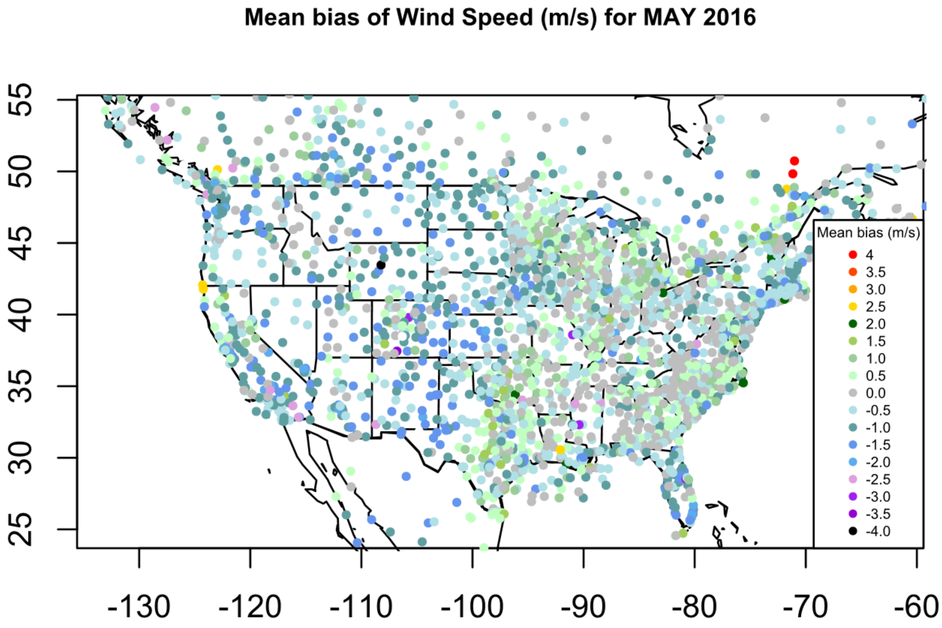

Figure 3-53: Mean Bias of Wind Speed for May 2016

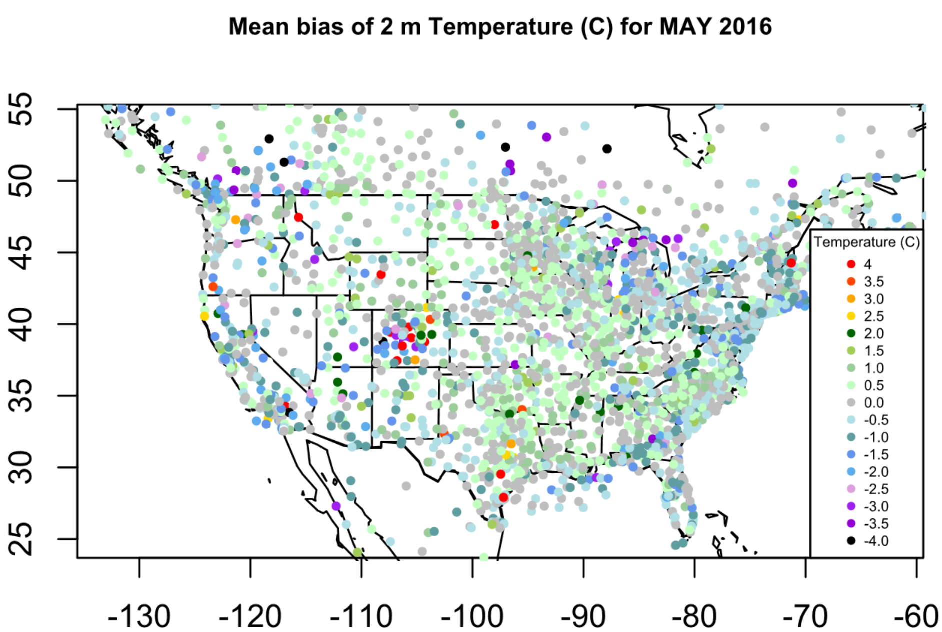

Figure 3-54: Mean Bias of Temperature for May 2016

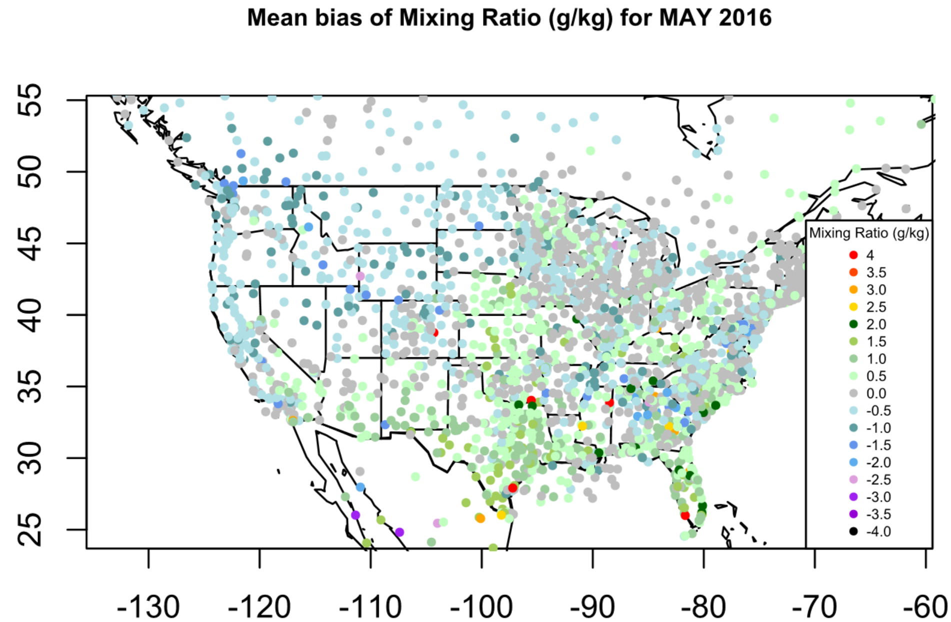

Figure 3-55: Mean Bias of Mixing Ratio for May 2016

3.6.4 May Accumulated Precipitation

WRF predicted precipitation (Figure 3-56: *WRF Accumulated Precipitation for May 2016*) was higher in Kansas and along the Texas coast than was reflected in the PRISM data (Figure 3-57: *PRISM Accumulated Precipitation for May 2016*). Otherwise, patterns of precipitation look broadly similar.

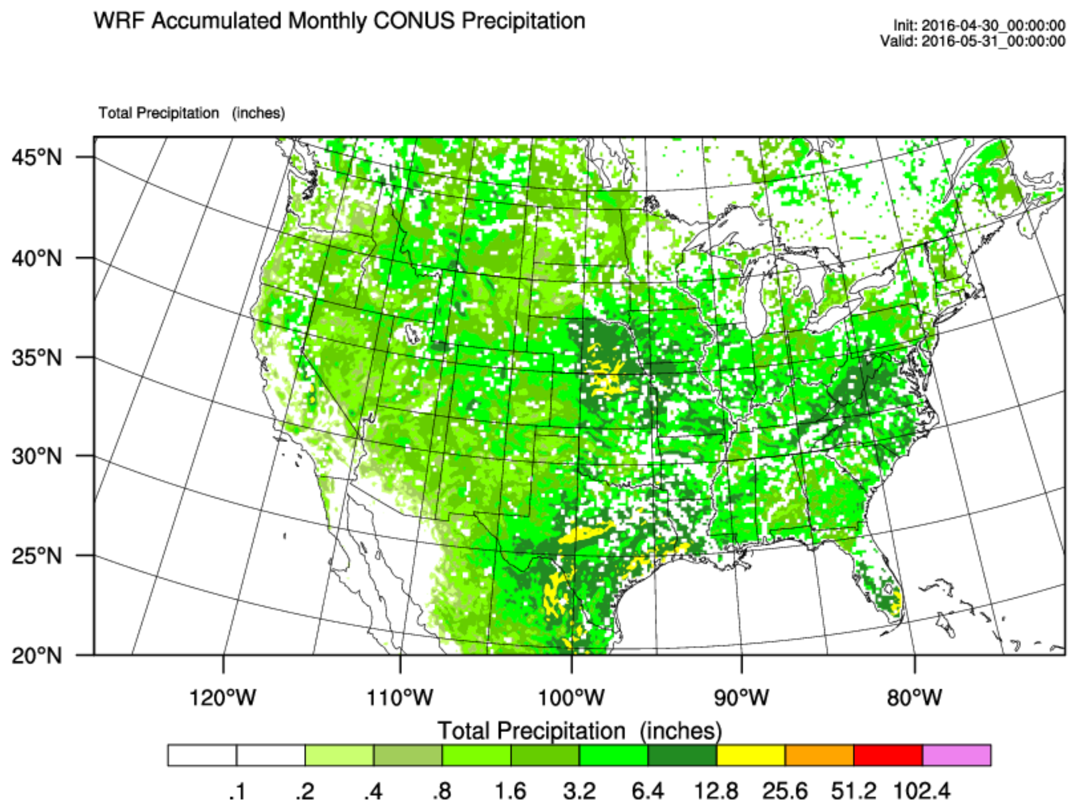

Figure 3-56: WRF Accumulated Precipitation for May 2016

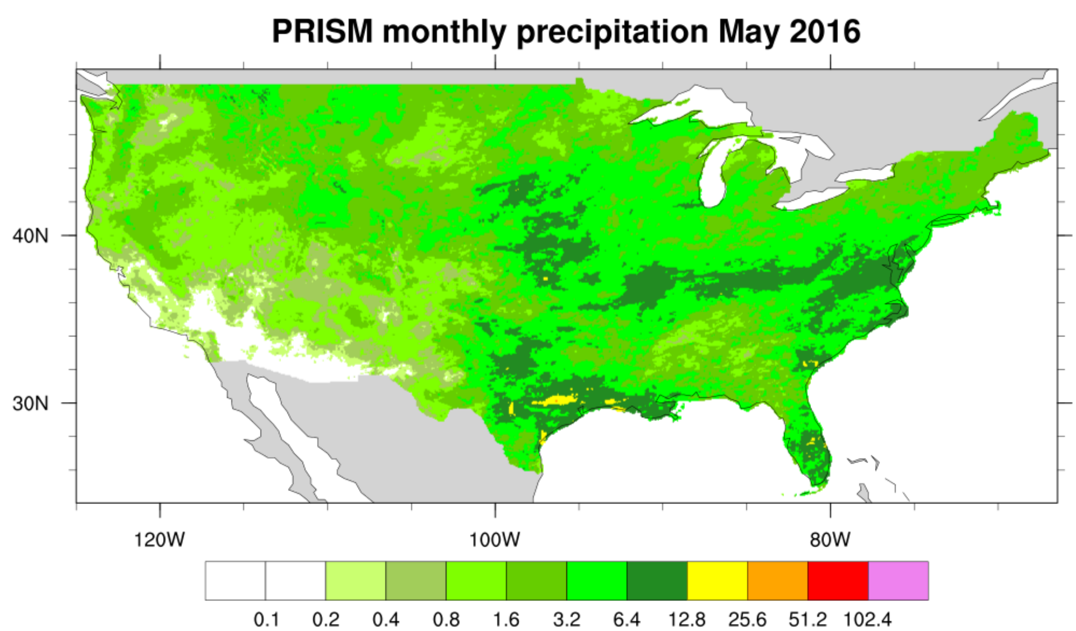

Figure 3-57: PRISM Accumulated Precipitation for May 2016

3.7 WRF JUNE PERFORMANCE

Although there is a persistent mild negative wind speed bias for June, as shown in Figure 3-58: *WRF CONUS Wind Performance for June 2016* and Figure 3-61: *WRF South-Central Region Performance for June 2016*, overall wind performance is good across the CONUS and the south-central region. Temperature performance is good as shown in Figure 3-59: *WRF CONUS Temperature Performance for June 2016* and Figure 3-62: *WRF South-Central Region Temperature Performance for June 2016*. A positive nocturnal humidity bias is observed across the CONUS, as seen in Figure 3-60: *WRF CONUS Humidity Performance for June 2016*, and in the south-central region, shown in Figure 3-63: *WRF South-Central Region Humidity Performance for June 2016*.

3.7.1 CONUS June Timeseries

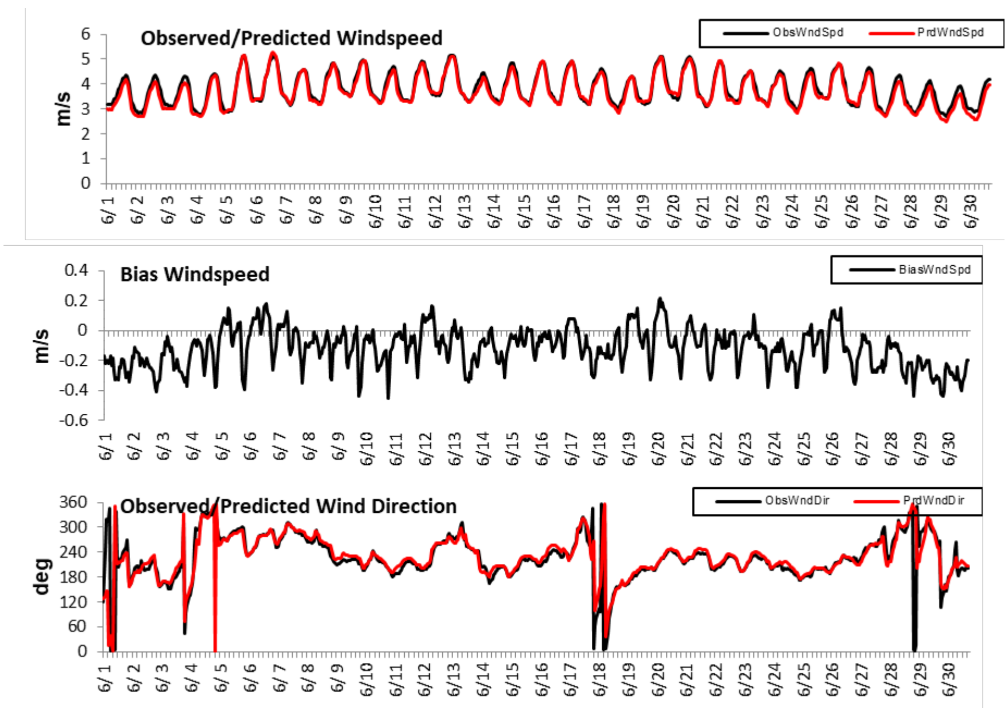

Figure 3-58: WRF CONUS Wind Performance for June 2016

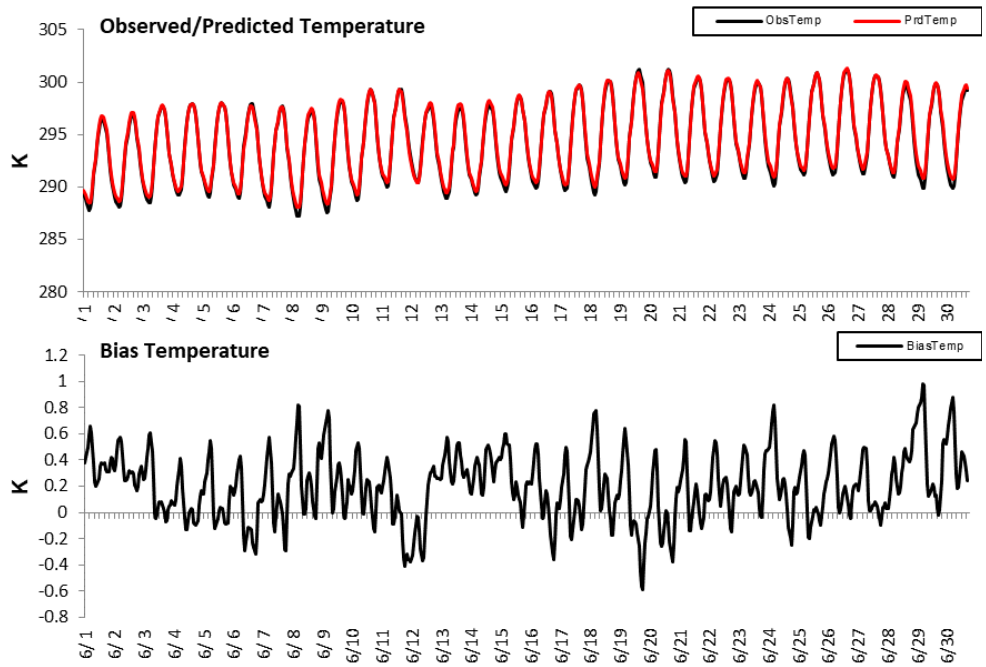

Figure 3-59: WRF CONUS Temperature Performance for June 2016

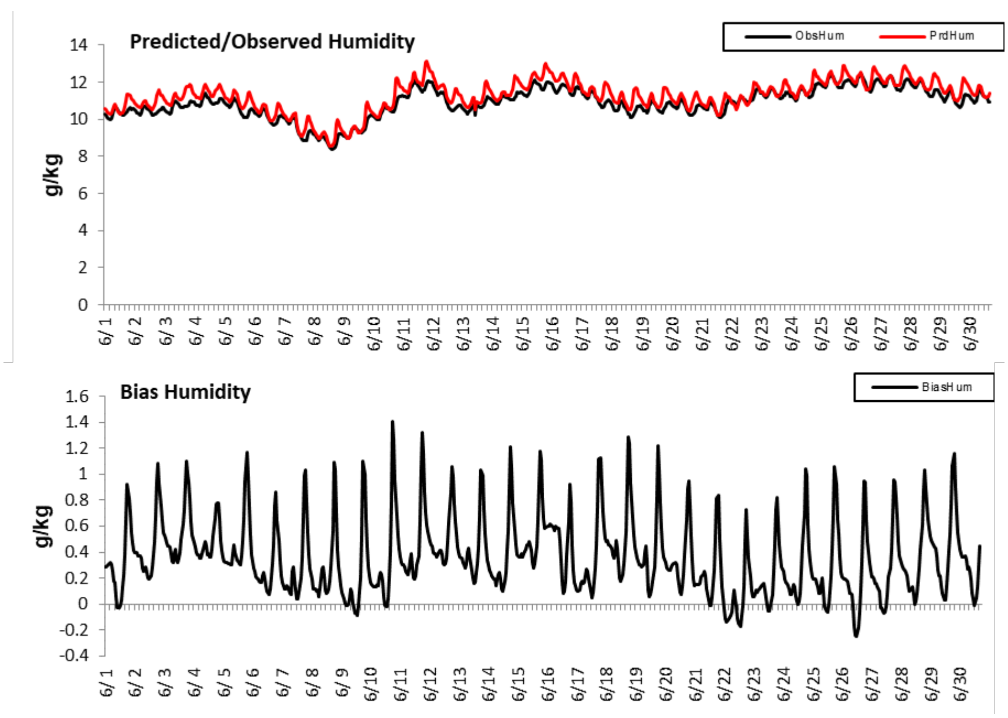

Figure 3-60: WRF CONUS Humidity Performance for June 2016

3.7.2 South-Central Region June Timeseries

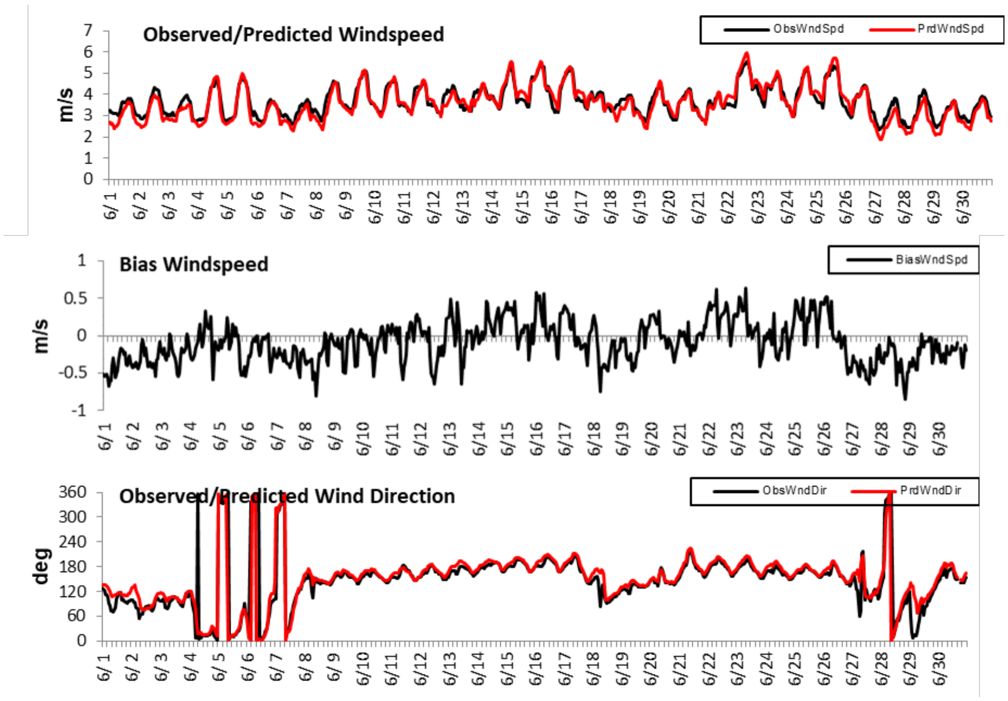

Figure 3-61: WRF South-Central Region Performance for June 2016

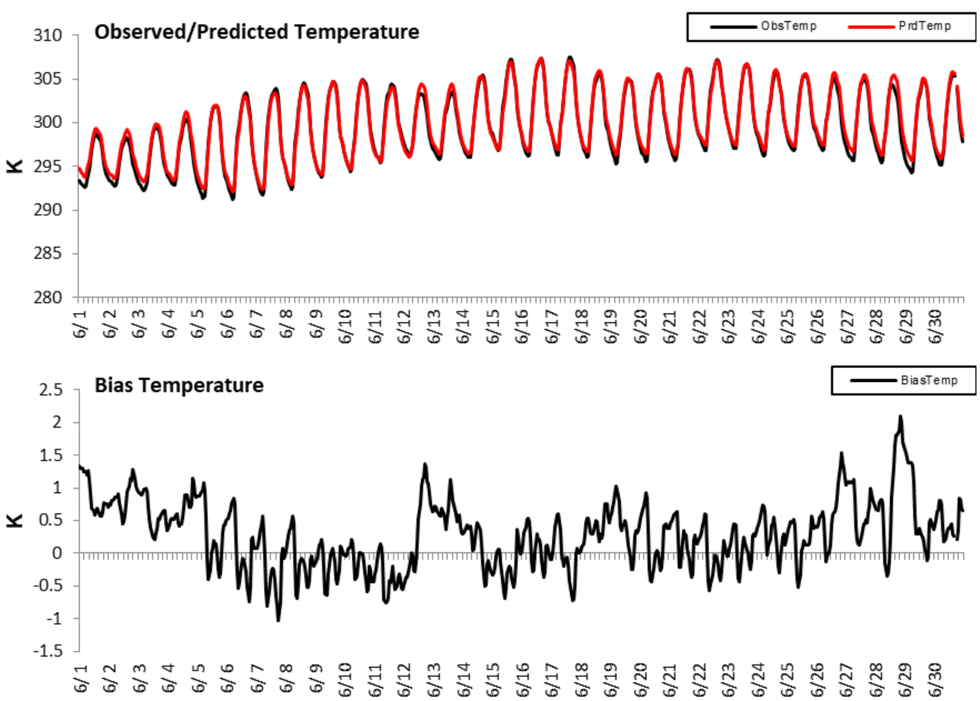

Figure 3-62: WRF South-Central Region Temperature Performance for June 2016

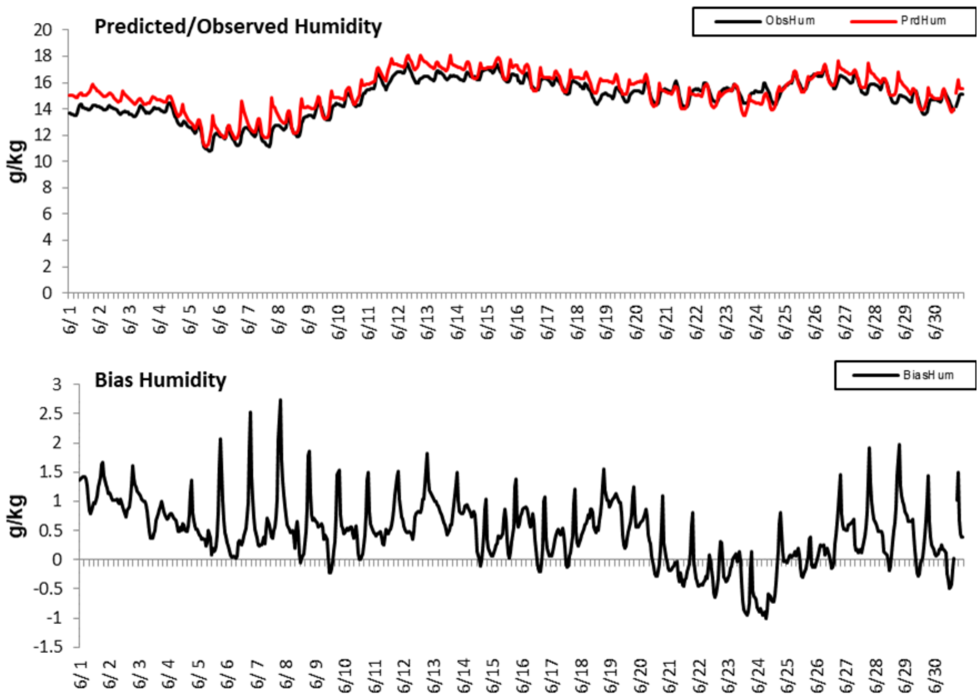

Figure 3-63: WRF South-Central Region Humidity Performance for June 2016

3.7.3 June Spatial Bias Plots

Generally, ds472 sites show good bias performance across the south-central region for June. However, a high wind speed bias at Guadalupe Mountains National Park is seen in Figure 3-64: *Mean Bias of Wind Speed for June 2016*, a high temperature biases occurs at one site along the south Texas coast as shown in Figure 3-65: *Mean Bias of Temperature for June 2016*, and high humidity biases are again seen along the Rio Grande border in south Texas and in southern New Mexico, shown in Figure 3-66: *Mean Bias of Mixing Ratio for June 2016*.

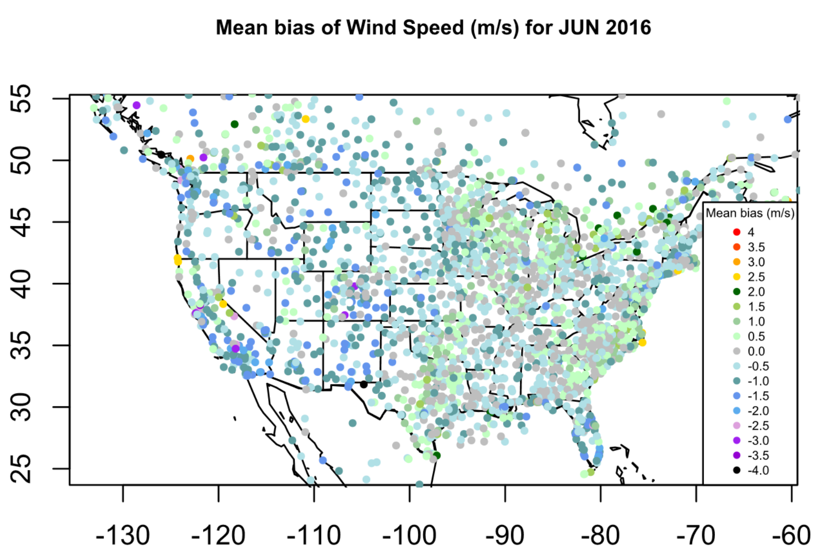

Figure 3-64: Mean Bias of Wind Speed for June 2016

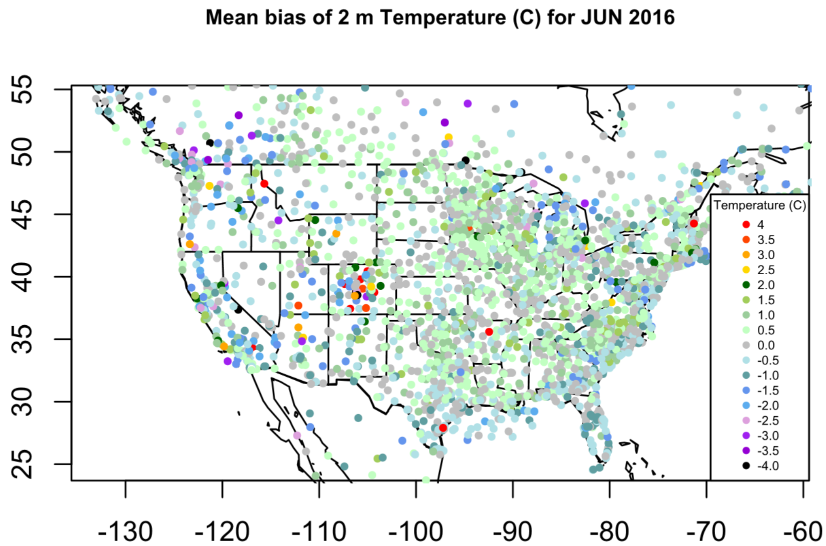

Figure 3-65: Mean Bias of Temperature for June 2016

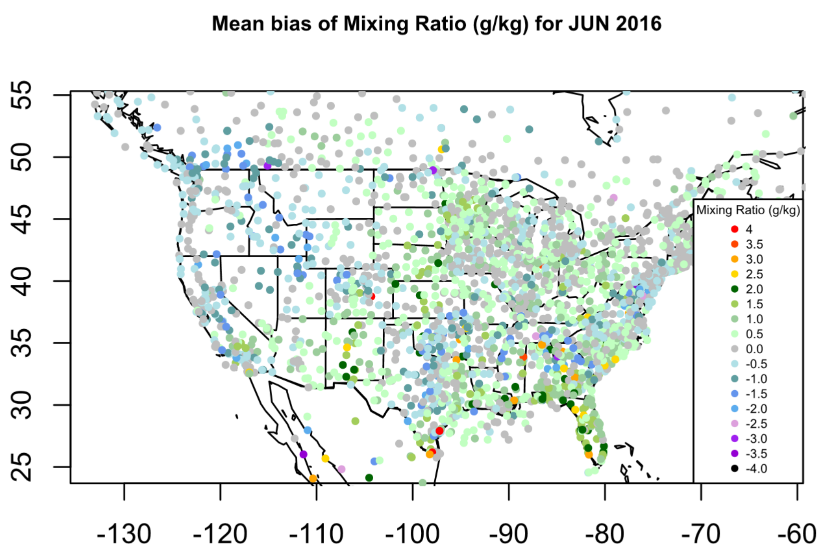

Figure 3-66: Mean Bias of Mixing Ratio for June 2016

3.7.4 June Accumulated Precipitation

Precipitation performance by WRF is reasonable for June. However, WRF predicted accumulations are higher in New Mexico and West Virginia, as shown in Figure 3-67: *WRF Accumulated Precipitation for June 2016*, compared to the PRISM data, as shown in Figure 3-68: *PRISM Accumulated Precipitation for June 2016*.

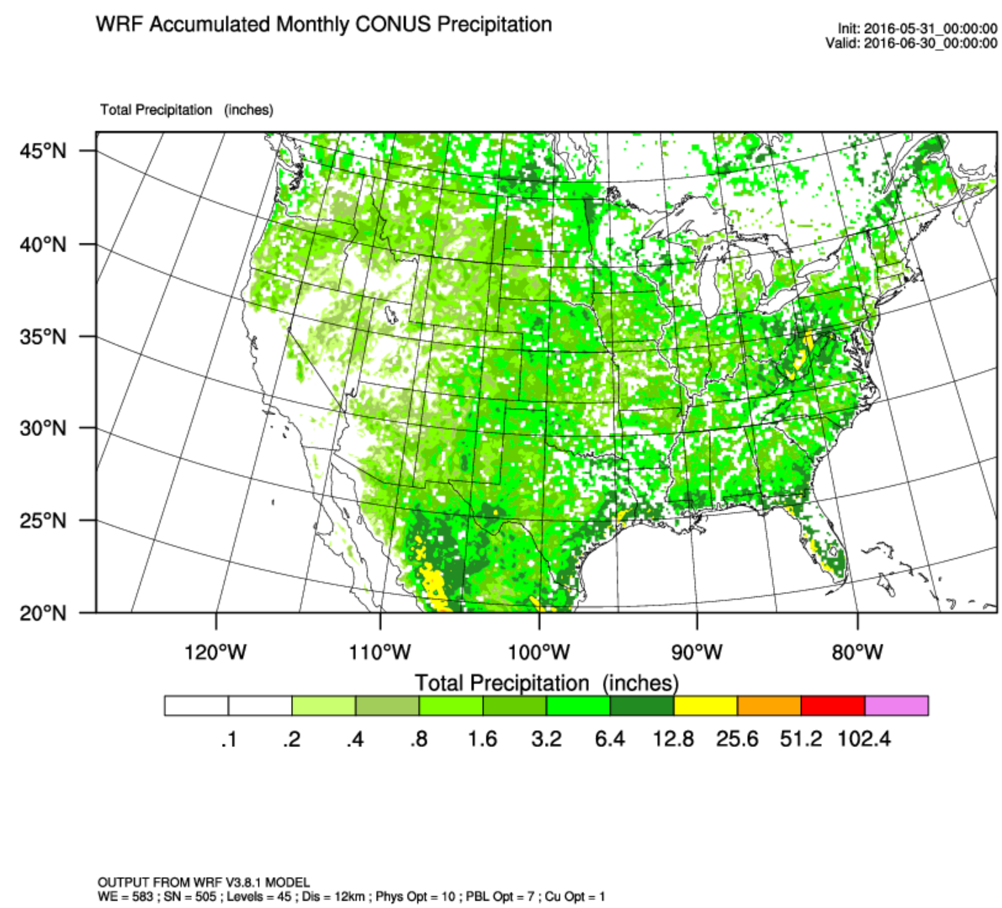

Figure 3-67: WRF Accumulated Precipitation for June 2016

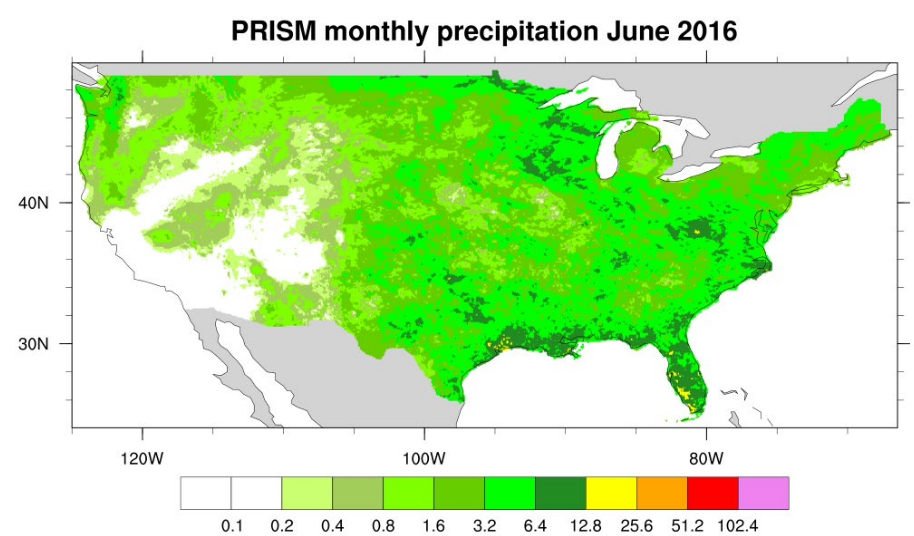

Figure 3-68: PRISM Accumulated Precipitation for June 2016

3.8 WRF JULY PERFORMANCE

Time series for winds (Figure 3-69: *WRF CONUS Wind Performance for July 2016* and Figure 3-72: *WRF South-Central Region Wind Performance for July 2016*), temperatures (Figure 3-70: *WRF CONUS Temperature Performance for July 2016* and Figure 3-73: *WRF South-Central Region Temperature Performance for July 2016*), and humidity (Figure 3-71: *WRF CONUS Humidity Performance for July 2016* and Figure 3-74: *WRF South-Central Region Humidity Performance for July 2016*)appear reasonable except for a brief transient error in WRF surface values on July 13.

3.8.1 CONUS July Timeseries

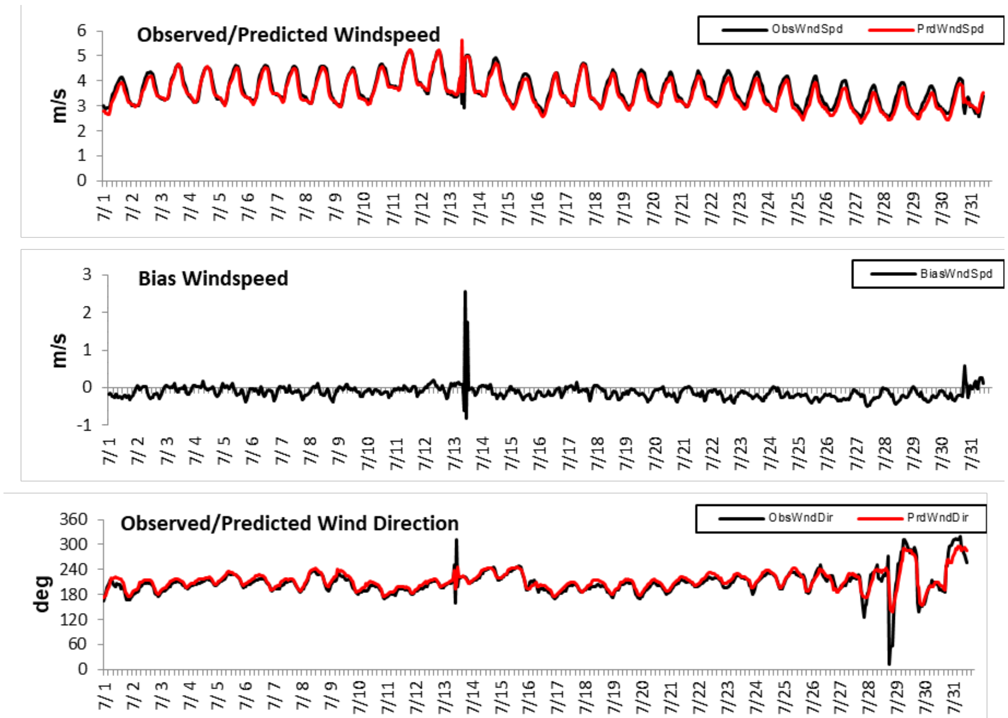

Figure 3-69: WRF CONUS Wind Performance for July 2016

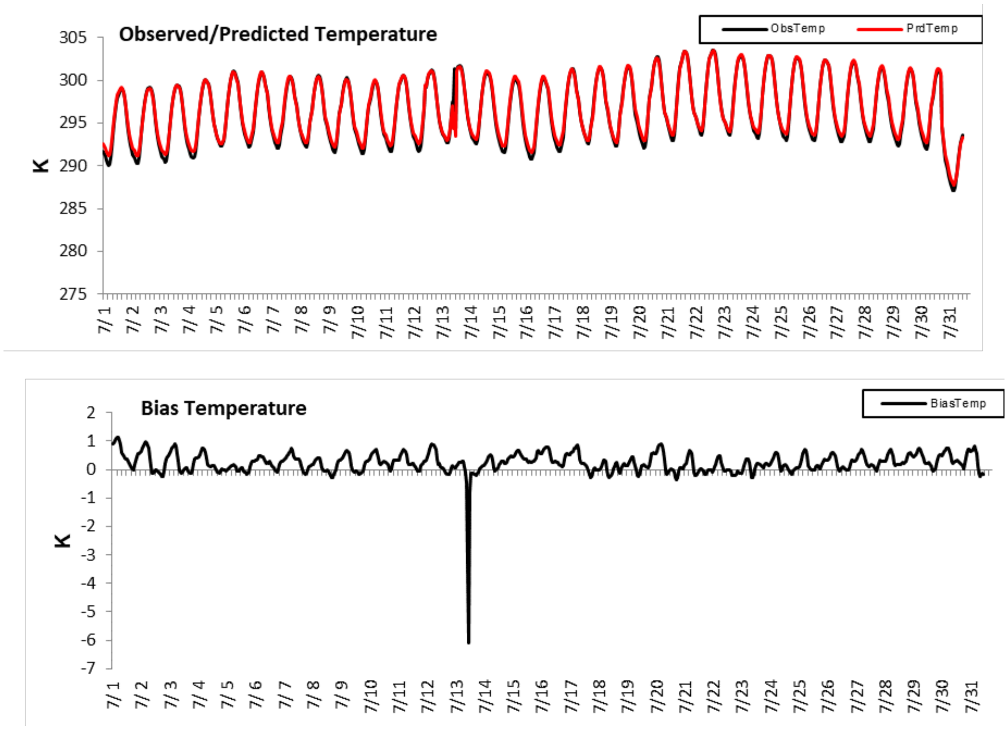

Figure 3-70: WRF CONUS Temperature Performance for July 2016

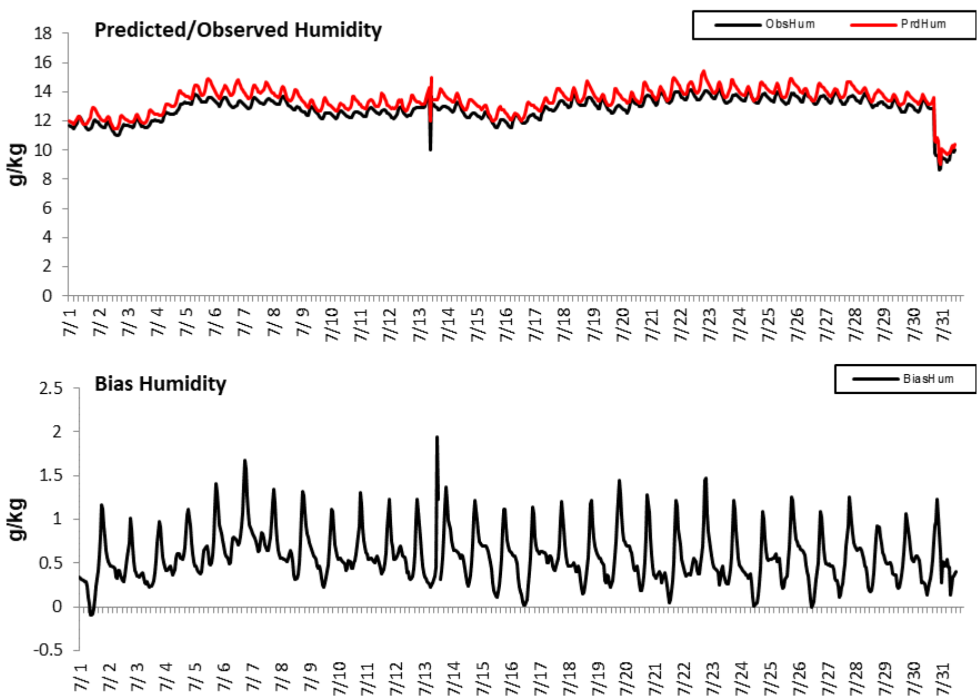

Figure 3-71: WRF CONUS Humidity Performance for July 2016

3.8.2 South-Central Region July Timeseries

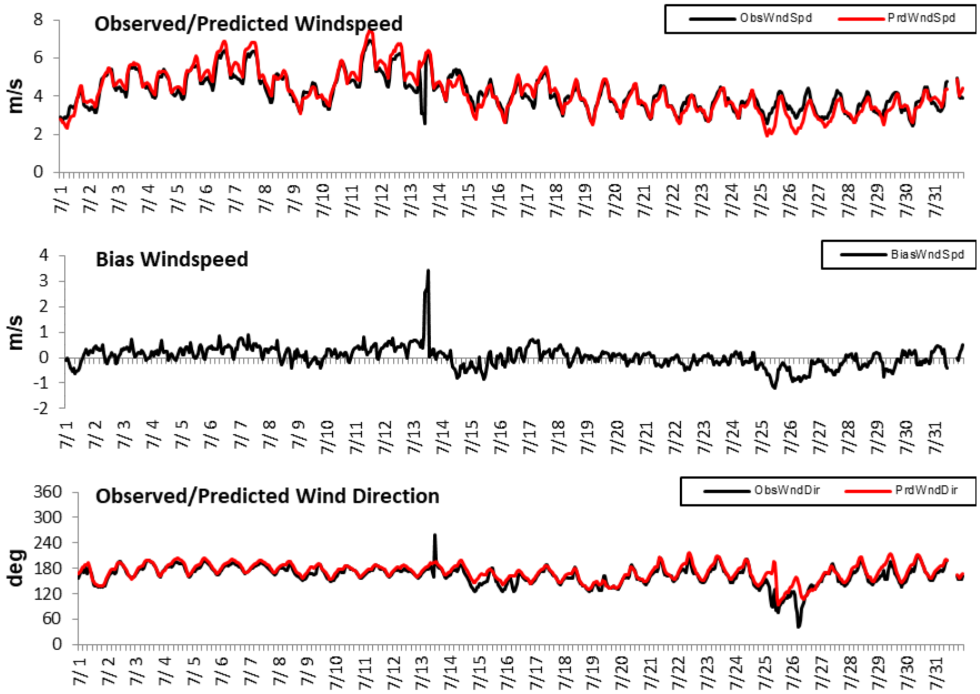

Figure 3-72: WRF South-Central Region Wind Performance for July 2016

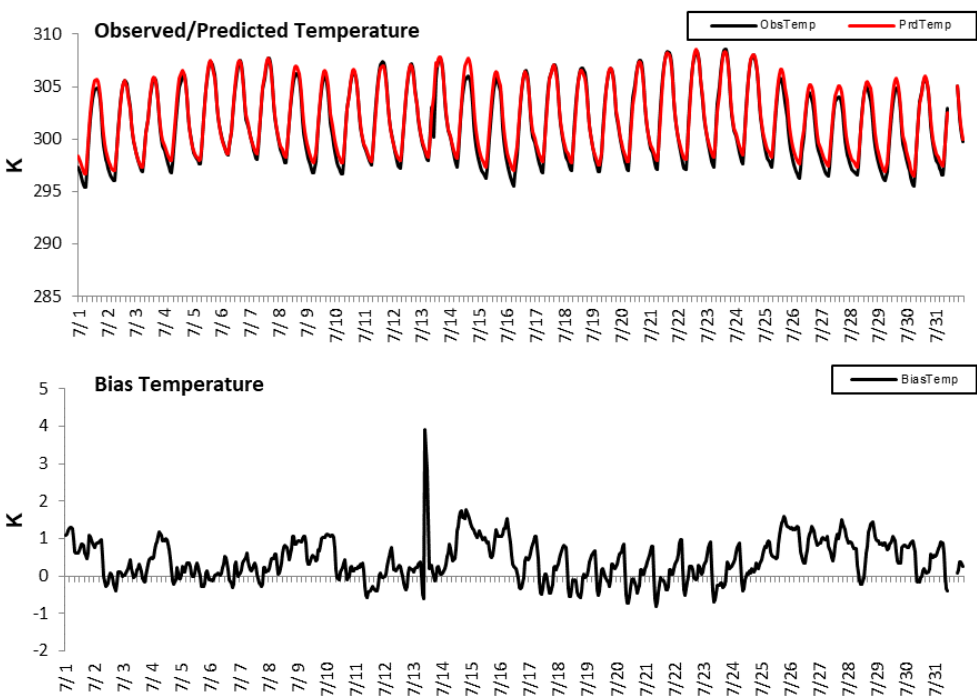

Figure 3-73: WRF South-Central Region Temperature Performance for July 2016

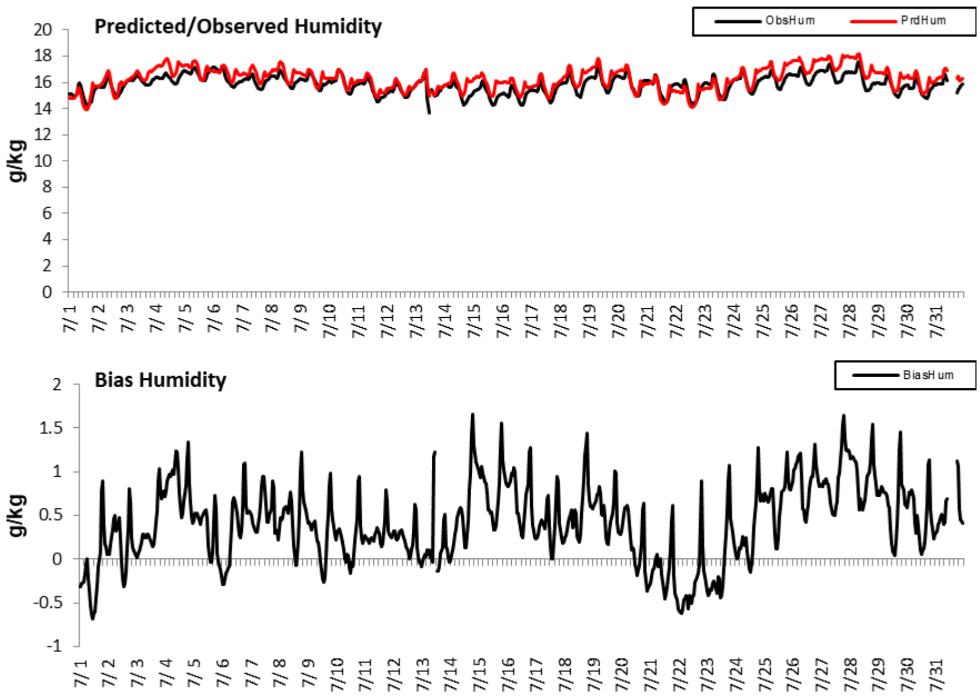

Figure 3-74: WRF South-Central Region Humidity Performance for July 2016

3.8.3 July Spatial Bias Plots

Except for a small number of sites in central Texas, wind speed biases throughout most of east Texas, Arkansas, and the Midwest, remained close to zero. Negative wind speed biases were predominant in the southwest as shown in Figure 3-75: *Mean Bias of Wind Speed for July 2016*. Temperature biases were low at sites throughout the south-central region as shown in Figure 3-76: *Mean Bias of Temperature for July 2016*. There was a modest positive bias for humidity in east Texas and Oklahoma, New Mexico, Arkansas, and Louisiana. The Wichita Mountains and parts of north and central Texas had a negative bias as shown in Figure 3-77: *Mean Bias of Mixing Ratio for July 2016*.

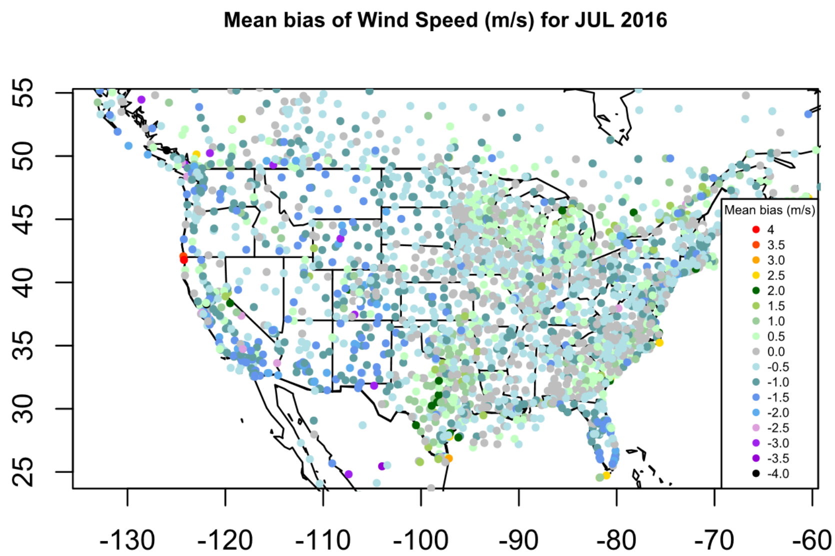

Figure 3-75: Mean Bias of Wind Speed for July 2016

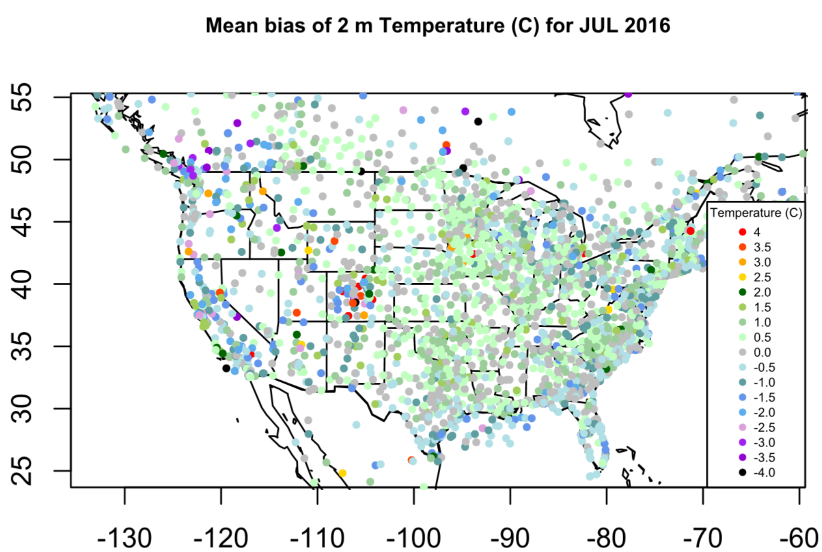

Figure 3-76: Mean Bias of Temperature for July 2016

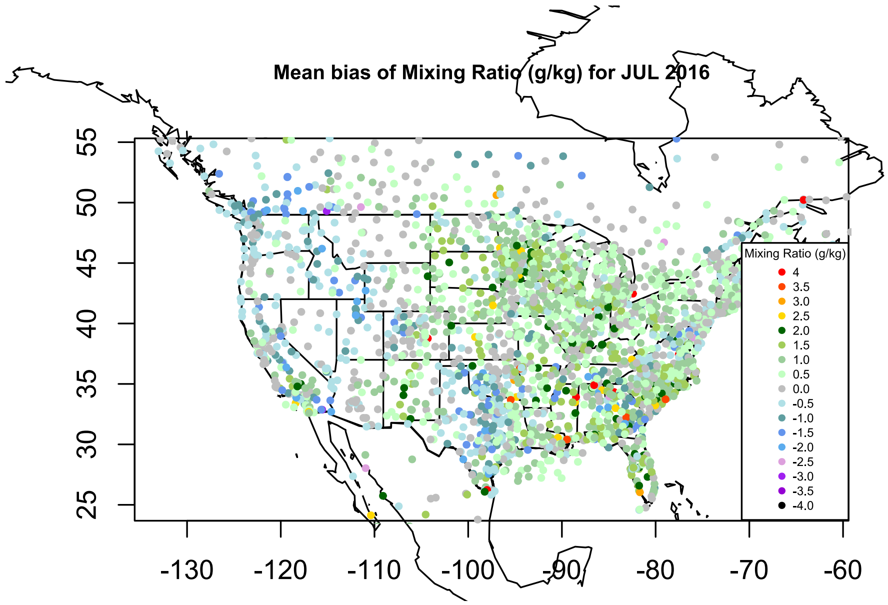

Figure 3-77: Mean Bias of Mixing Ratio for July 2016

3.8.4 July Accumulated Precipitation

PRISM data showed significant accumulation of precipitation in the east-central United States and in the Pacific northwest as depicted in Figure 3-79: *PRISM Accumulated Precipitation for July 2016*. This was not well captured in WRF as shown in Figure 3-78: *WRF Accumulated Precipitation for July 2016*; however, the dry areas of central Texas and the southwest are well represented.

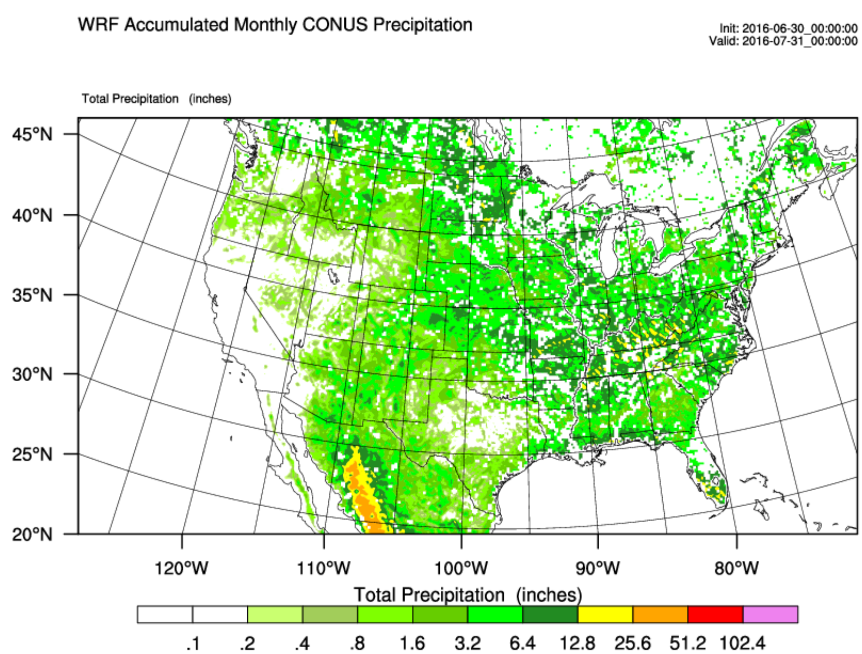

Figure 3-78: WRF Accumulated Precipitation for July 2016

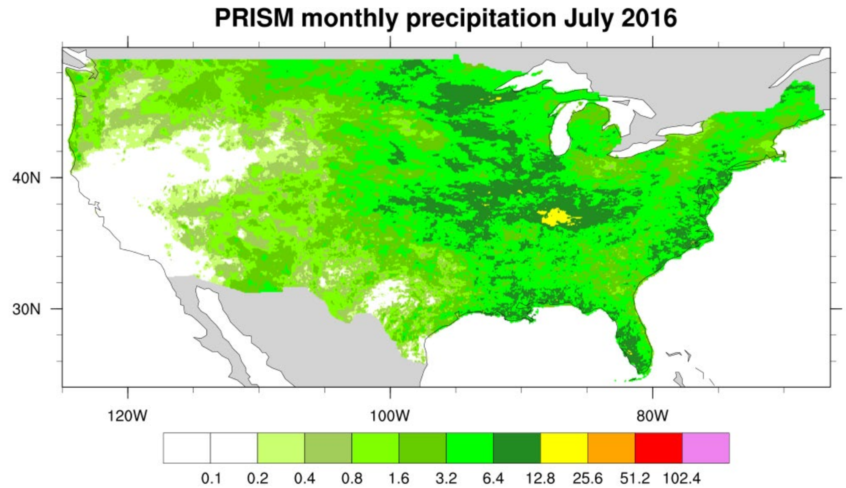

Figure 3-79: PRISM Accumulated Precipitation for July 2016

3.9 WRF AUGUST PERFORMANCE

Wind speed and direction show good performance during August. The average wind speed bias is approximately -0.2 m/s as shown in Figure 3-80: *WRF CONUS Wind Performance for August 2016* and Figure 3-83: *WRF South-Central Region Wind Performance for August 2016*. Temperatures across the country have a strong diurnal bias pattern from consistent nocturnal overprediction, but the bias averages about 0.5 degrees Celsius for the month as shown in Figure 3-81: *WRF CONUS Temperature Performance for August 2016* and Figure 3-84: *WRF South-Central Region Temperature Performance for August 2016*. Humidity also has a persistent positive bias of about 1.0 g/kg as shown in Figure 3-82: *WRF CONUS Humidity Performance for August 2016* and Figure 3-85: *WRF South-Central Region Humidity Performance for August 2016*. However, both can be viewed as acceptable when averaged across the month by meeting the model performance benchmarks of Table 3-1.

3.9.1 CONUS August Timeseries

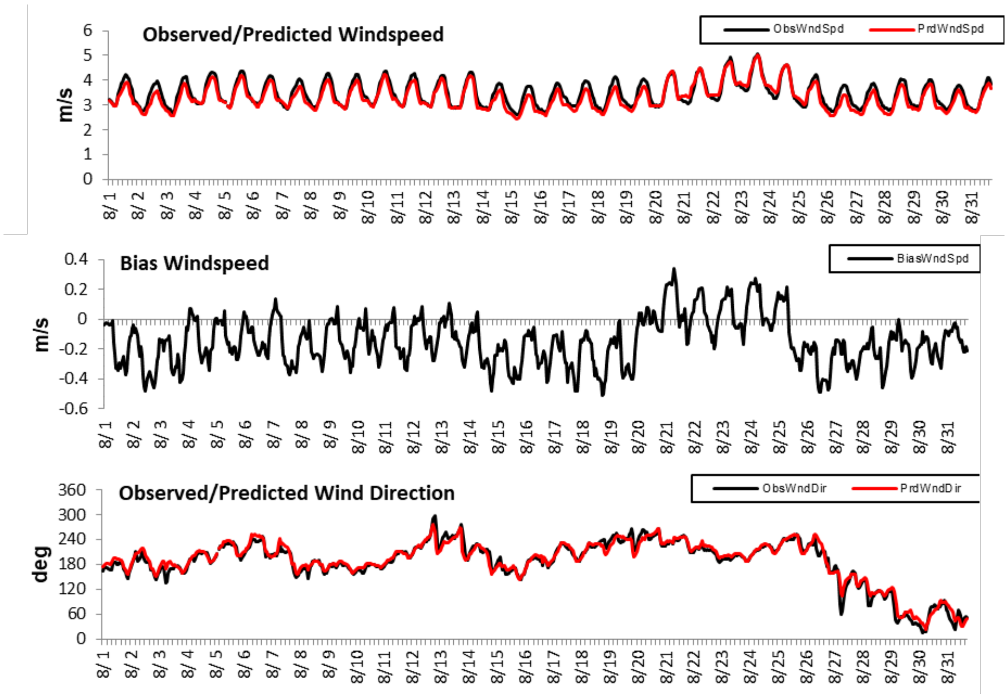

Figure 3-80: WRF CONUS Wind Performance for August 2016

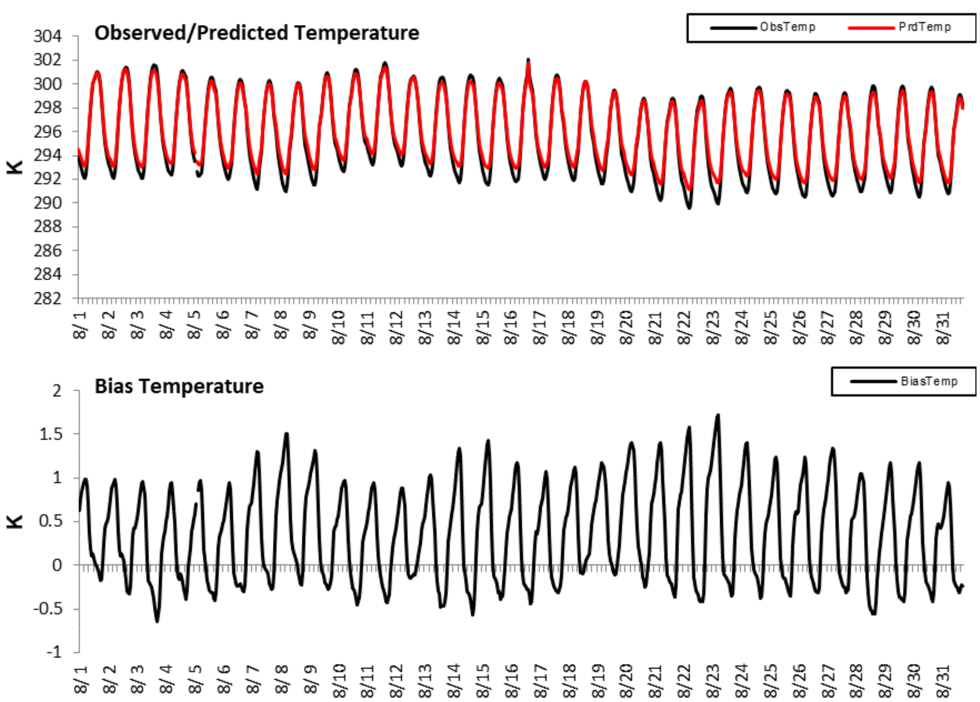

Figure 3-81: WRF CONUS Temperature Performance for August 2016

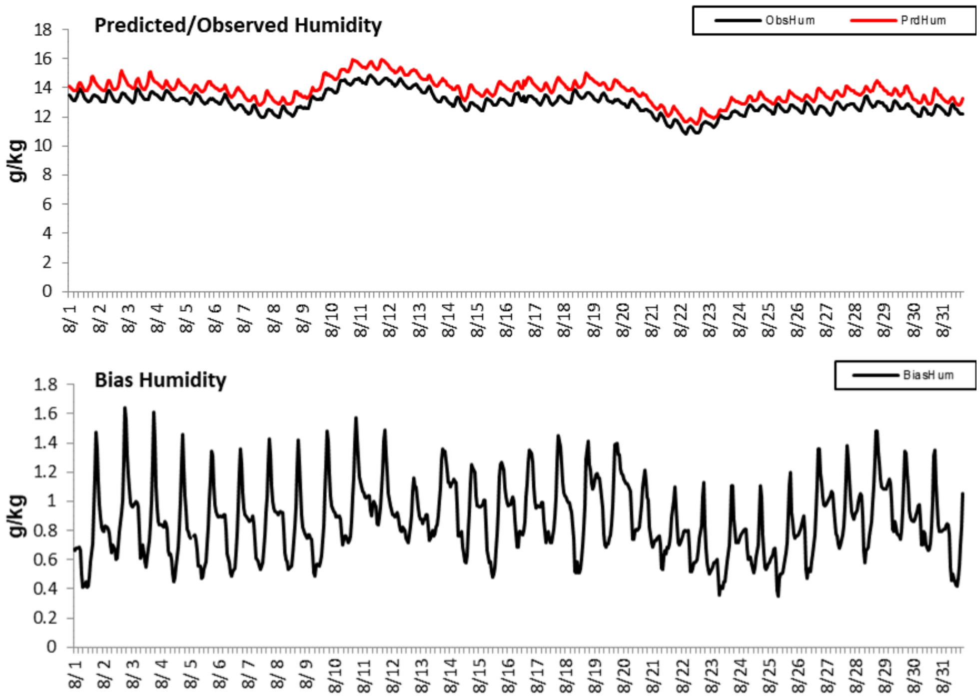

Figure 3-82: WRF CONUS Humidity Performance for August 2016

3.9.2 South-Central Region August Timeseries

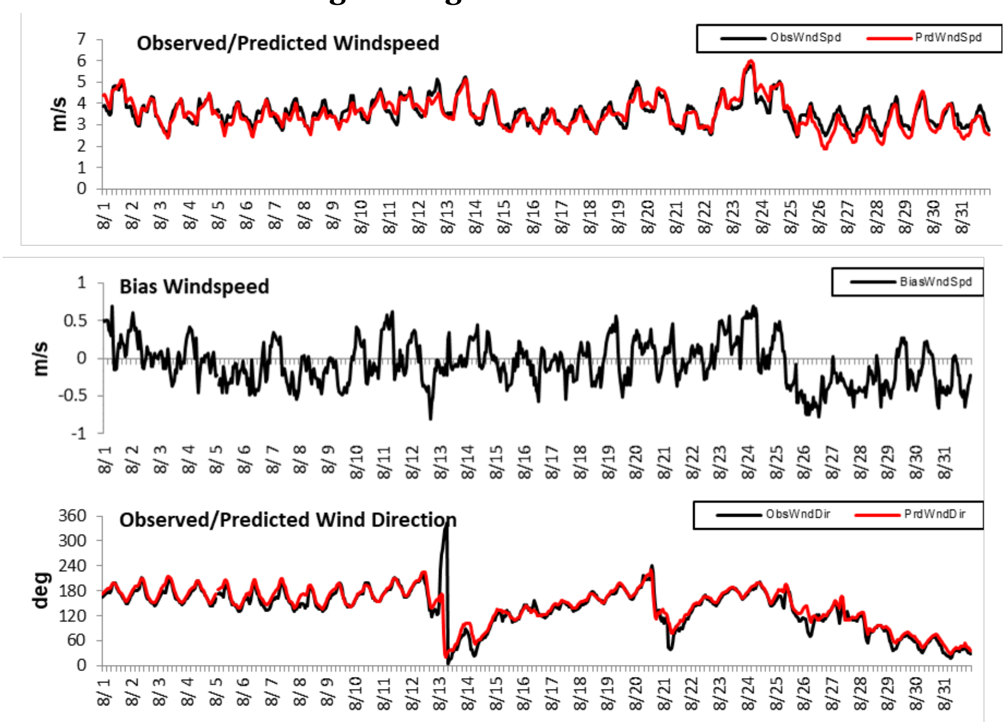

Figure 3-83: WRF South-Central Region Wind Performance for August 2016

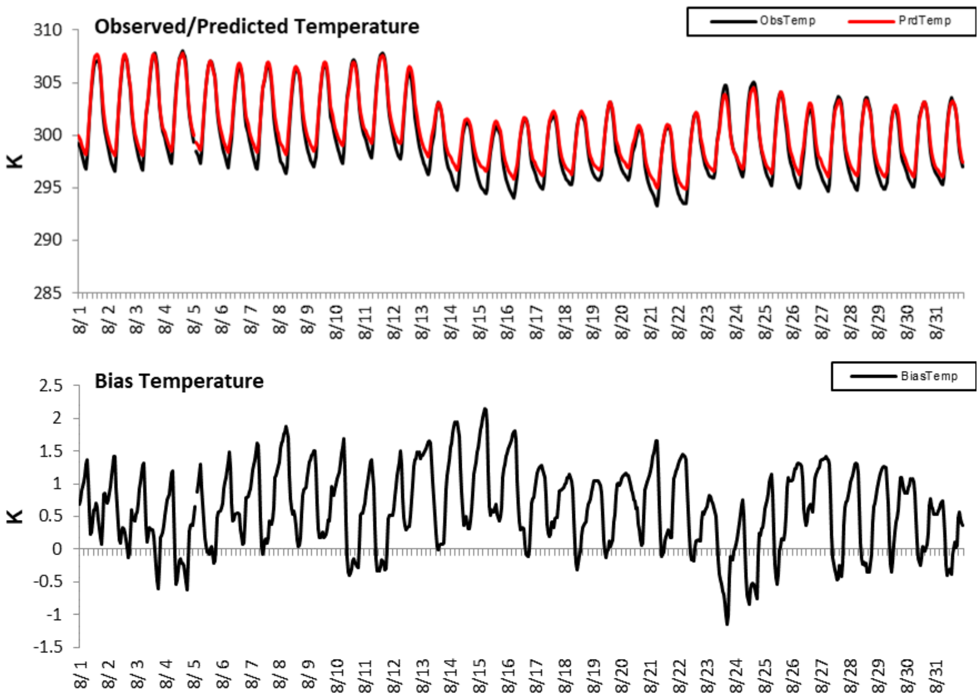

Figure 3-84: WRF South-Central Region Temperature Performance for August 2016

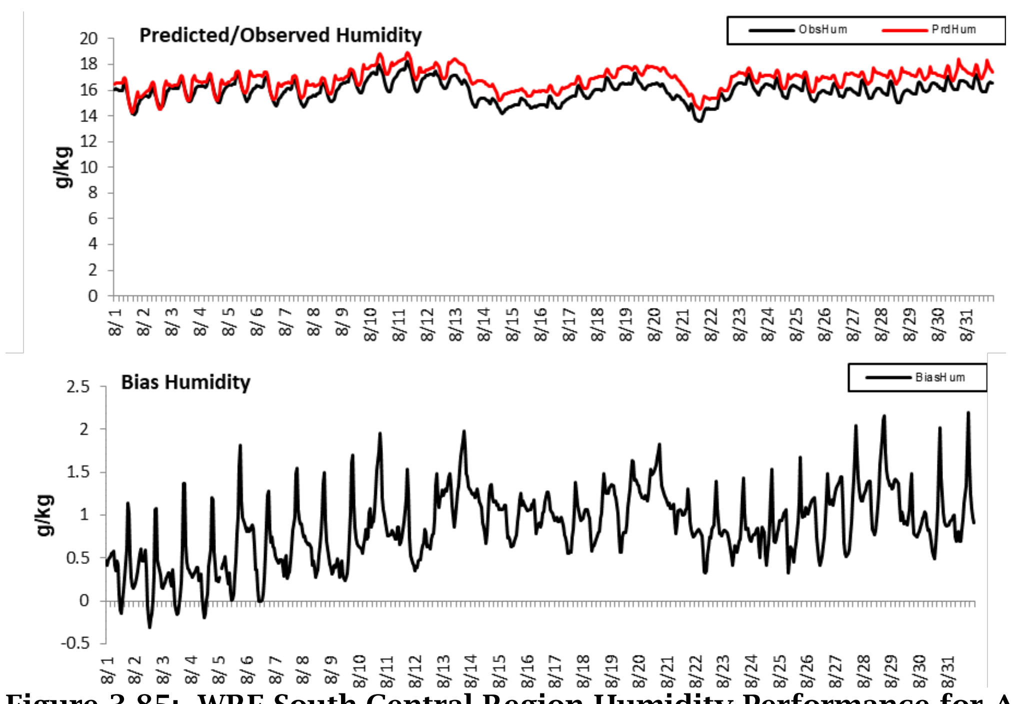

Figure 3-85: WRF South-Central Region Humidity Performance for August 2016

3.9.3 August Spatial Bias Plots

The spatial distribution of wind speed bias shows more negative values in the western states and to a lesser degree more positive values in the eastern half of the country as shown in Figure 3-86: *Mean Bias of Wind Speed for August 2016*. However, Figure 3-87: *Mean Bias of Temperature for August 2016* shows more spatial variability for temperature, with Colorado and other mountain states showing several sites with significant positive bias. Also, California coastal sites have positive temperature bias and the Sierra Nevada and coastal ranges have negative biases. The variability seen in Figure 3-88: *Mean Bias of Mixing Ratio for August 2016* clearly show New Mexico sites with a positive humidity bias for this month, while sites in Mississippi, Georgia, and South Carolina have significant positive bias as does the Great Lakes region.

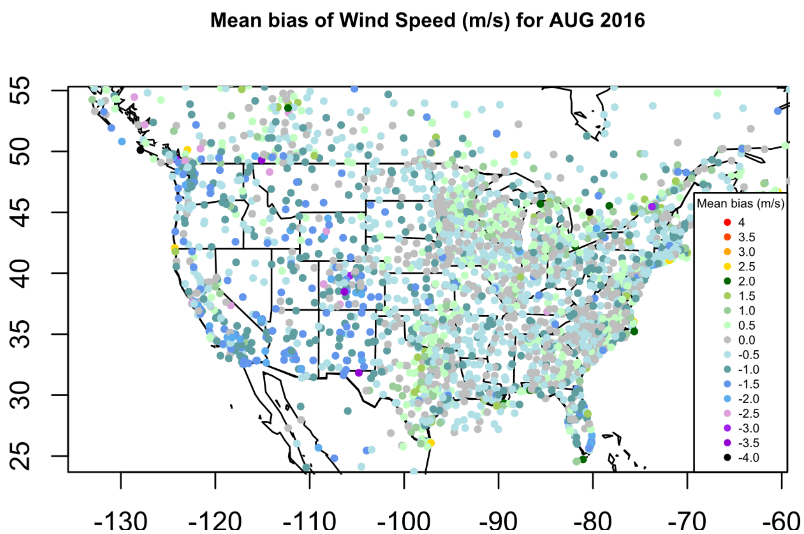

Figure 3-86: Mean Bias of Wind Speed for August 2016

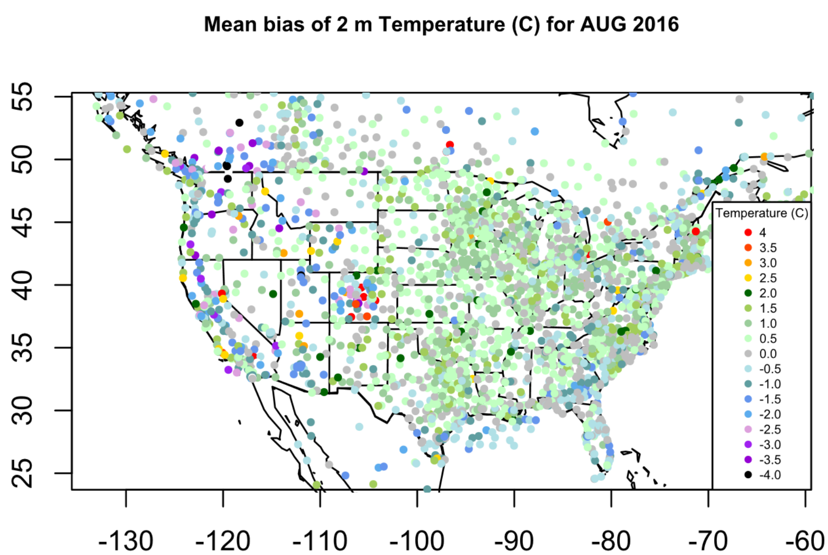

Figure 3-87: Mean Bias of Temperature for August 2016

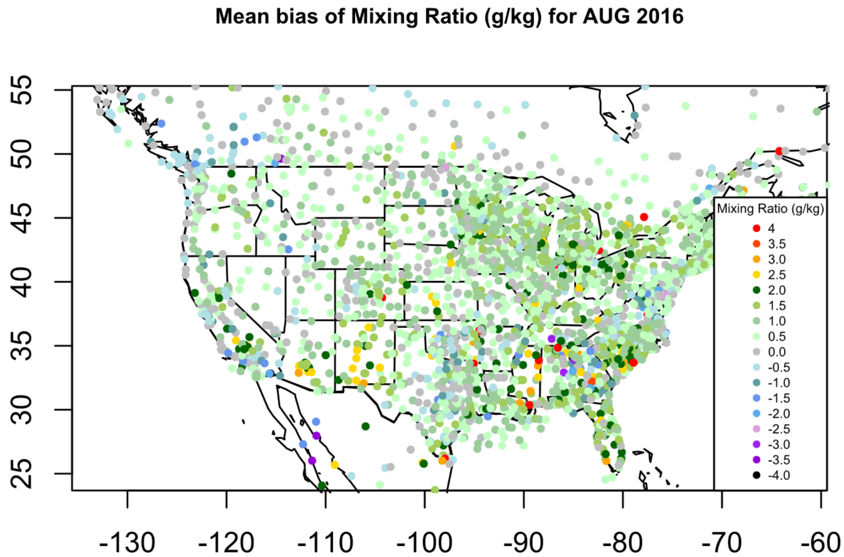

Figure 3-88: Mean Bias of Mixing Ratio for August 2016

3.9.4 August Accumulated Precipitation

The August WRF precipitation patterns exhibit a dry west, and precipitation magnitudes greater than six inches up the Mississippi valley, and in excess of 12.8 inches in southern Louisiana as shown in Figure 3-89: *WRF Accumulated Precipitation for August 2016*. PRISM data in Figure 3-90: *PRISM Accumulated Precipitation for August 2016* shows a broader extent compared to the spatial granularity in the WRF output.

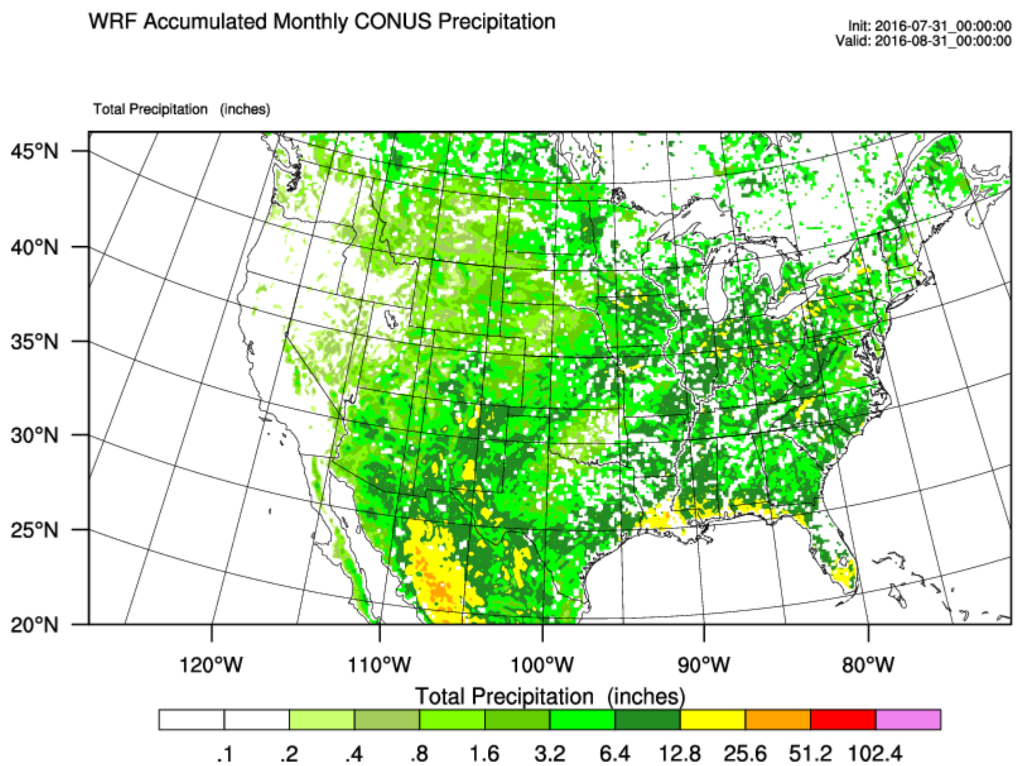

Figure 3-89: WRF Accumulated Precipitation for August 2016

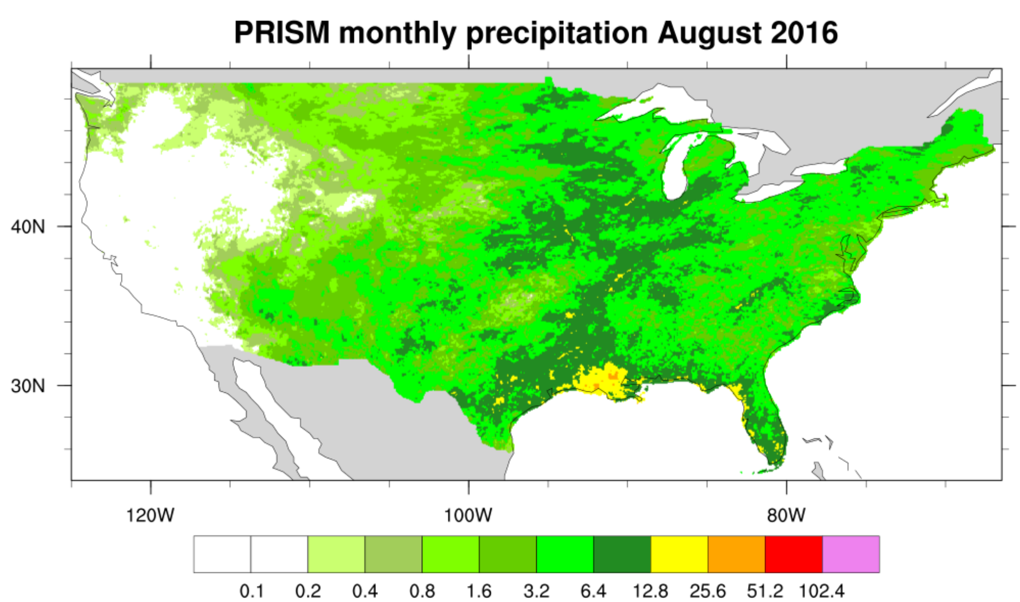

Figure 3-90: PRISM Accumulated Precipitation for August 2016

3.10 WRF SEPTEMBER PERFORMANCE

Wind speed and direction (Figure 3-91: *WRF CONUS Wind Performance for September 2016* and Figure 3-94: *WRF South-Central Region Wind Performance for September 2016*), temperature (Figure 3-92: *WRF CONUS Temperature Performance for September 2016* and Figure 3-95: *WRF South-Central Region Temperature Performance for September 2016*), and humidity (Figure 3-93: *WRF CONUS Humidity Performance for September 2016* and Figure 3-96: *WRF South-Central Region Humidity Performance for September 2016*) showed good performance time series statistics across the CONUS and south-central region for the month of September.

3.10.1 CONUS September Timeseries

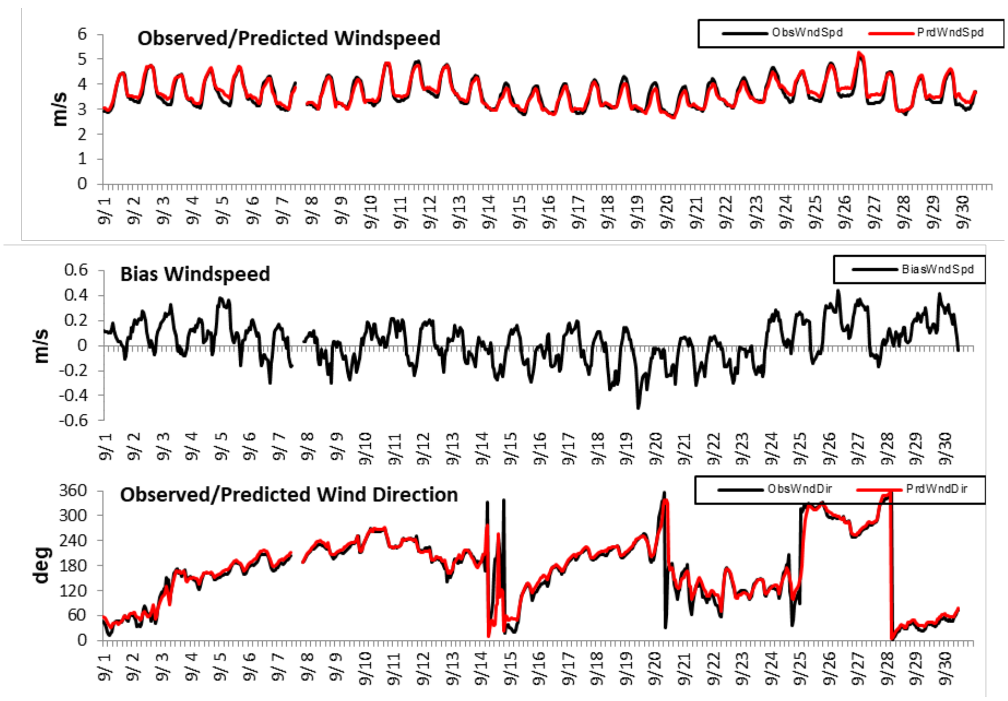

Figure 3-91: WRF CONUS Wind Performance for September 2016

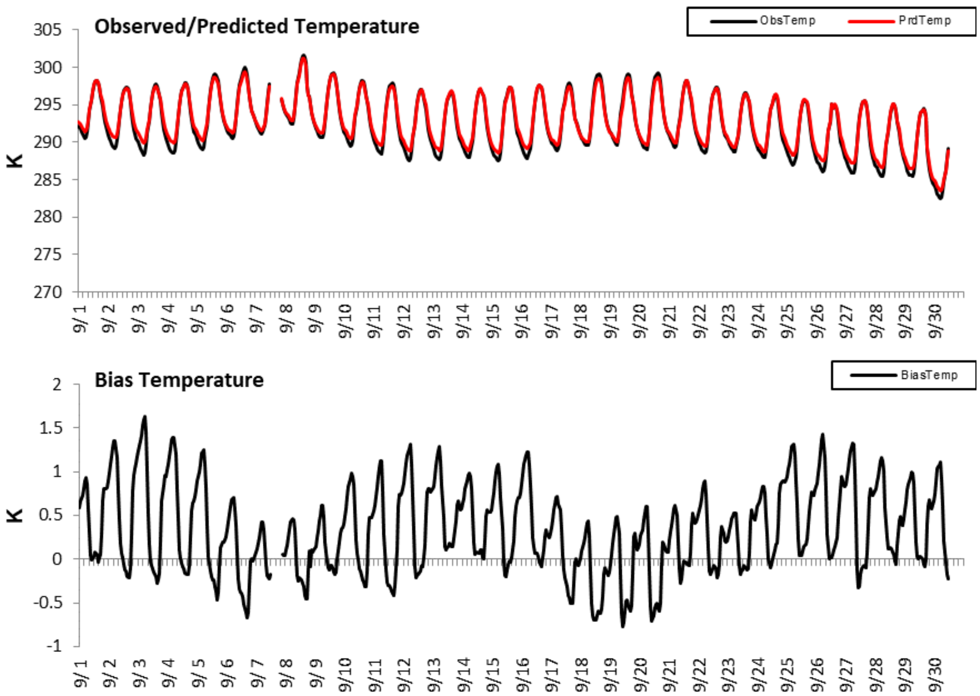

Figure 3-92: WRF CONUS Temperature Performance for September 2016

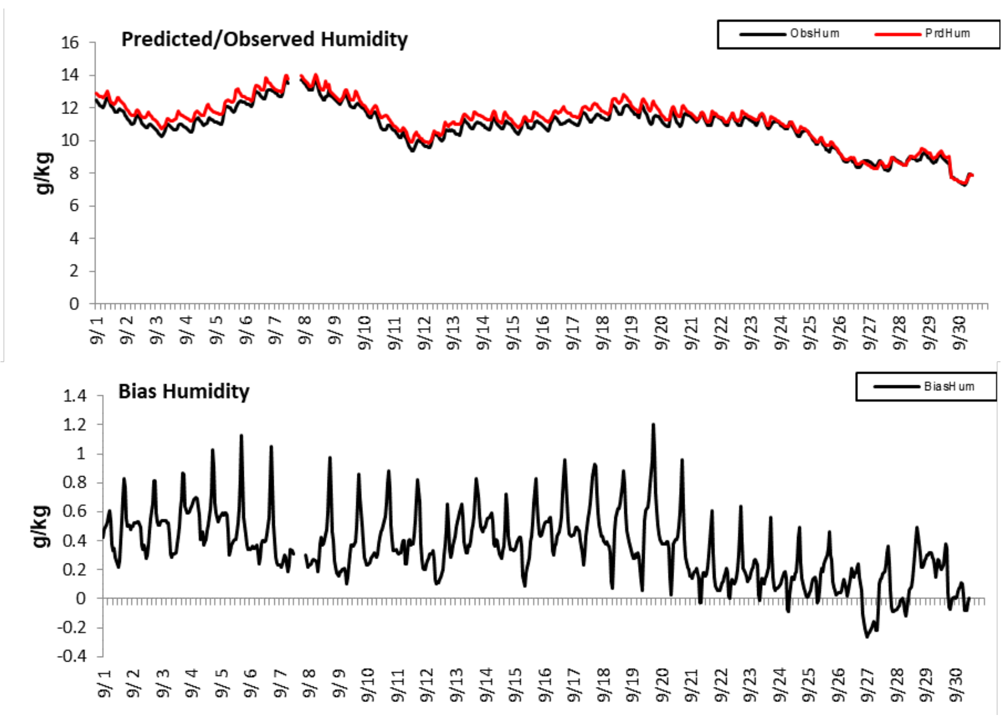

Figure 3-93: WRF CONUS Humidity Performance for September 2016

3.10.2 South-Central Region September Timeseries

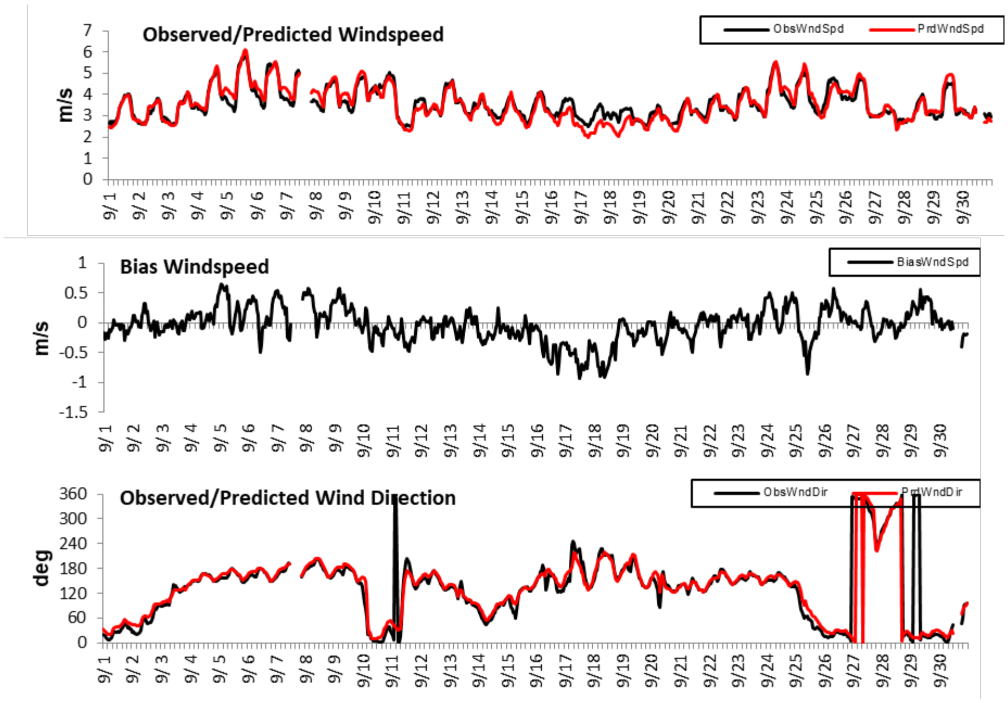

Figure 3-94: WRF South-Central Region Wind Performance for September 2016

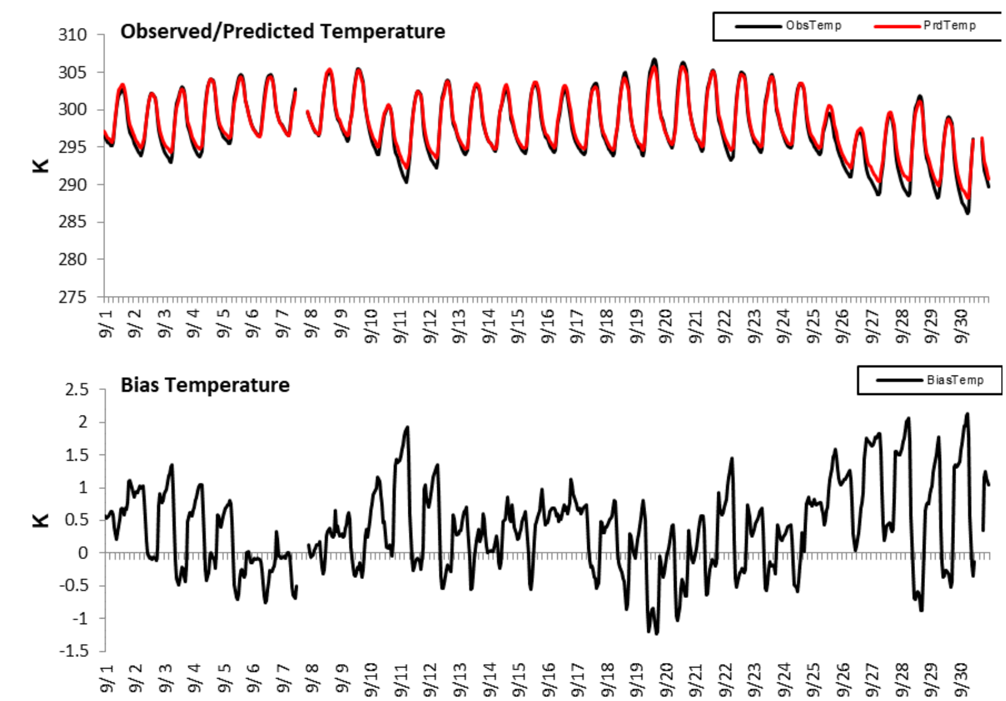

Figure 3-95: WRF South-Central Region Temperature Performance for September 2016

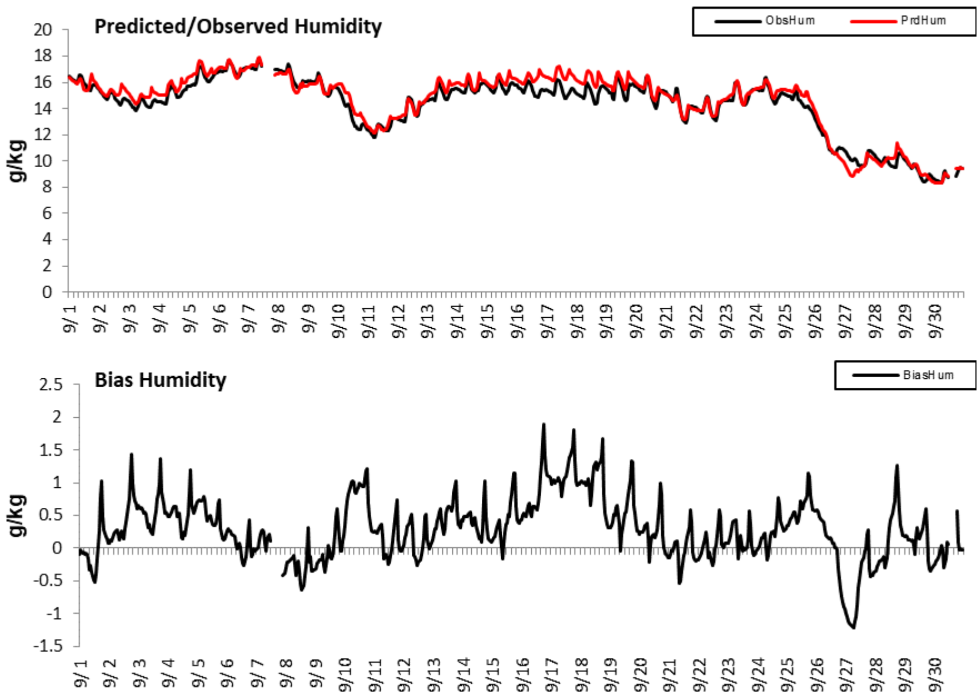

Figure 3-96: WRF South-Central Region Humidity Performance for September 2016

3.10.3 September Spatial Bias Plots

Individual ds472 sites across the United States showed low biases for wind speed, with a negative bias in the western states and a slightly positive bias in the Midwest and Atlantic states as shown in Figure 3-97: *Mean Bias of Wind Speed for September 2016*. Figure 3-98: *Mean Bias of Temperature for September 2016* exhibits modeled temperature biases were within 1.0 degrees Celsius, except for sites in Colorado where WRF produced higher values. Humidity biases were within 1.5 g/kg for much of the CONUS as shown in Figure 3-99: *Mean Bias of Mixing Ratio for September 2016*.

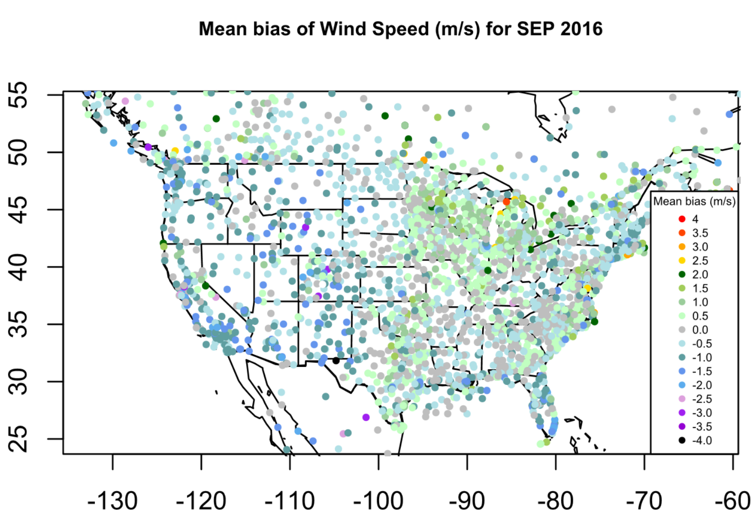

Figure 3-97: Mean Bias of Wind Speed for September 2016

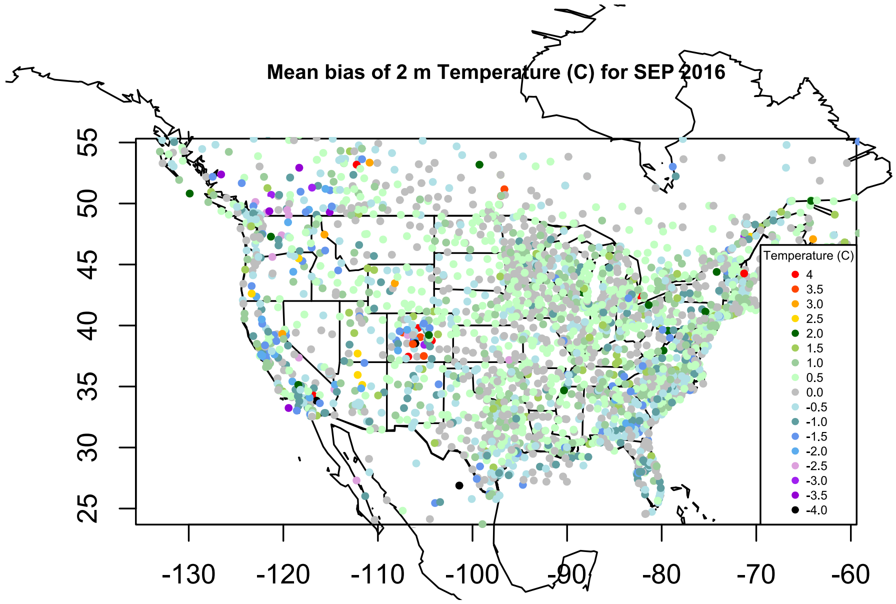

Figure 3-98: Mean Bias of Temperature for September 2016

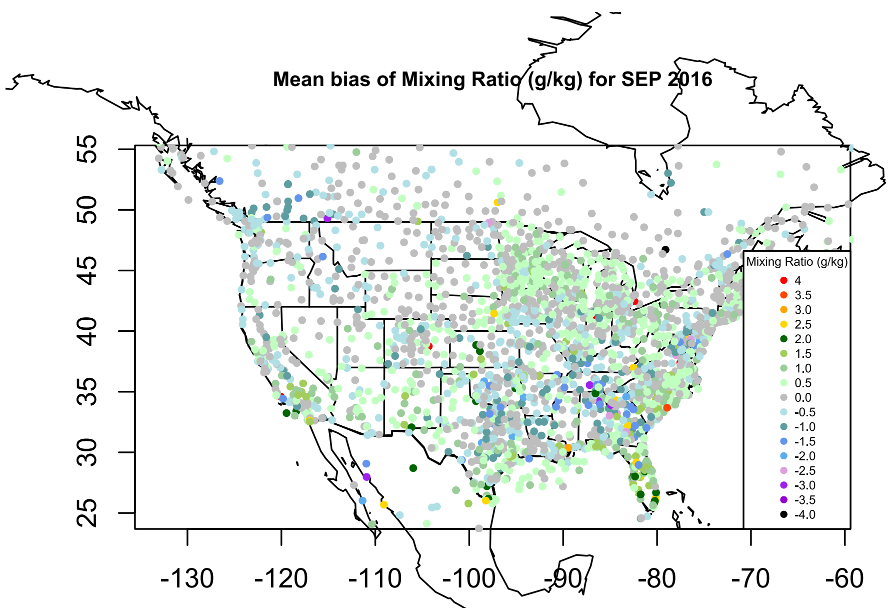

Figure 3-99: Mean Bias of Mixing Ratio for September 2016

3.10.4 September Accumulated Precipitation

Comparing Figure 3-100: *WRF Accumulated Precipitation for September 2016* and Figure 3-101: *PRISM Accumulated Precipitation for September 2016*, WRF had more rainfall in the mountains and in southeastern New Mexico than the PRISM data. However, PRISM showed more accumulated precipitation across northeast Texas. Most differences are not large, and the patterns are similar, which indicates acceptable model performance.

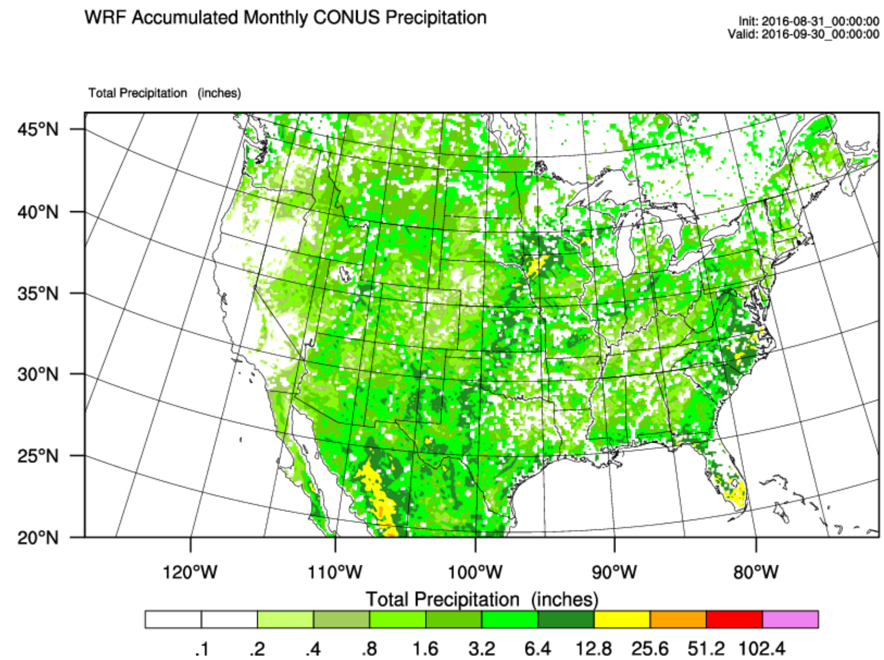

Figure 3-100: WRF Accumulated Precipitation for September 2016

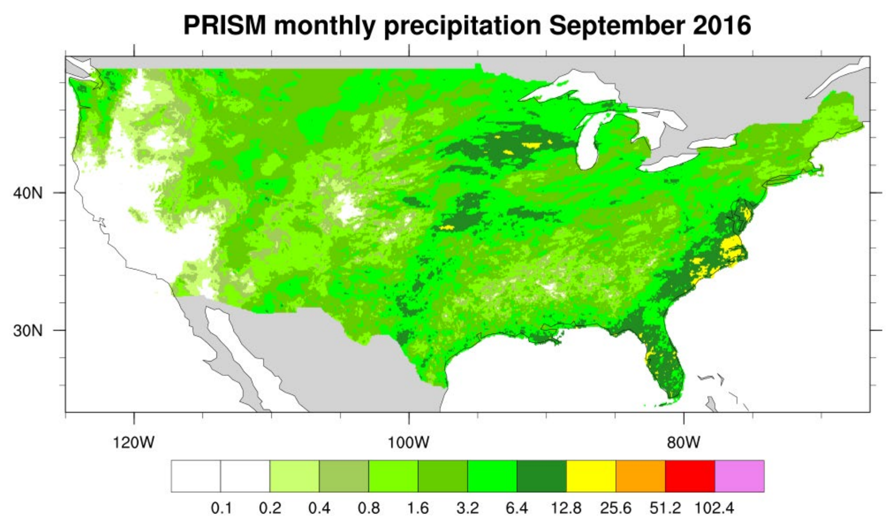

Figure 3-101: PRISM Accumulated Precipitation for September 2016

3.11 WRF OCTOBER PERFORMANCE

Wind speed, direction, temperature, and humidity exhibited good performance across the CONUS and the south-central region during the month of October. Nighttime wind speeds showed a high bias of less than 1.0 m/s as shown in Figure 3-102: *WRF CONUS Wind Performance for October 2016* and Figure 3-105: *WRF South-Central Region Wind Performance for October 2016*. Modeled temperatures also had a minimal high bias at night as shown in Figure 3-103: *WRF CONUS Temperature Performance for October*

2016 and Figure 3-106: *WRF South-Central Region Temperature Performance for October 2016*. The average WRF humidity values matched the ds472 monitored values well over the CONUS and the south-central region as shown in Figure 3-104: *WRF CONUS Humidity Performance for October 2016* and Figure 3-107: *WRF South-Central Region Humidity Performance for October 2016*.

3.11.1 CONUS October Timeseries

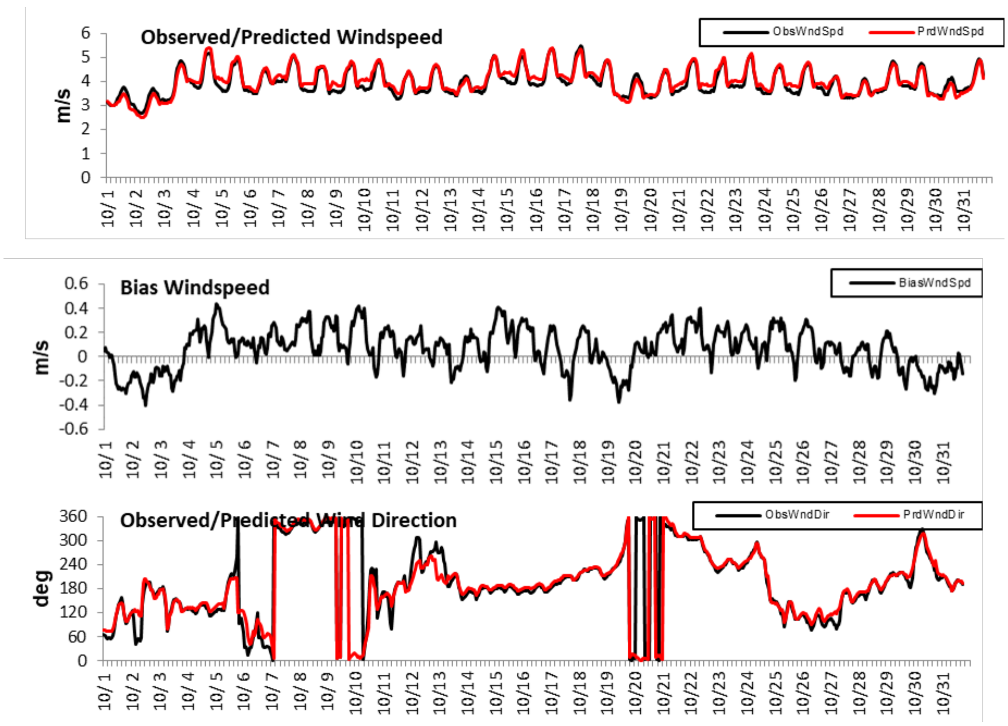

Figure 3-102: WRF CONUS Wind Performance for October 2016

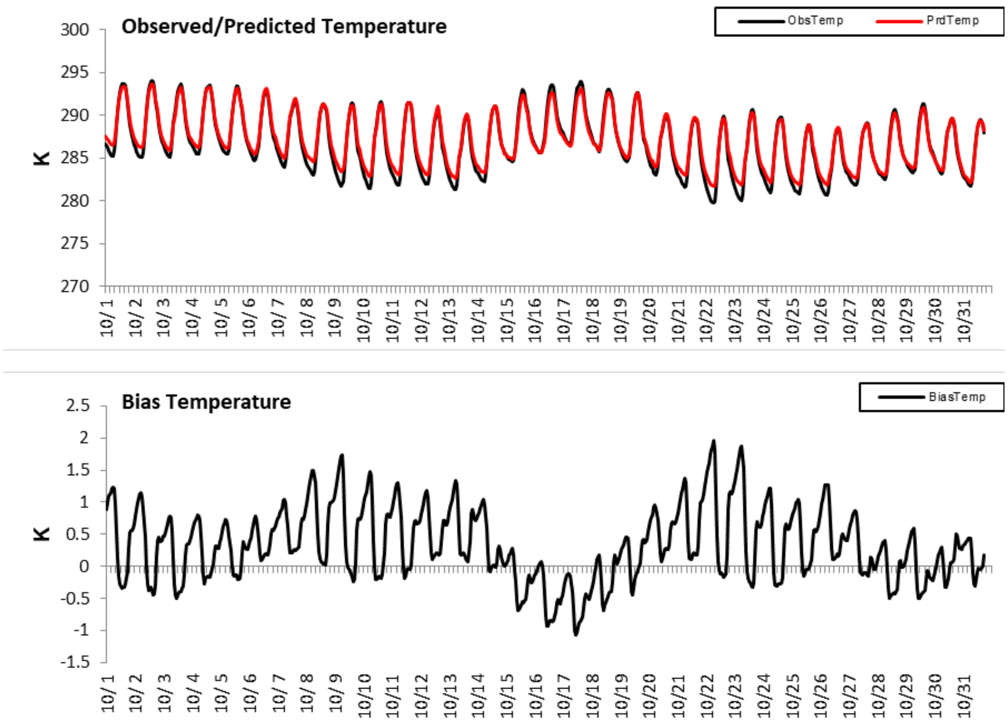

Figure 3-103: WRF CONUS Temperature Performance for October 2016

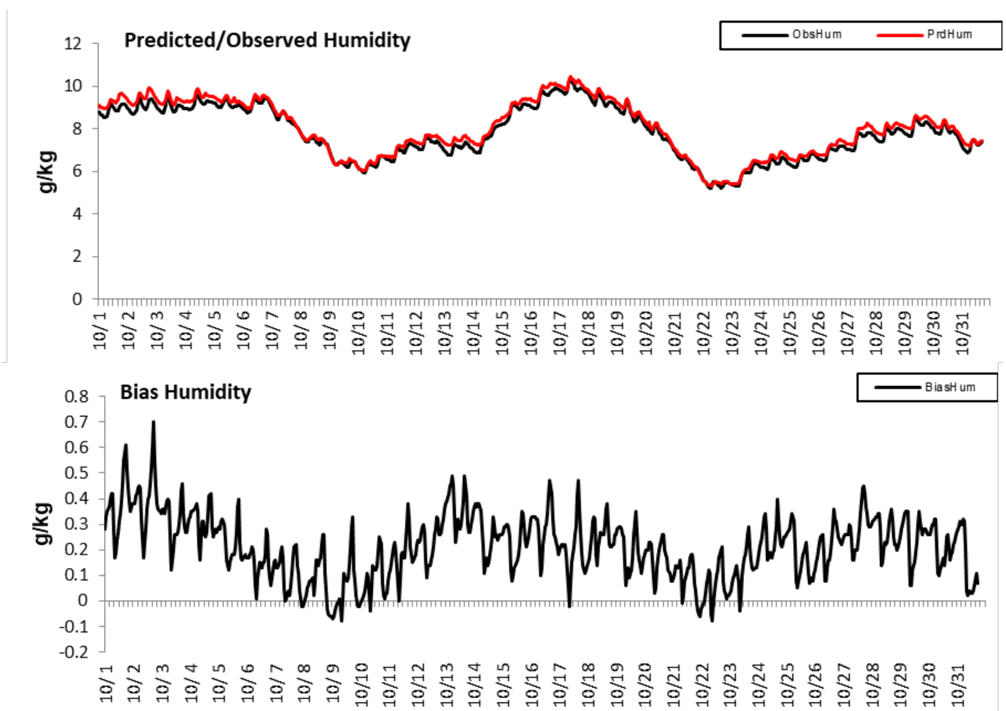

Figure 3-104: WRF CONUS Humidity Performance for October 2016

3.11.2 South-Central Region October Timeseries

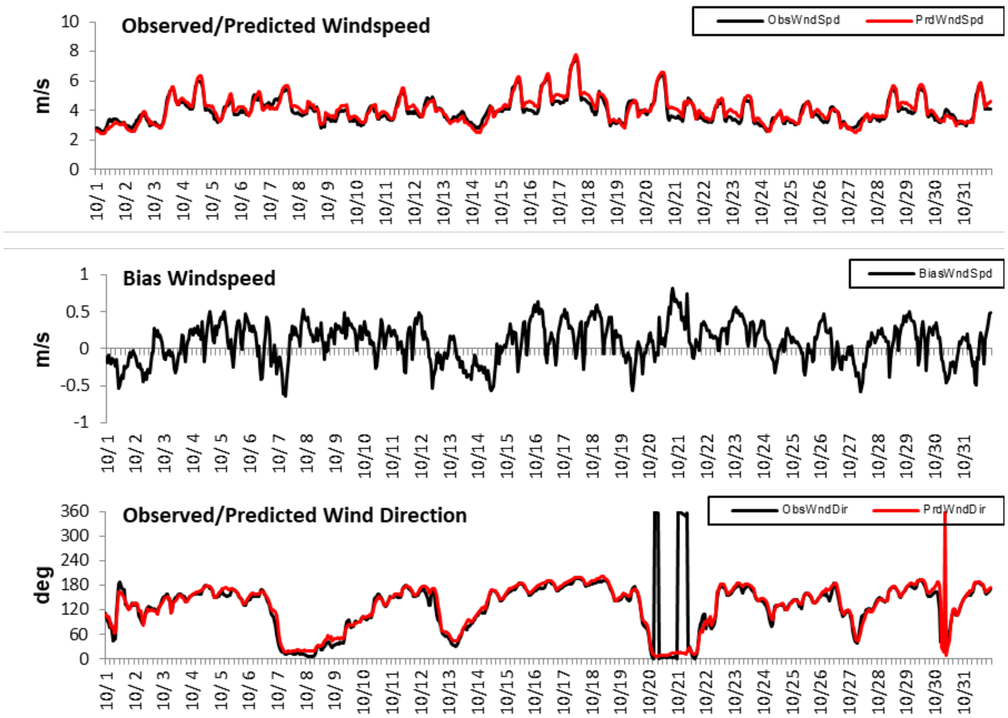

Figure 3-105: WRF South-Central Region Wind Performance for October 2016

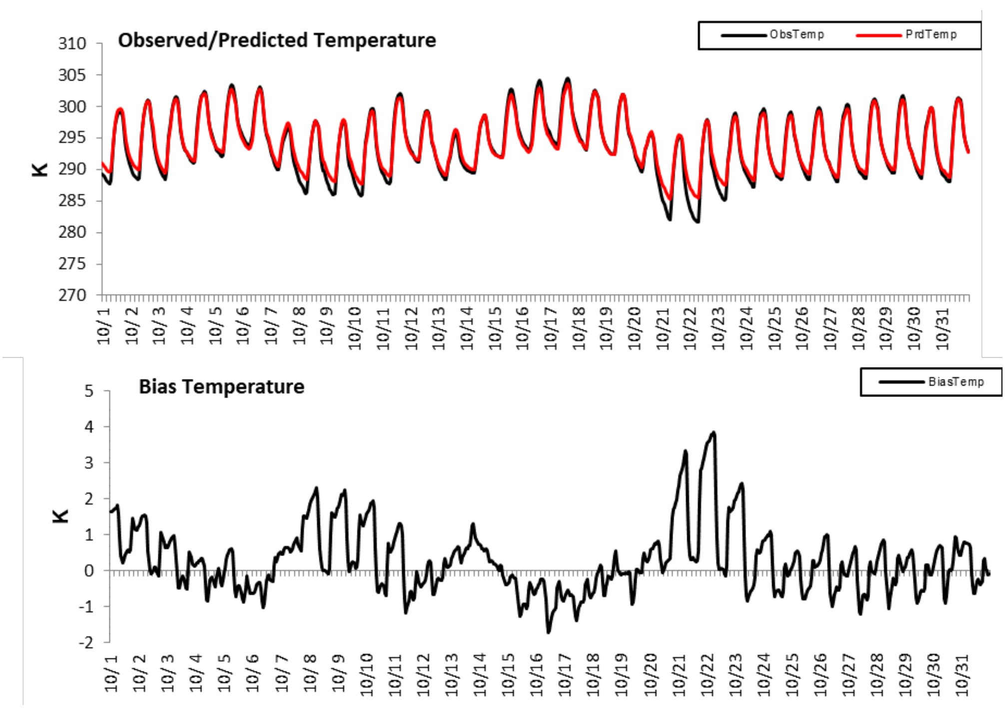

Figure 3-106: WRF South-Central Region Temperature Performance for October 2016

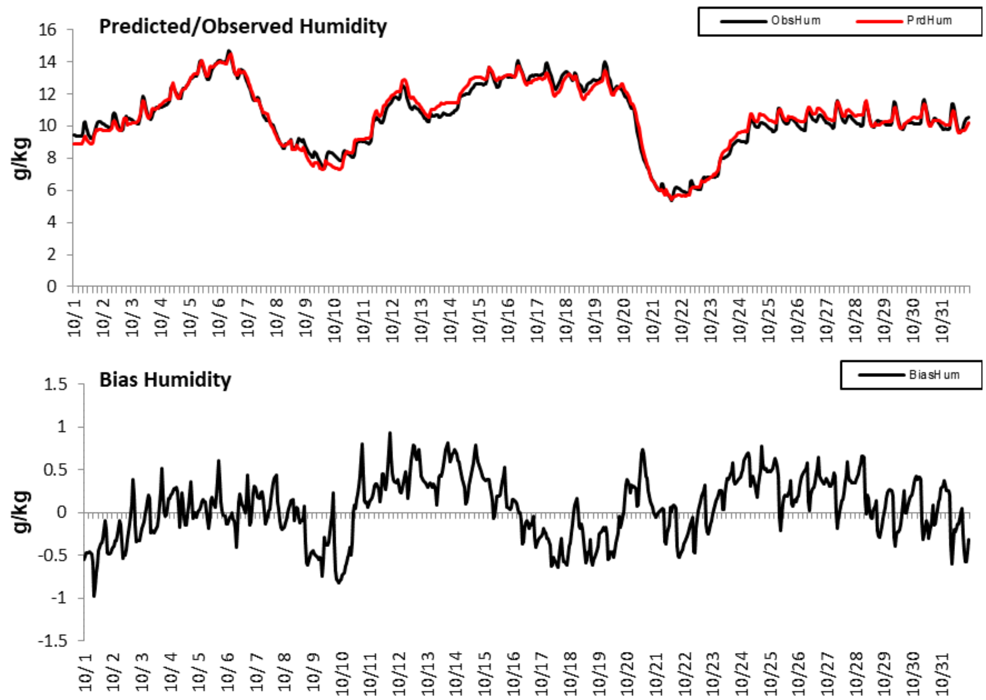

Figure 3-107: WRF South-Central Region Humidity Performance for October 2016

3.11.3 October Spatial Bias Plots

Similar spatial patterns as September for wind speed bias occurred in October with a negative bias in the western states and a positive bias in the eastern states as shown in Figure 3-108: *Mean Bias of Wind Speed for October 2016*. Spatially, the temperature bias was generally within 1.5 degrees Celsius as shown in Figure 3-109: *Mean Bias of Temperature for October 2016*. Humidity bias was near zero for most areas of the CONUS except the southeastern states as depicted in Figure 3-110: *Mean Bias of Mixing Ratio for October 2016*.

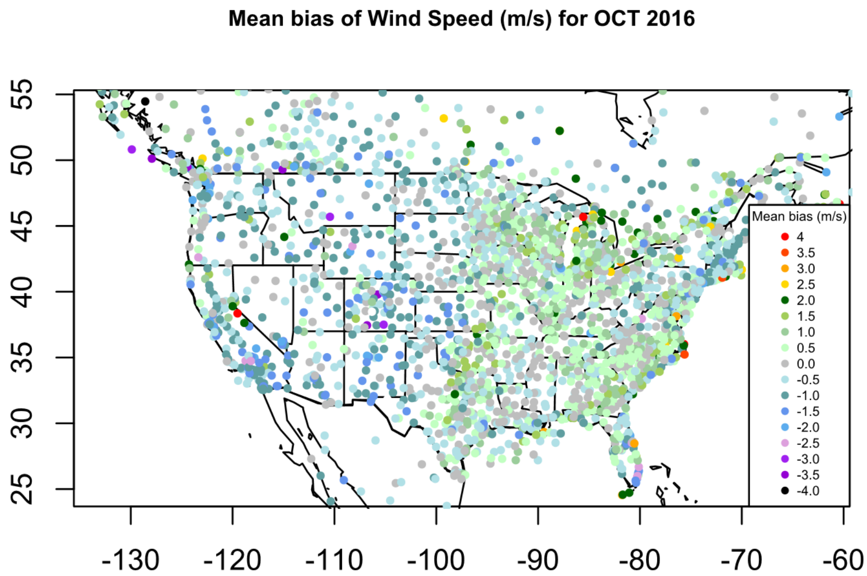

Figure 3-108: Mean Bias of Wind Speed for October 2016

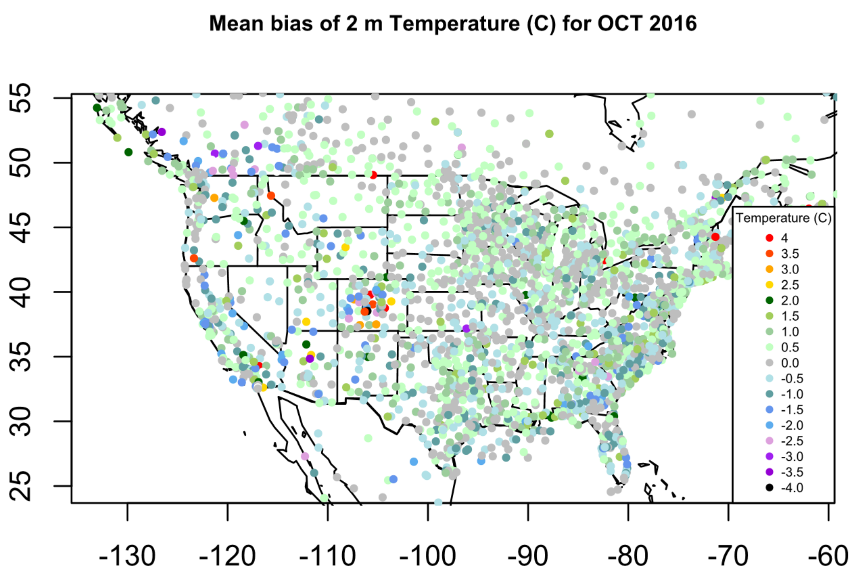

Figure 3-109: Mean Bias of Temperature for October 2016

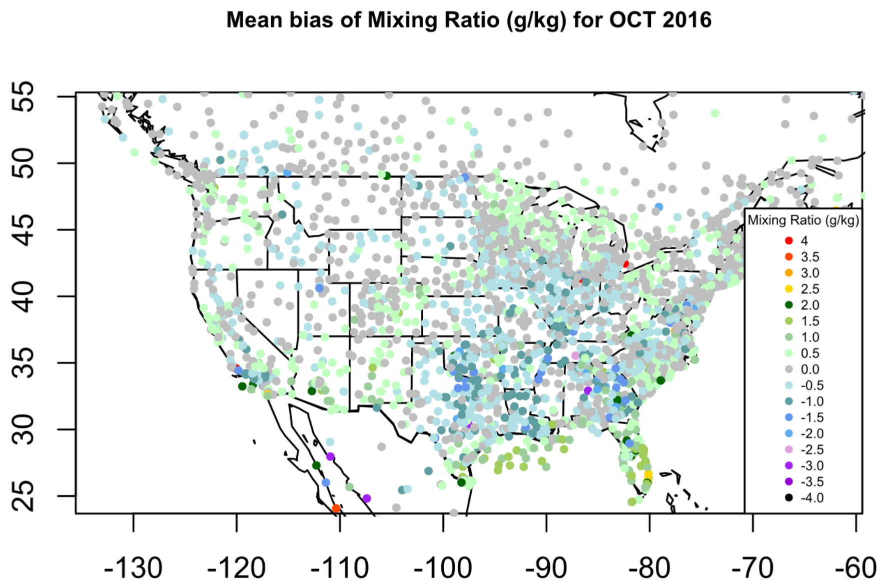

Figure 3-110: Mean Bias of Mixing Ratio for October 2016

3.11.4 October Accumulated Precipitation

October had very modest predicted and observed monthly precipitation. WRF predicted values compared well with PRISM data, although there was some additional predicted precipitation over New Mexico, as seen when comparing Figure 3-111: *WRF Accumulated Precipitation for October 2016* with Figure 3-112: *PRISM Accumulated Precipitation for October 2016*.

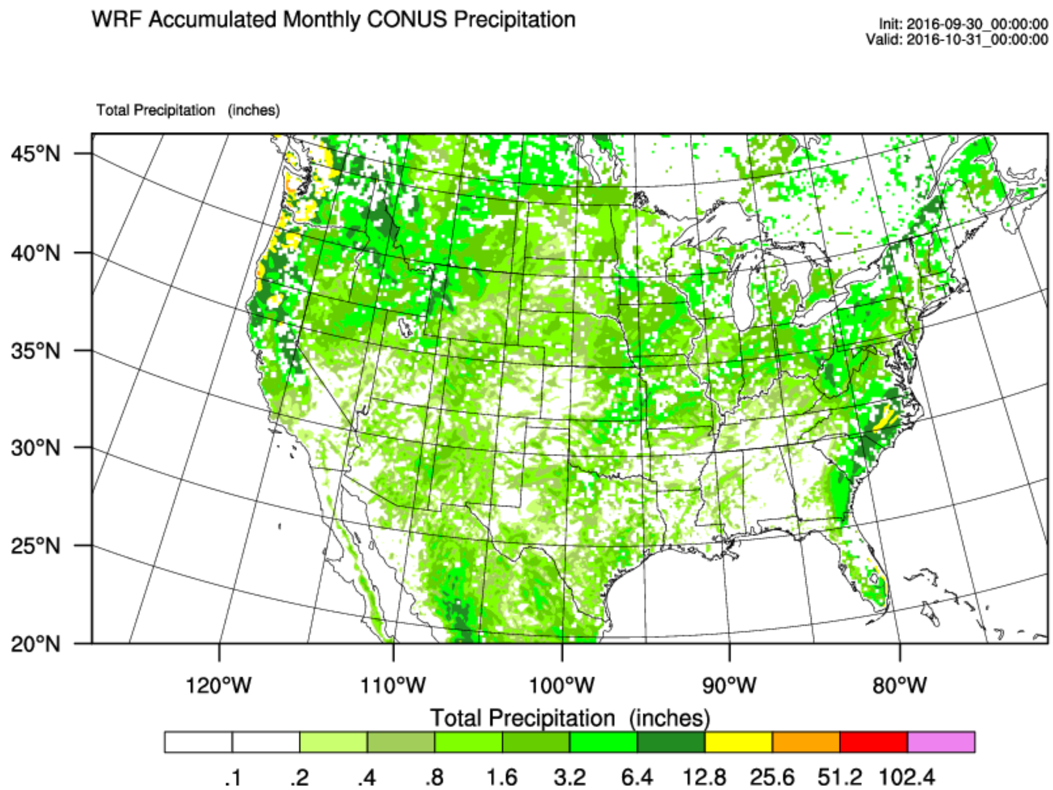

Figure 3-111: WRF Accumulated Precipitation for October 2016

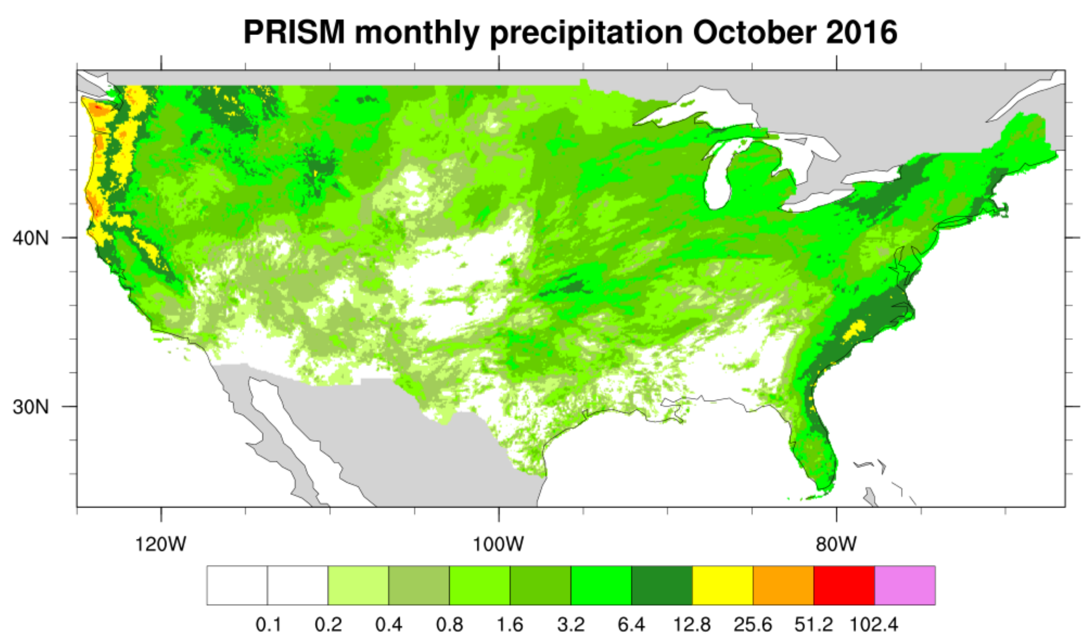

Figure 3-112: PRISM Accumulated Precipitation for October 2016

3.12 WRF NOVEMBER PERFORMANCE

Model performance for wind speed, direction, and humidity were within the benchmarks across the CONUS and the south-central region for the month of November. Average wind speed bias was less as shown in Figure 3-113: *WRF CONUS Wind Performance for November 2016* and Figure 3-116: *WRF South-Central Region Wind Performance for November 2016*. Temperatures were reasonable, but there was a modest persistent high bias to nocturnal temperatures as seen in Figure 3-114: *WRF CONUS Temperature Performance for November 2016* and Figure 3-117: *WRF South-Central Region Temperature Performance for November 2016*. Humidity performance was acceptable with the largest errors in the middle of the month as shown in Figure 3-115: *WRF CONUS Humidity Performance for November 2016* and Figure 3-118: *WRF South-Central Region Humidity Performance for November 2016*.

3.12.1 CONUS November Timeseries

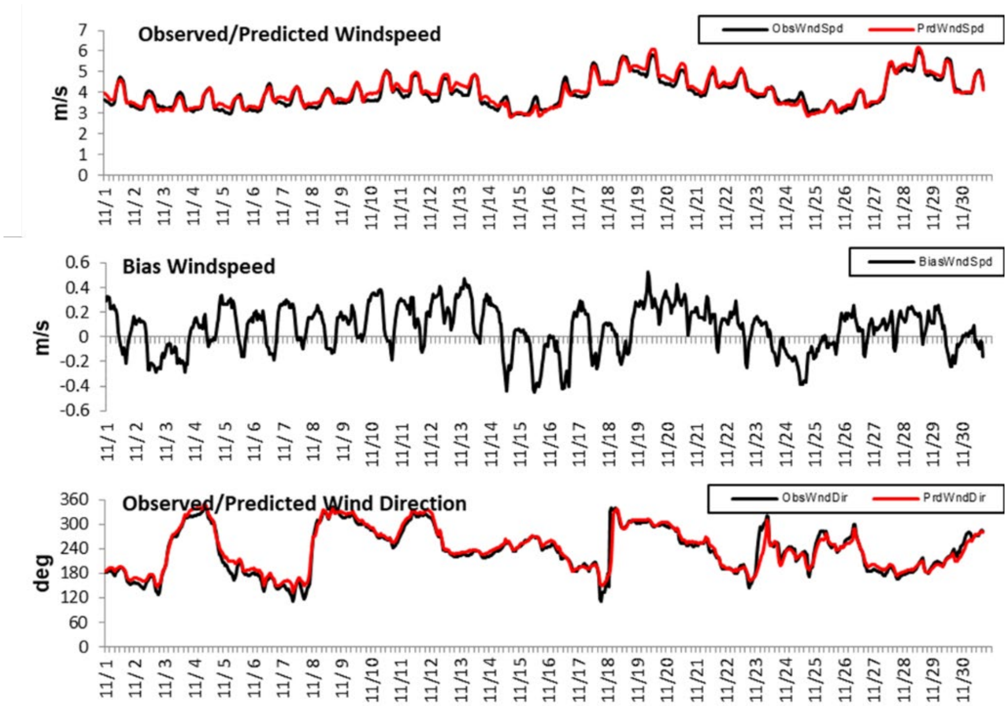

Figure 3-113: WRF CONUS Wind Performance for November 2016

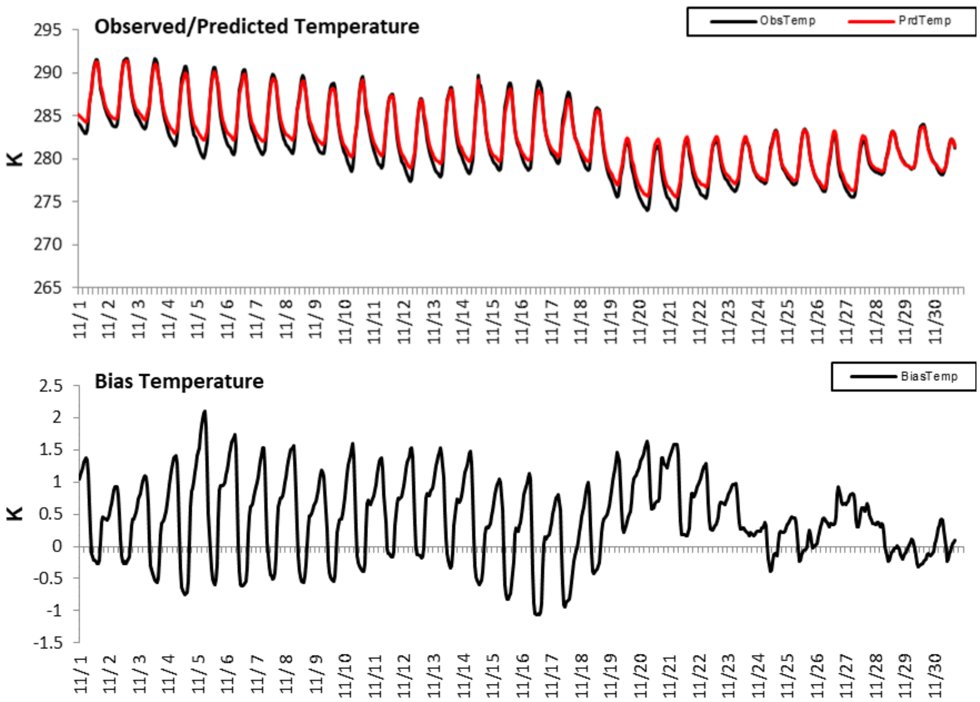

Figure 3-114: WRF CONUS Temperature Performance for November 2016

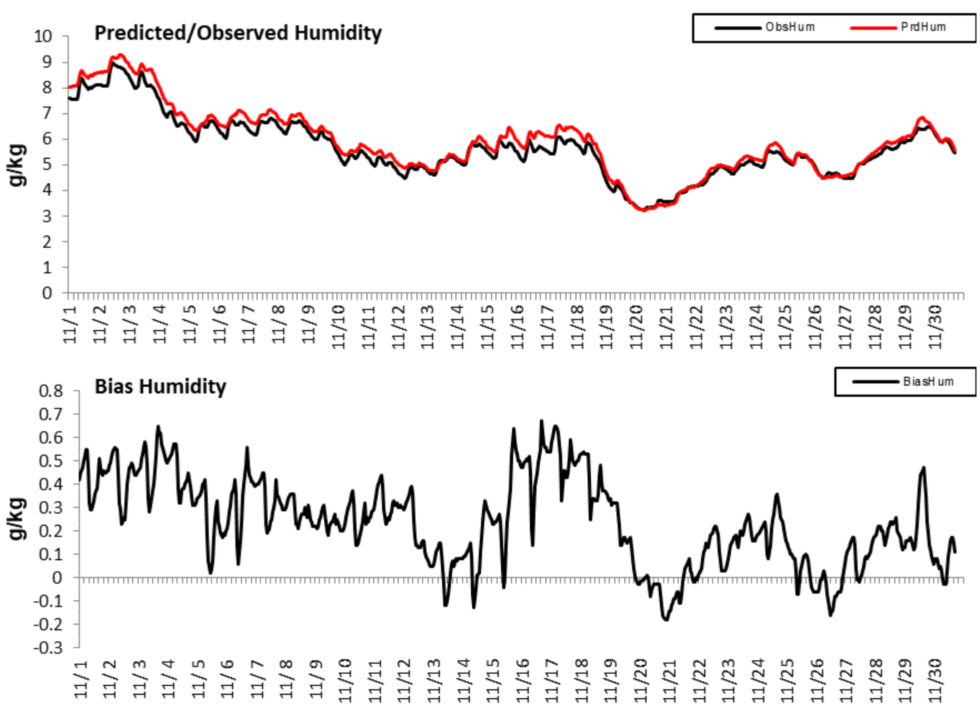

Figure 3-115: WRF CONUS Humidity Performance for November 2016

3.12.2 South-Central Region November Timeseries

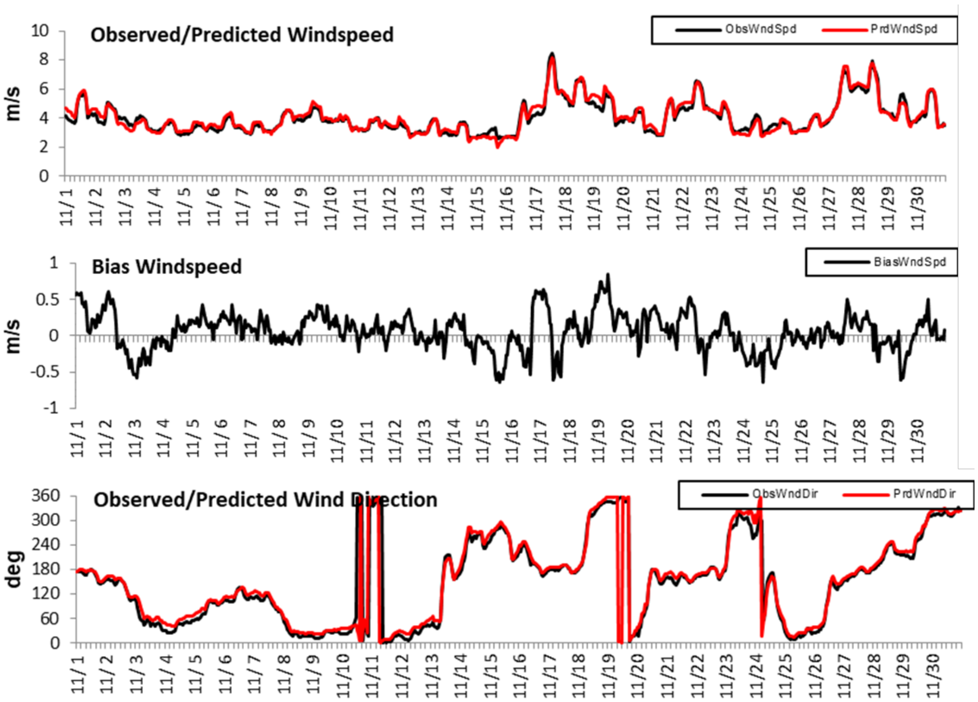

Figure 3-116:WRF South-Central Region Wind Performance for November 2016

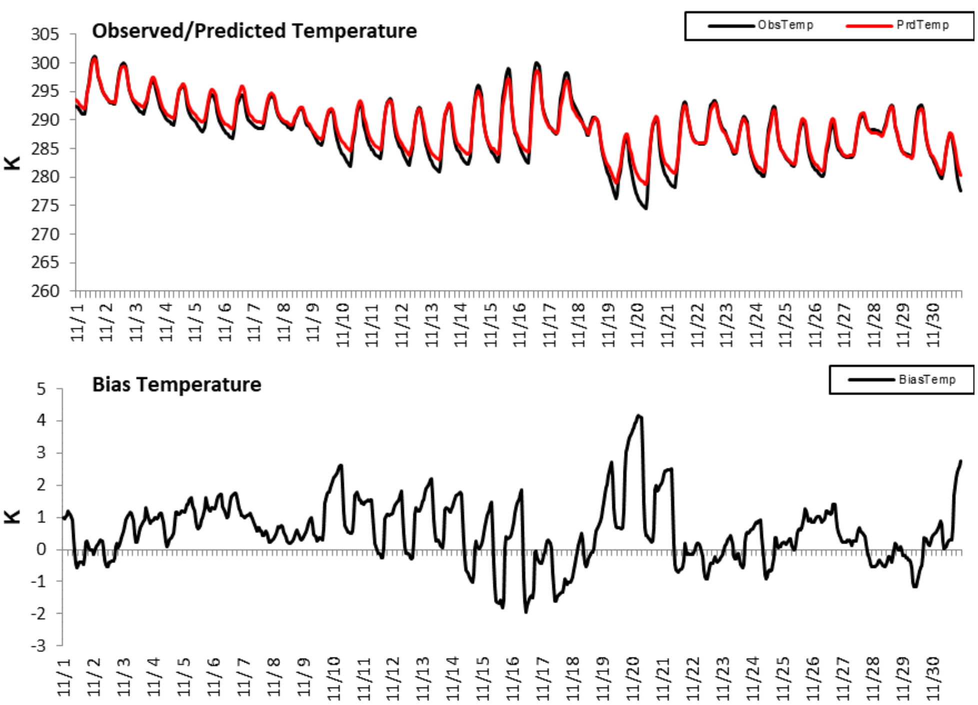

Figure 3-117: WRF South-Central Region Temperature Performance for November 2016

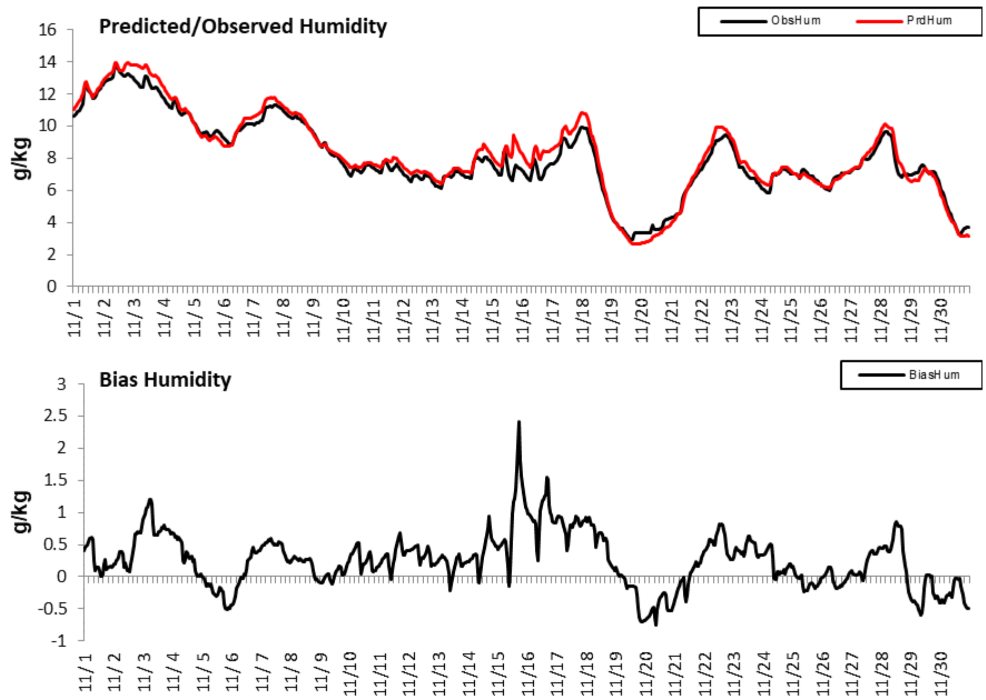

Figure 3-118: WRF South-Central Region Humidity Performance for November 2016

3.12.3 November Spatial Bias Plots

Figure 3-119: *Mean Bias of Wind Speed for November 2016* displays larger negative wind speed biases in the west in November compared to previous months, which may be expected due to increased frontal passages. Larger temperature biases are also observed at more sites in the western states but biases near Texas are close to zero as shown in Figure 3-120: *Mean Bias of Temperature for November 2016*. Humidity biases are also close to zero over the CONUS, with the largest values along the coasts as depicted in Figure 3-121: *Mean Bias of Humidity for November 2016*. The November spatial plots demonstrate that the WRF model is generally performing within the benchmarks throughout the modeling domain.

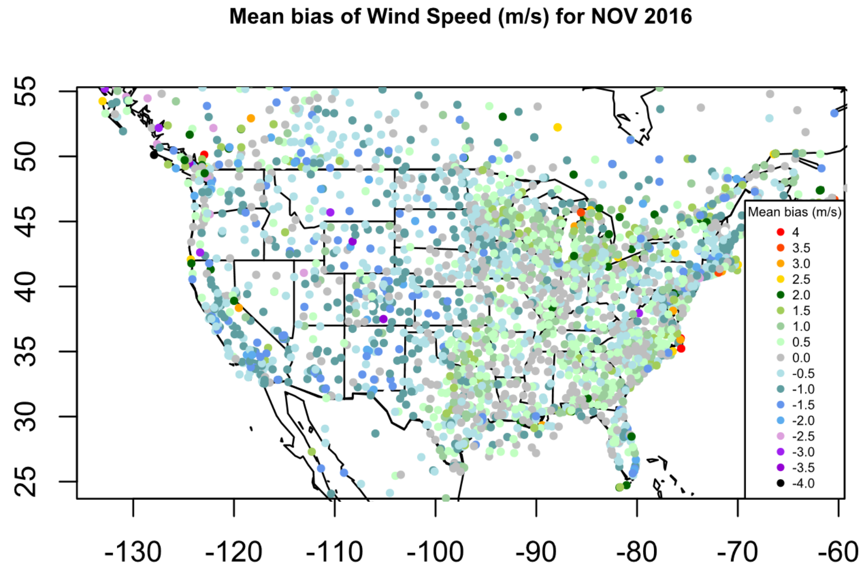

Figure 3-119: Mean Bias of Wind Speed for November 2016

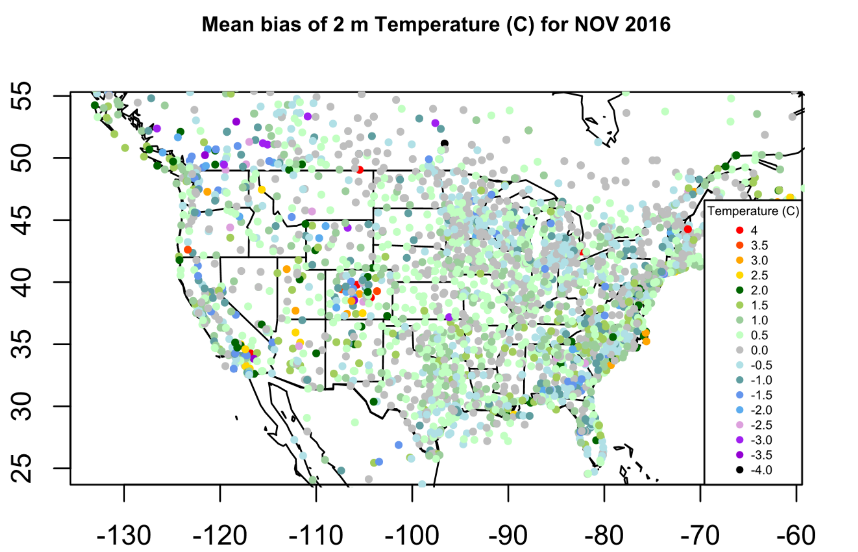

Figure 3-120: Mean Bias of Temperature for November 2016

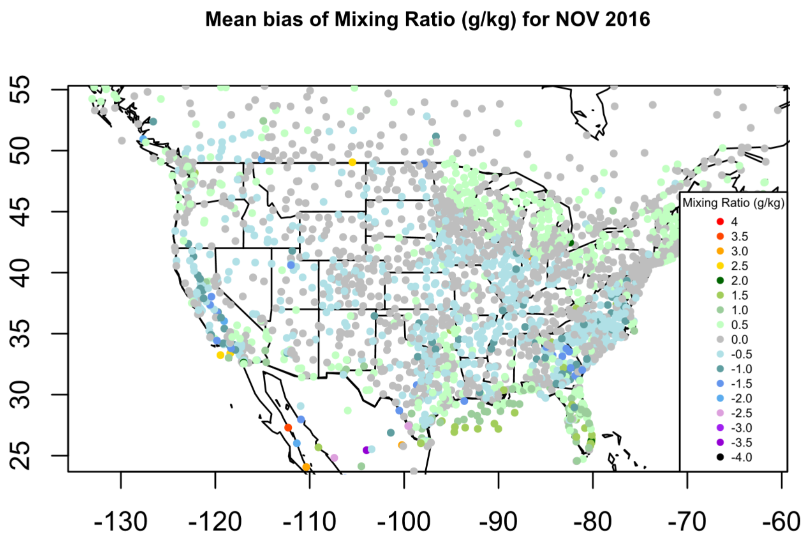

Figure 3-121: Mean Bias of Humidity for November 2016

3.12.4 November Accumulated Precipitation

WRF monthly precipitation broadly matched observed patterns across the U.S. as shown when comparing Figure 3-122: *WRF Accumulated Precipitation for November 2016* with Figure 3-123: *PRISM Accumulated Precipitation for November 2016*. However, predicted values are lower than observed in north-central Texas, Oklahoma, Arkansas, and Missouri. The model underestimated the precipitation in the Pacific Northwest.

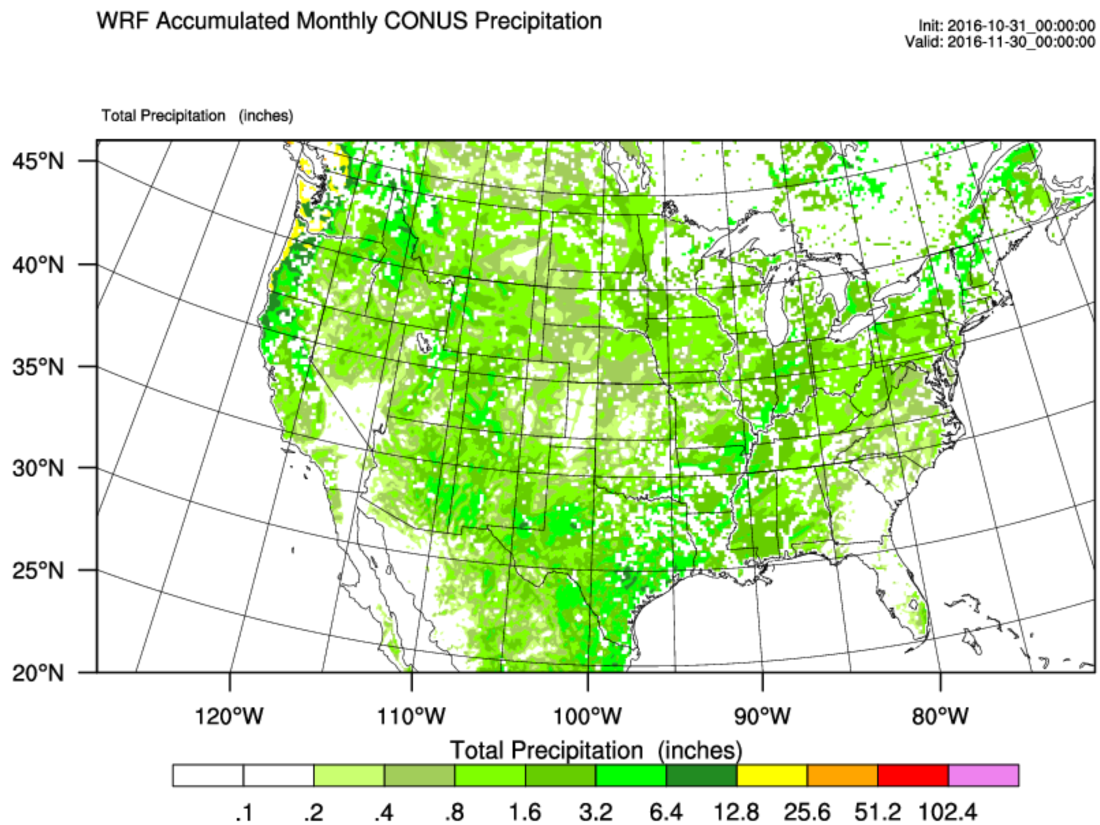

Figure 3-122: WRF Accumulated Precipitation for November 2016

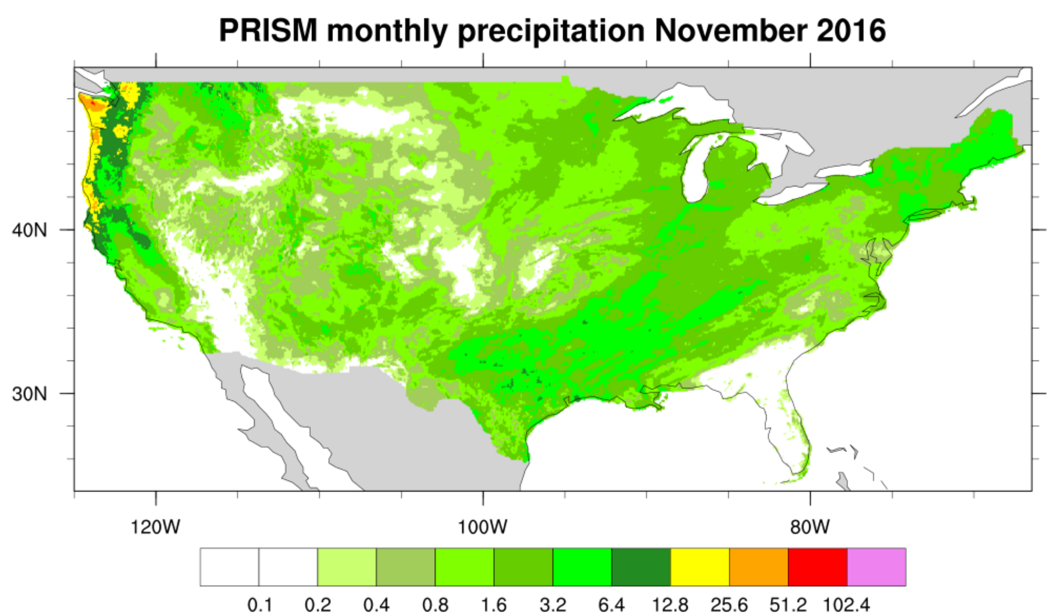

Figure 3-123: PRISM Accumulated Precipitation for November 2016

3.13 WRF DECEMBER PERFORMANCE

Wind speed performance was good across the CONUS and the south-central region as shown in Figure 3-124: *WRF CONUS Wind Performance for December 2016* and Figure 3-127: *WRF South-Central Region Wind Performance for December 2016*. The WRF modeling tracked observed multi-day temperature trends, although there were overpredictions of night time values as seen in Figure 3-125: *WRF CONUS Temperature Performance for December 2016* and Figure 3-128: *WRF South-Central Region Temperature Performance for December 2016*. Humidity values were simulated well by WRF during the December winter month as shown in Figure 3-126: *WRF CONUS Humidity Performance for December 2016* and Figure 3-129: *WRF South-Central Region Humidity Performance for December 2016*.

3.13.1 CONUS December Timeseries

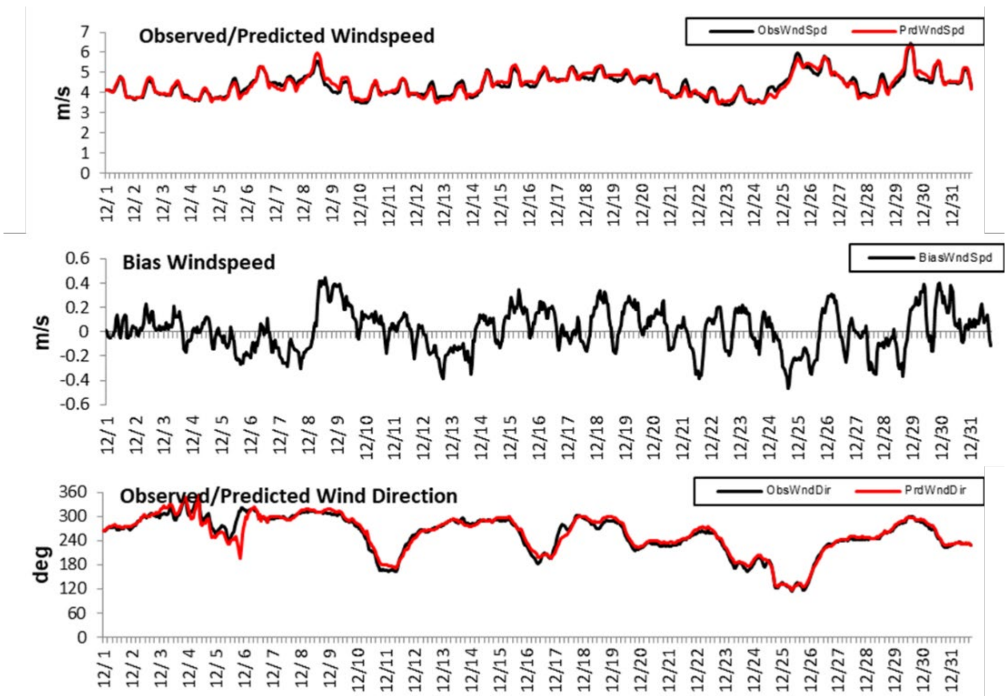

Figure 3-124: WRF CONUS Wind Performance for December 2016

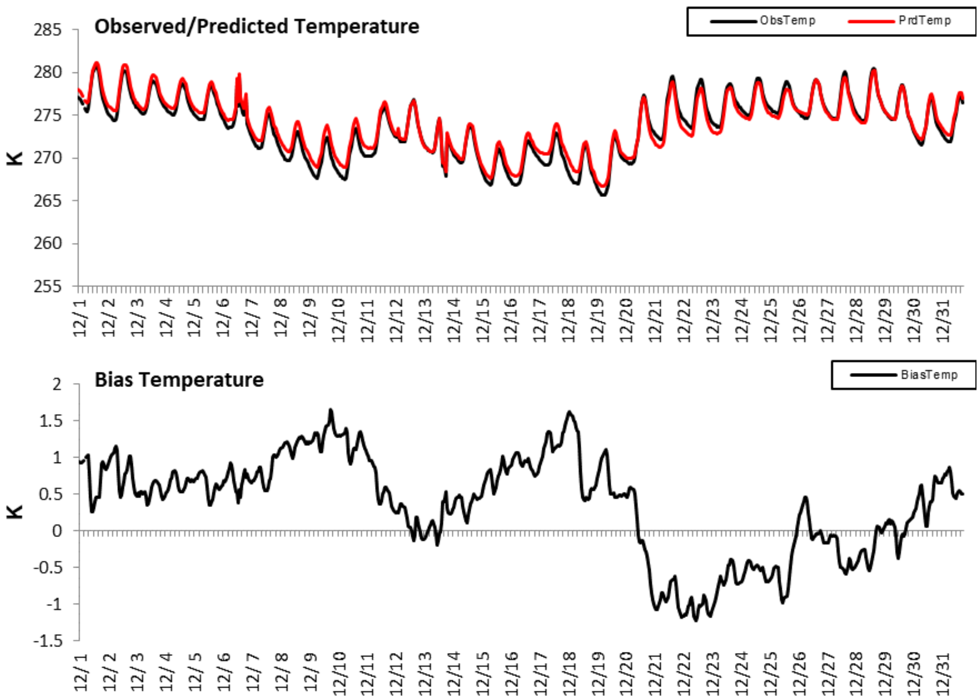

Figure 3-125: WRF CONUS Temperature Performance for December 2016

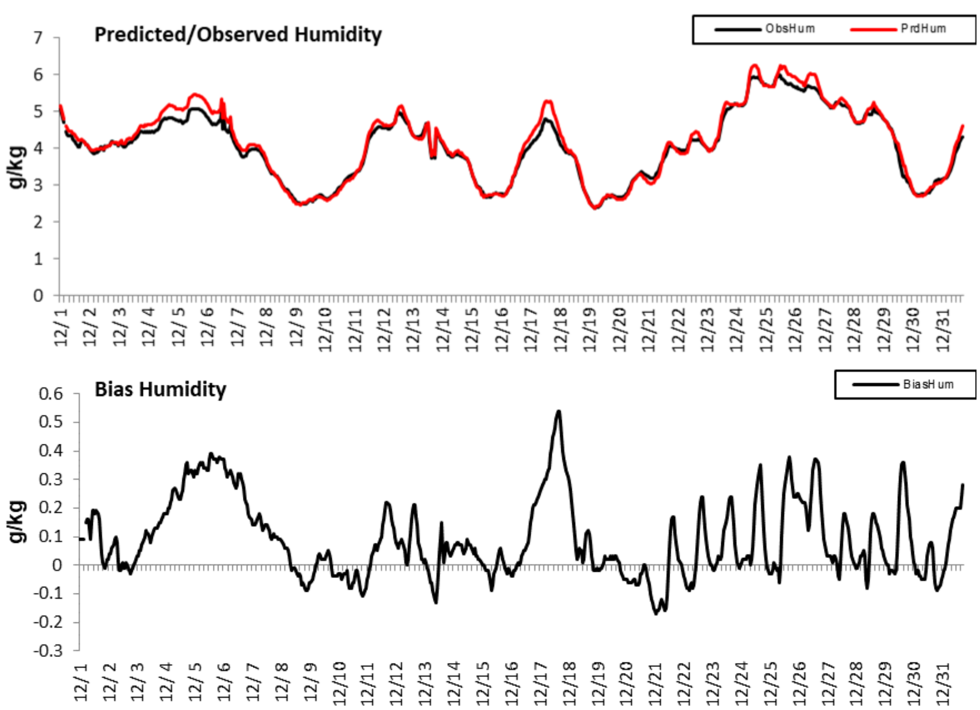

Figure 3-126: WRF CONUS Humidity Performance for December 2016

3.13.2 South-Central Region December Timeseries

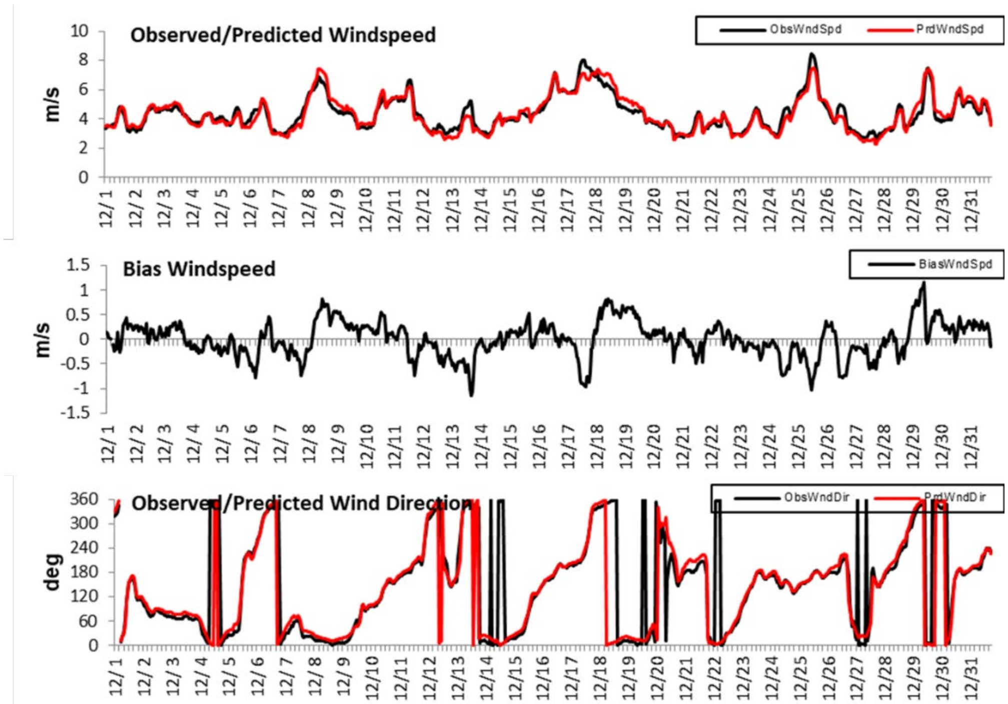

Figure 3-127: WRF South-Central Region Wind Performance for December 2016

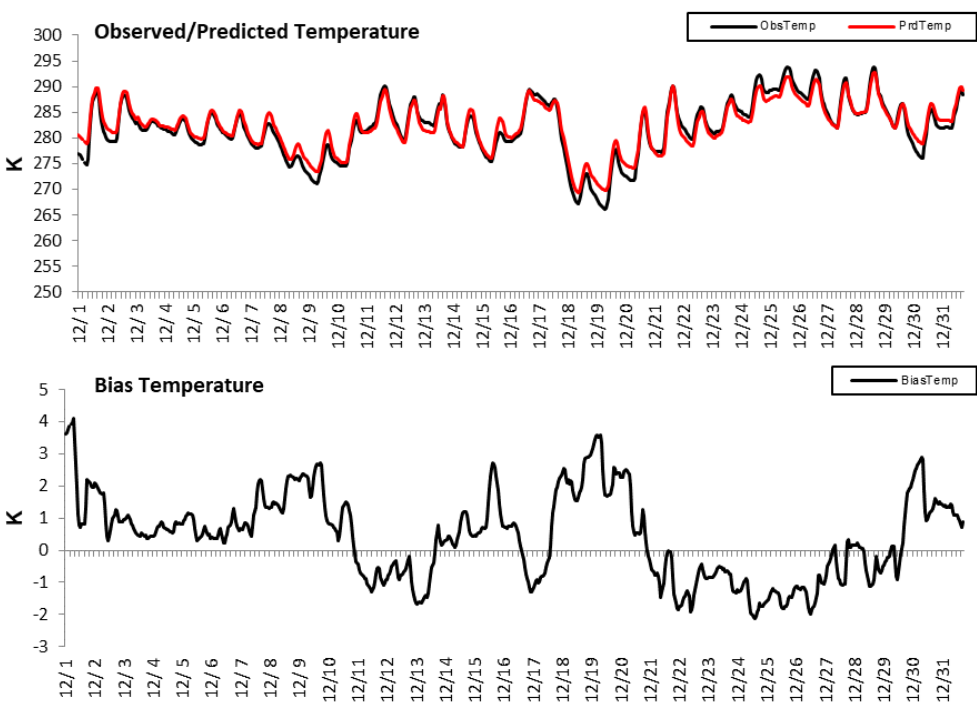

Figure 3-128: WRF South-Central Region Temperature Performance for December 2016

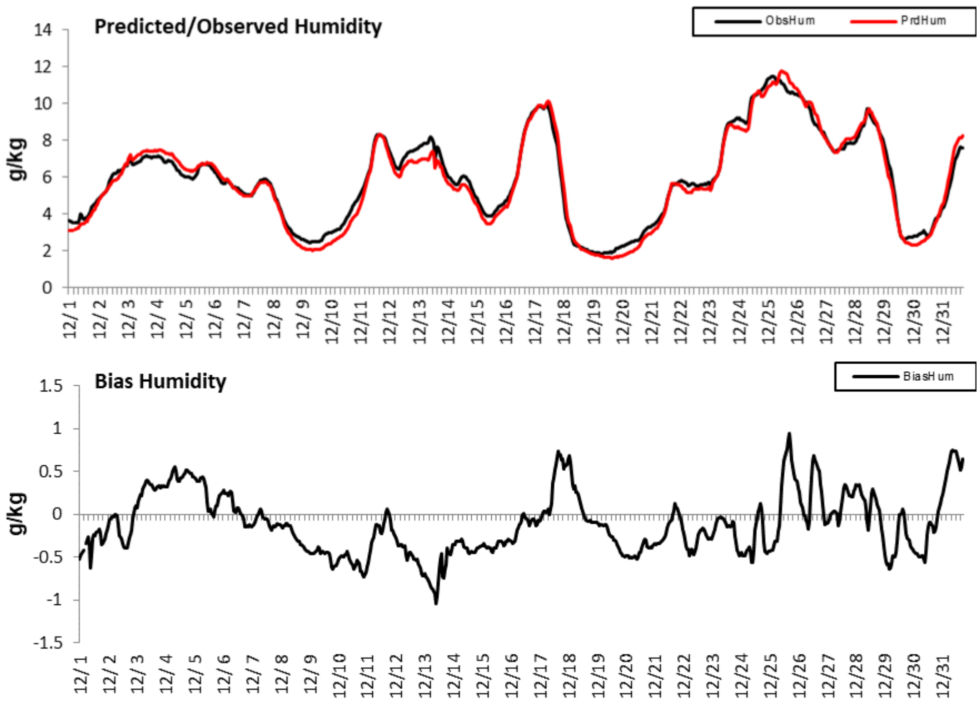

Figure 3-129: WRF South-Central Region Humidity Performance for December 2016

3.13.3 December Spatial Bias Plots

The spatial bias performance for wind speed was similar to November with larger negative biases in the west but good performance in and near Texas as shown in Figure 3-130: *Mean Bias of Wind Speed for December 2016*. Figure 3-131: *Mean Bias for Temperature for December 2016* exhibits that temperature was predicted well near Texas, but large biases were observed in Colorado and the Pacific Northwest. Humidity performance biases were near zero over much of the CONUS, though WRF underpredicted slightly in eastern Texas and the Gulf coast states, as shown in Figure 3-132: *Mean Bias of Humidity for December 2016*.

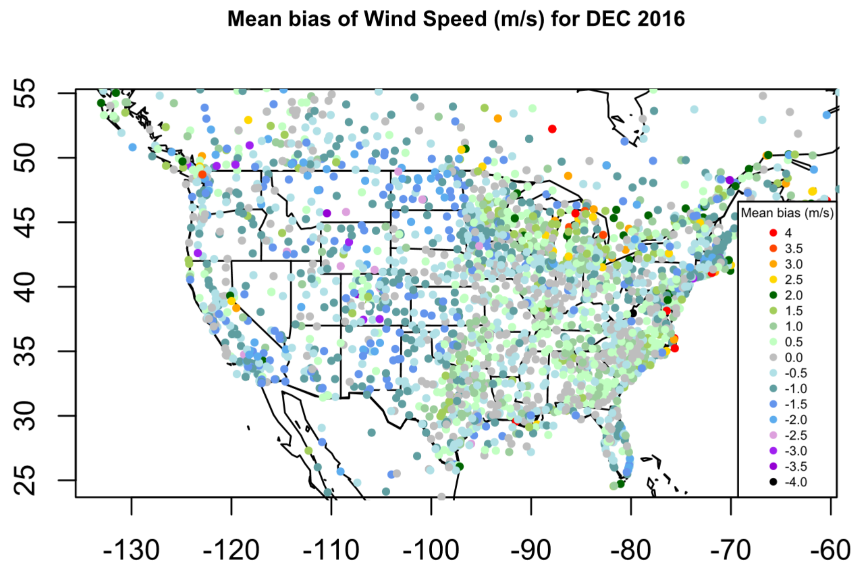

Figure 3-130: Mean Bias of Wind Speed for December 2016

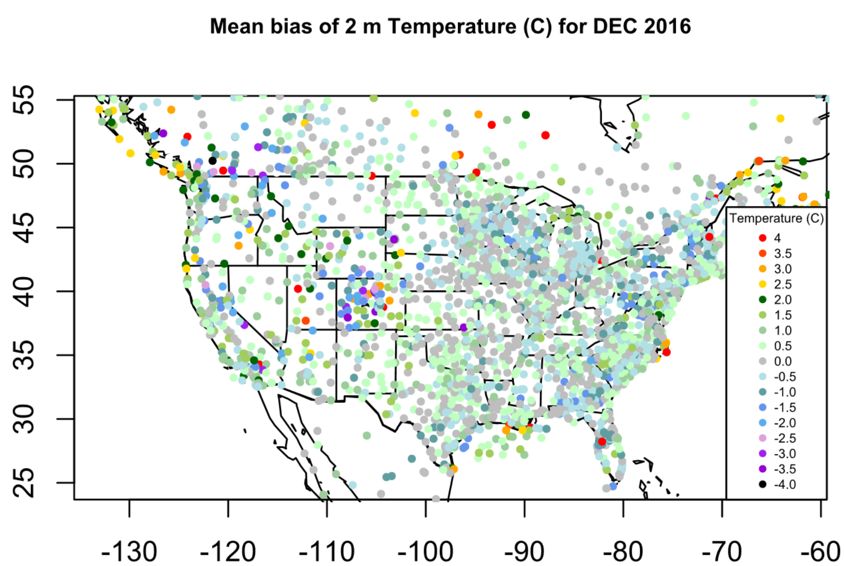

Figure 3-131: Mean Bias for Temperature for December 2016

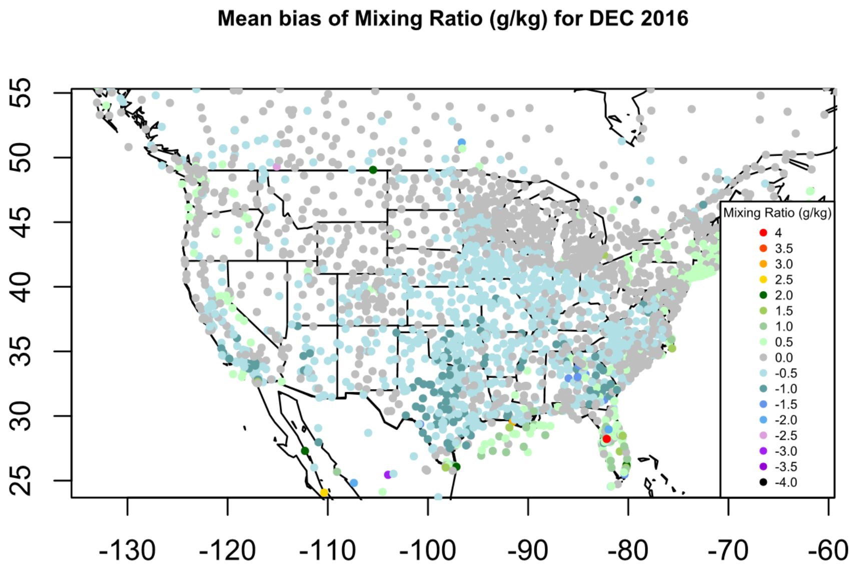

Figure 3-132: Mean Bias of Humidity for December 2016

3.13.4 December Accumulated Precipitation

WRF precipitation values in December matched the overall pattern of the observed PRISM data very well, as shown when comparing Figure 3-133: *WRF Accumulated Precipitation for December 2016* to Figure 3-134: *PRISM Accumulated Precipitation for December 2016*. The WRF model underpredicted the precipitation from in Mississippi, Alabama, and Georgia.

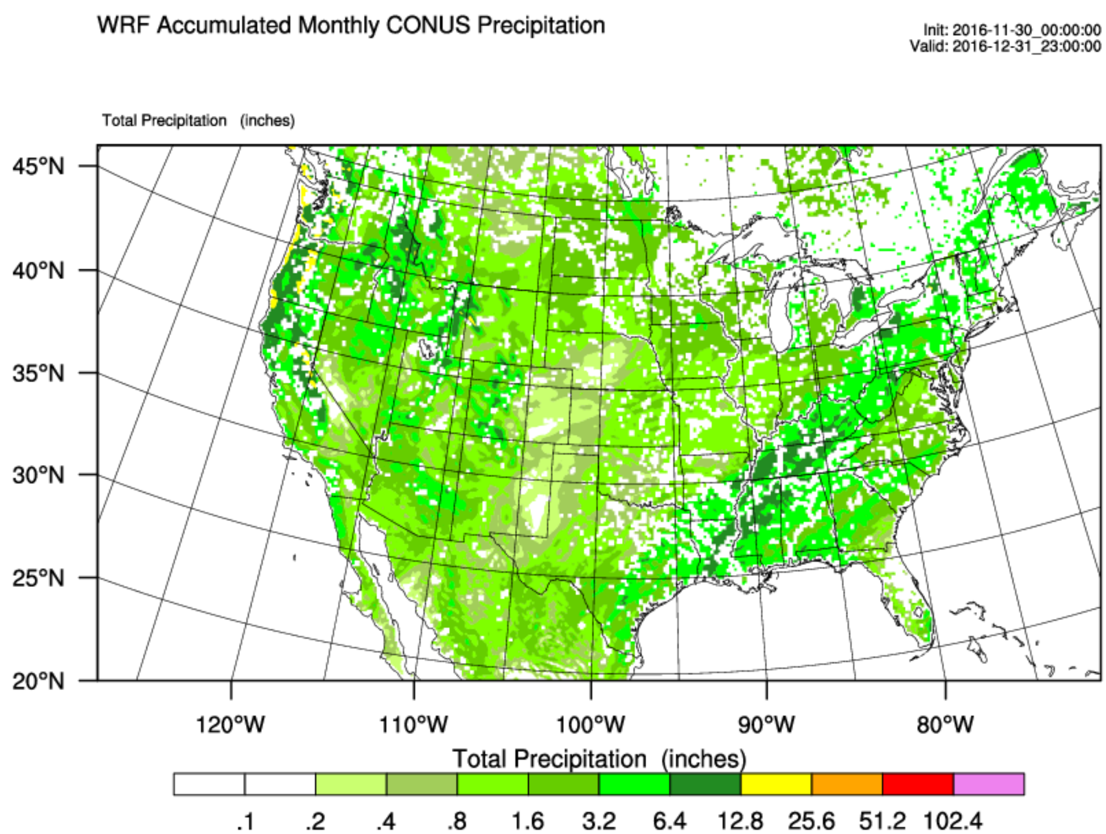

Figure 3-133: WRF Accumulated Precipitation for December 2016

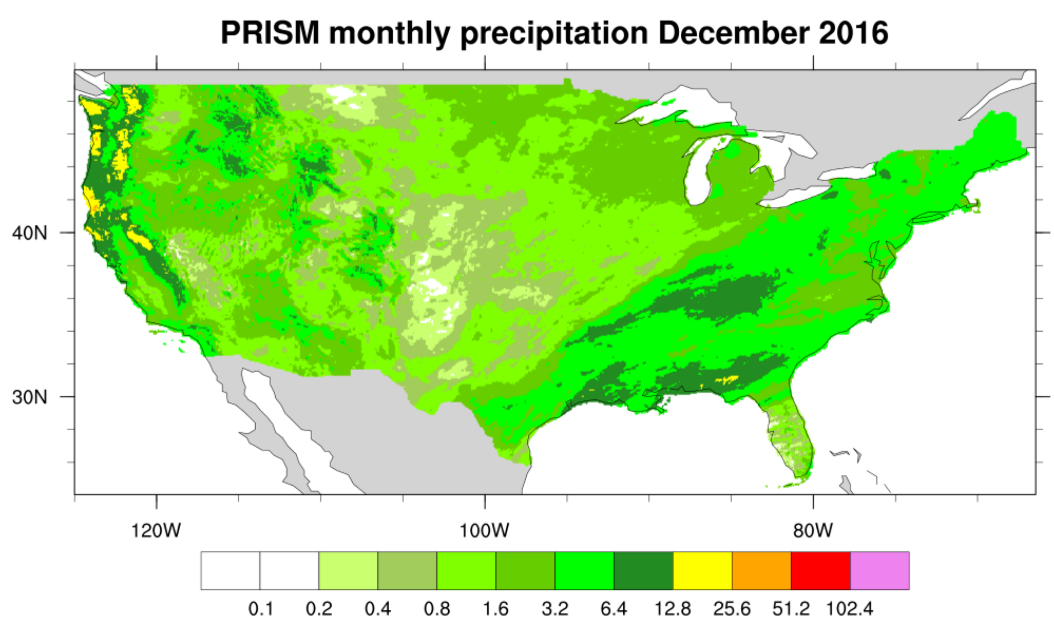

Figure 3-134: PRISM Accumulated Precipitation for December 2016

3.14 CONCLUSIONS

This appendix presented monthly time series comparing mean daily observed and predicted wind speed, wind direction, temperature, and humidity as well as mean daily biases for these variables across the entire CONUS and the south-central region. The monthly average of these mean daily values compares favorably with the benchmarks presented in Table 3-1. Although many data pairs are included in the mean daily calculations, these time series evaluate all months including those with high seasonal variability. Spatial bias plots for each site in the modeling domain reflected both the impact of complex terrain in mountainous areas and coastal areas. However, across the south-central region which includes the Class I areas of Texas and surrounding states, performance was consistently acceptable with few outliers. Accumulated precipitation from WRF and PRISM data were very consistent in magnitude and overall patterns. These collected statistical summaries support the use of this WRF modeling as input for the CAMx photochemical modeling used in this regional haze SIP revision.

REFERENCES

Bullock Jr., O. R., K. Alapaty, J. Herwehe, and J. Kain, 2015. A Dynamically Computed Convective Time Scale for the Kain-Fritsch Convective Parameterization Scheme, Mon. Wea. Rev., 143(6), 2105-2120.

Emery, C., Tai, E., and Yarwood, G., 2001. Enhanced Meteorological Modeling and Performance Evaluation for Two Texas Ozone Episodes, Environ International Company, https://www.tceq.texas.gov/assets/public/implementation/air/am/contracts/reports/mm/EnhancedMetModelingAndPerformanceEvaluation.pdf, August 2001.

McNally, D. E., 2009. 12 km MM5 Performance Goals, Presentation to the Ad-Hoc Meteorology Group, https://www3.epa.gov/scram001/adhoc/mcnally2009.pdf, June 2009.

Ramboll, 2018. User's Guide for the Comprehensive Air Quality Model with Extensions, Version 6.5, Ramboll-Environ, 2018.

Ramboll, 2019. WRFCAMx Post-Processing Tool, Ramboll, http://www.camx.com/download/support-software.aspx, February 2019.

WRAP, 2013. Western Regional Air Partnership (WRAP) West-wide Jump-start Air Quality Modeling Study (WestJumpAQMS), Environ and Alpine Geophysics, https://www.wrapair2.org/pdf/WestJumpAQMS_FinRpt_Finalv2.pdf, September 2013.

WRF, 2017. WRF Model Version 3.8.1: Updates, https://www2.mmm.ucar.edu/wrf/users/wrfv3.8/updates-3.8.1.html, March, 2017.